Chapter 2
State Feedback Control

Abstract In this chapter we explore the advantages of feedback control assuming that all the state variables are measurable. This is not a realistic assumption since the rotor variables are usually not measured but it allows us to explore fully the potentiality of feedback control. In Section 2.1 we establish that the feedforward control does not guarantee the asymptotic stability of the desired operating point for every initial condition and for every parameter value: the load torque in particular is a critical parameter. Hence, feedback control is needed to achieve the asymptotic stability of the desired operating condition, for any load torque and for any initial condition. Six feedback control algorithms are then presented. The most complex is the dynamic feedback linearizing control presented in the last Section 2.6, which imposes an arbitrary linear dynamic behavior to the controlled motor. The input–output feedback linearizing control is presented in Section 2.4: it achieves arbitrary and decoupled linear dynamics for the two tracking errors of rotor speed and flux modulus; it is generalized in Section 2.5 by an adaptive input–output feedback linearizing control which identifies both the load torque and the rotor resistance in realistic operating conditions. The identification of these two parameters allows computation online of the optimal value of the rotor flux modulus which minimizes the power losses. All three feedback linearizing control schemes have excellent performances provided that the initial errors are sufficiently small: this is a significant limitation which is removed by the global control with arbitrary rate of convergence presented in Section 2.7. It is the evolution of the historically important direct field-oriented control which is presented in Section 2.2 and its variant, the indirect field-oriented control, which is discussed in Section 2.3 and can operate from any initial conditions. The field-oriented controls constitute a modification of the feedforward control discussed in Section 2.1 and contain the key steps to design the global control with arbitrary rate of convergence, which can operate from any motor initial conditions. The indirect field-oriented control is tested by experiments in Section 2.8 and its robustness with respect to rotor resistance variations is explored.

2.1 Stability Analysis of Feedforward Control

In this section we assume that the left inverse control (1.74) is applied as a feedforward control to the induction motor fixed frame model (1.26) and we study the case in which the initial conditions are not compatible in (1.74). We have seen in the previous chapter that if the initial conditions of the induction motor and of the inverse system are compatible and the inverse feedforward control (1.74) is applied, then the induction motor satisfies the equations

$$\begin{aligned}
\frac{\mathrm{d}\omega^*}{\mathrm{d}t} &= \mu\psi^* i_{sq}^* - \frac{T_L}{J} \\
\frac{\mathrm{d}\psi^*}{\mathrm{d}t} &= -\alpha\psi^* + \alpha M i_{sd}^* \\
0 &= -(\omega_0^* - \omega^*)\psi^* + \alpha M i_{sq}^* \\
\frac{\mathrm{d}i_{sd}^*}{\mathrm{d}t} &= -\gamma i_{sd}^* + \omega_0^* i_{sq}^* + \beta\alpha\psi^* + \frac{u_{sd}^*}{\sigma} \\
\frac{\mathrm{d}i_{sq}^*}{\mathrm{d}t} &= -\gamma i_{sq}^* - \omega_0^* i_{sd}^* - \beta\omega^*\psi^* + \frac{u_{sq}^*}{\sigma}
\end{aligned} \tag{2.1}$$

in which the (d,q) reference rotating frame rotates at speed

$$\frac{\mathrm{d}\varepsilon_0^*}{\mathrm{d}t} = \omega_0^* = \omega^* + \frac{\alpha M i_{sq}^*}{\psi^*} = \omega^* + \omega_s^* \tag{2.2}$$

and it is identified by the angle $\varepsilon_0^*(t) = \rho^*(t) = \rho(t)$ in the fixed (a,b) frame. The crucial question we are going to answer in this section is the following: what happens when the initial conditions of the inverse control (1.74) are not compatible and in particular when $\rho^*(0) \neq \arctan\frac{\psi_{rb}(0)}{\psi_{ra}(0)}$, which is very likely to happen since measurements of (ψ_{ra}, ψ_{rb}) are typically not available? In other words we are going to explore the stability and the attractivity (see Appendix A) of the steady-state solution $(\omega^*, \psi^*, 0, i_{sd}^*, i_{sq}^*)$. Since the rotor flux angle ρ no longer coincides with the angle ρ^*, consider the (d,q) frame identified by the angle ε_0^*. In the considered (d,q) frame the induction motor satisfies (1.31) with ω_0^* in place of ω_0. If we now subtract (2.1) from (1.31) we obtain the tracking error dynamics

$$\begin{aligned}
\frac{\mathrm{d}(\omega - \omega^*)}{\mathrm{d}t} &= \mu\left[(\psi_{rd} - \psi^*) i_{sq}^* - \psi_{rq} i_{sd}^*\right] + \mu\psi^*\left(i_{sq} - i_{sq}^*\right) \\
&\quad + \mu\left[(\psi_{rd} - \psi^*)\left(i_{sq} - i_{sq}^*\right) - \psi_{rq}\left(i_{sd} - i_{sd}^*\right)\right] \\
\frac{\mathrm{d}(\psi_{rd} - \psi^*)}{\mathrm{d}t} &= -\alpha(\psi_{rd} - \psi^*) - (\omega - \omega^*)\psi_{rq} \\
&\quad + \omega_s^*\psi_{rq} + \alpha M\left(i_{sd} - i_{sd}^*\right) \\
\frac{\mathrm{d}\psi_{rq}}{\mathrm{d}t} &= -\alpha\psi_{rq} + (\omega - \omega^*)(\psi_{rd} - \psi^*) \\
&\quad - \omega_s^*(\psi_{rd} - \psi^*) + (\omega - \omega^*)\psi^* + \alpha M\left(i_{sq} - i_{sq}^*\right)
\end{aligned}$$

$$\begin{aligned}
\frac{\mathrm{d}\left(i_{sd}-i_{sd}^{*}\right)}{\mathrm{d}t} &= -\gamma\left(i_{sd}-i_{sd}^{*}\right)+\omega_0^{*}\left(i_{sq}-i_{sq}^{*}\right)+\beta\alpha\left(\psi_{rd}-\psi^{*}\right)\\
&\quad +\beta\omega^{*}\psi_{rq}+\beta\left(\omega-\omega^{*}\right)\psi_{rq}\\
\frac{\mathrm{d}\left(i_{sq}-i_{sq}^{*}\right)}{\mathrm{d}t} &= -\gamma\left(i_{sq}-i_{sq}^{*}\right)-\omega_0^{*}\left(i_{sd}-i_{sd}^{*}\right)+\beta\alpha\psi_{rq}\\
&\quad -\beta\omega^{*}\left(\psi_{rd}-\psi^{*}\right)-\beta\left(\omega-\omega^{*}\right)\left(\psi_{rd}-\psi^{*}\right)\\
&\quad -\beta\left(\omega-\omega^{*}\right)\psi^{*}
\end{aligned} \tag{2.3}$$

where we recall that

$$\begin{aligned}
i_{sd}^{*} &= \frac{\psi^{*}}{M}+\frac{\dot{\psi}^{*}}{\alpha M}\\
i_{sq}^{*} &= \frac{\dot{\omega}^{*}}{\mu\psi^{*}}+\frac{T_L}{J\mu\psi^{*}}
\end{aligned} \tag{2.4}$$

and ω_s^{*} is defined in (2.2). The origin

$$\left[\left(\omega-\omega^{*}\right),\left(\psi_{rd}-\psi^{*}\right),\psi_{rq},\left(i_{sd}-i_{sd}^{*}\right),\left(i_{sq}-i_{sq}^{*}\right)\right]^{\mathrm{T}}=0\,,$$

which corresponds to zero tracking errors, is clearly an equilibrium point for the tracking error dynamics (2.3): this is the case of compatible initial conditions in which

$$\begin{aligned}
\omega(0) &= \omega^{*}(0)\\
\psi_{ra}(0) &= \psi^{*}(0)\cos\rho^{*}(0)\\
\psi_{rb}(0) &= \psi^{*}(0)\sin\rho^{*}(0)\\
\begin{bmatrix} i_{sa}(0)\\ i_{sb}(0)\end{bmatrix} &= \begin{bmatrix}\cos\rho^{*}(0) & -\sin\rho^{*}(0)\\ \sin\rho^{*}(0) & \cos\rho^{*}(0)\end{bmatrix}\begin{bmatrix}\frac{\psi^{*}(0)}{M}+\frac{\dot{\psi}^{*}(0)}{\alpha M}\\ \frac{\dot{\omega}^{*}(0)}{\mu\psi^{*}(0)}+\frac{T_L}{J\mu\psi^{*}(0)}\end{bmatrix}\\
\rho^{*}(0) &= \rho(0)\,.
\end{aligned}$$

In order to have a more compact notation, let us rewrite the tracking error dynamics in terms of the tracking errors

$$\begin{aligned}
\tilde{\omega} &= \omega-\omega^{*}\\
\tilde{\psi}_{rd} &= \psi_{rd}-\psi^{*}\\
\tilde{\psi}_{rq} &= \psi_{rq}\\
\tilde{i}_{sd} &= i_{sd}-i_{sd}^{*}\\
\tilde{i}_{sq} &= i_{sq}-i_{sq}^{*}
\end{aligned}$$

as

$$\frac{\mathrm{d}\tilde{\omega}}{\mathrm{d}t}=\mu i_{sq}^{*}\tilde{\psi}_{rd}-\mu i_{sd}^{*}\tilde{\psi}_{rq}+\mu\psi^{*}\tilde{i}_{sq}+\mu\tilde{\psi}_{rd}\tilde{i}_{sq}-\mu\tilde{\psi}_{rq}\tilde{i}_{sd}$$

$$\begin{aligned}
\frac{\mathrm{d}\tilde{\psi}_{rd}}{\mathrm{d}t} &= -\alpha\tilde{\psi}_{rd} + \omega_s^*\tilde{\psi}_{rq} - \tilde{\omega}\tilde{\psi}_{rq} + \alpha M\tilde{i}_{sd} \\
\frac{\mathrm{d}\tilde{\psi}_{rq}}{\mathrm{d}t} &= -\alpha\tilde{\psi}_{rq} - \omega_s^*\tilde{\psi}_{rd} + \tilde{\omega}\tilde{\psi}_{rd} + \alpha M\tilde{i}_{sq} + \psi^*\tilde{\omega} \\
\frac{\mathrm{d}\tilde{i}_{sd}}{\mathrm{d}t} &= -\gamma\tilde{i}_{sd} + \omega_0^*\tilde{i}_{sq} + \beta\alpha\tilde{\psi}_{rd} + \beta\omega^*\tilde{\psi}_{rq} + \beta\tilde{\omega}\tilde{\psi}_{rq} \\
\frac{\mathrm{d}\tilde{i}_{sq}}{\mathrm{d}t} &= -\gamma\tilde{i}_{sq} - \omega_0^*\tilde{i}_{sd} + \beta\alpha\tilde{\psi}_{rq} - \beta\omega^*\tilde{\psi}_{rd} - \beta\tilde{\omega}\tilde{\psi}_{rd} - \beta\psi^*\tilde{\omega}\,. \qquad (2.5)
\end{aligned}$$

Many questions are naturally posed on the tracking error dynamics (2.5): is the origin stable, asymptotically stable, exponentially stable, globally asymptotically stable, globally exponentially stable? How large is the region of attraction of the origin and what is the influence of critical parameters, such as rotor resistance R_r and load torque T_L, on the region of attraction and on the dynamic behavior? These questions have no simple answers since the system (2.5) is nonlinear and time-varying when the reference signals (ω^*, ψ^*) are time-varying. On the other hand, these questions are extremely important since, for instance, if the origin were globally exponentially stable with satisfactory transient properties and robustness with respect to parameter variations then no feedback control would be needed and the feedforward control (1.74) would achieve the tracking of (ω^*, ψ^*) from any initial condition. To examine one of those questions, consider the error system dynamics (2.5) and compute the equilibrium points for (2.5) in the case of constant references (ω^*, ψ^*) and $T_L \neq 0$. In order to use a more compact notation and simplify the analysis, define the tracking error variables

$$\begin{aligned}
z_d &= \tilde{i}_{sd} + \beta\tilde{\psi}_{rd} \\
z_q &= \tilde{i}_{sq} + \beta\tilde{\psi}_{rq}
\end{aligned}$$

so that the error system (2.5) in the case of constant references (ω^*, ψ^*) may be rewritten in the simpler form

$$\begin{aligned}
\dot{\tilde{\omega}} &= A\tilde{\psi}_{rd} - B\tilde{\psi}_{rq} + Cz_q + \mu\tilde{\psi}_{rd}z_q - \mu\tilde{\psi}_{rq}z_d \\
\dot{\tilde{\psi}}_{rd} &= -D\tilde{\psi}_{rd} - \tilde{\omega}\tilde{\psi}_{rq} + E\tilde{\psi}_{rq} + \alpha M z_d \\
\dot{\tilde{\psi}}_{rq} &= -D\tilde{\psi}_{rq} + \tilde{\omega}\tilde{\psi}_{rd} - E\tilde{\psi}_{rd} + \psi^*\tilde{\omega} + \alpha M z_q \\
\dot{z}_d &= Fz_q - kz_d + k\beta\tilde{\psi}_{rd} \\
\dot{z}_q &= -Fz_d - kz_q + k\beta\tilde{\psi}_{rq} \qquad (2.6)
\end{aligned}$$

in which the following reparameterization is used

$$\begin{aligned}
&A = \frac{T_L}{J\psi^*}, \quad B = \mu\psi^*\left(\frac{1}{M} + \beta\right), \\
&C = \mu\psi^*, \quad D = \alpha + \alpha M\beta, \\
&E = \frac{\alpha M T_L}{\mu J\psi^{*2}}, \quad F = \omega^* + E, \quad k = \frac{R_s}{\sigma}\,.
\end{aligned}$$

By direct computation it is possible to show that there exist constant references (ω^*, ψ^*) and $T_L \neq 0$, which are within physical bounds such that the tracking error dynamics (2.6) have an explicitly computable additional equilibrium point besides the origin whose first component

$$\tilde{\omega}_e = \left(\beta kCF - \beta k\psi^* \mu F - k^2 A - AF^2\right)^{-1} \Big[\alpha\beta^2 MCk^2 - \alpha\beta MBk^2 - \alpha\beta MAFk - \beta CDk^2 + \beta kCFE - k^2 AE + k^2 BD + BF^2 D - AF^2 E\Big]$$

is nonzero. Hence, for such references and load torque values, the origin is not a globally attractive equilibrium point for (2.6) and rotor speed tracking cannot be achieved for any motor initial condition. Furthermore, consider the linear approximation about the origin of system (2.5):

$$\begin{aligned}
\frac{\mathrm{d}\tilde{\omega}}{\mathrm{d}t} &= \mu i_{sq}^* \tilde{\psi}_{rd} - \mu i_{sd}^* \tilde{\psi}_{rq} + \mu\psi^* \tilde{i}_{sq} \\
\frac{\mathrm{d}\tilde{\psi}_{rd}}{\mathrm{d}t} &= -\alpha\tilde{\psi}_{rd} + \omega_s^* \tilde{\psi}_{rq} + \alpha M \tilde{i}_{sd} \\
\frac{\mathrm{d}\tilde{\psi}_{rq}}{\mathrm{d}t} &= \psi^* \tilde{\omega} - \omega_s^* \tilde{\psi}_{rd} - \alpha\tilde{\psi}_{rq} + \alpha M \tilde{i}_{sq} \\
\frac{\mathrm{d}\tilde{i}_{sd}}{\mathrm{d}t} &= \beta\alpha\tilde{\psi}_{rd} + \beta\omega^* \tilde{\psi}_{rq} - \gamma\tilde{i}_{sd} + (\omega^* + \omega_s^*)\tilde{i}_{sq} \\
\frac{\mathrm{d}\tilde{i}_{sq}}{\mathrm{d}t} &= -\beta\psi^* \tilde{\omega} - \beta\omega^* \tilde{\psi}_{rd} + \beta\alpha\tilde{\psi}_{rq} - (\omega^* + \omega_s^*)\tilde{i}_{sd} - \gamma\tilde{i}_{sq}\,.
\end{aligned} \tag{2.7}$$

According to the linear approximation Theorem A.7 in Appendix A, if the load torque satisfies the inequality

$$T_L^2 \geq \frac{(1 + M\beta)^2 \psi^{*4}}{L_r^2}$$

then the origin is an unstable equilibrium point for the error system (2.5). Recall that in the analysis of the torque–speed characteristic curve in Section 1.3 we observed in Figures 1.5 and 1.6 that unstable operating conditions at low rotor speed correspond to low rotor flux modulus and high load torques.

In conclusion, there exist constant references (ω^*, ψ^*) and $T_L \neq 0$ such that the feedforward control (1.74), specialized to the case of constant rotor speed and flux modulus references (see Figure 2.1 for current-fed motors),

$$\begin{bmatrix} u_{sa}^* \\ u_{sb}^* \end{bmatrix} = \begin{bmatrix} \cos\rho^* & -\sin\rho^* \\ \sin\rho^* & \cos\rho^* \end{bmatrix} \begin{bmatrix} u_{sd}^* \\ u_{sq}^* \end{bmatrix}$$

$$u_{sd}^* = \sigma \left[\frac{R_s \psi^*}{\sigma M} - \frac{\omega^* T_L}{\mu J \psi^*} - \frac{\alpha M}{\psi^*} \left(\frac{T_L}{J\mu\psi^*} \right)^2 \right]$$

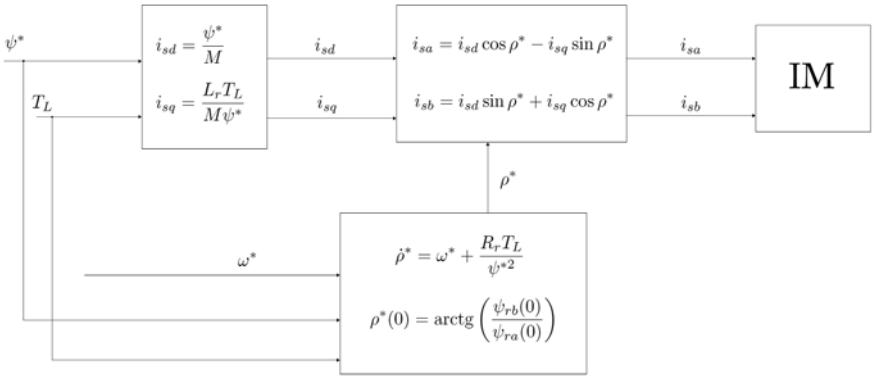

Fig. 2.1 Feedforward control for current-fed motors (constant references ω^*, ψ^*)

$$u_{sq}^* = \sigma\left[\frac{\gamma T_L}{J\mu\psi^*} + \frac{\omega^*\psi^*}{M} + \frac{\alpha T_L}{J\mu\psi^*} + \beta\omega^*\psi^*\right]$$
$$\dot{\rho}^* = \omega^* + \frac{\alpha M T_L}{\mu J\psi^{*2}} \tag{2.8}$$

depending on the reference signals (ω^*, ψ^*), on the initial condition $\rho^*(0)$, and on the machine parameters M, R_r, L_r, J, R_s, L_s, does not guarantee rotor speed tracking for any motor initial condition. Furthermore, the origin of the error system (2.5), which implies zero tracking error, is unstable if the inequality $|T_L| \geq \frac{(1+M\beta)\psi^{*2}}{L_r}$ is satisfied.

Illustrative Simulations

We tested the feedforward control (2.8) by simulations for the three-phase single pole pair 0.6-kW induction motor whose parameters have been reported in Chapter 1. All the motor initial conditions have been set equal to zero except for $\psi_{ra}(0) = \psi_{rb}(0) = 0.1\,\text{Wb}$. The references for the speed and flux modulus along with the applied load torque are reported in Figures 2.2–2.4. The rotor flux modulus reference signal starts from 0.001 Wb at $t = 0\,\text{s}$ and grows up to the constant value 1.16 Wb. The speed reference is zero until $t = 0.32\,\text{s}$ and grows up to the constant value 100 rad/s; at $t = 1.5\,\text{s}$ the reference for the flux modulus is reduced to 0.5 Wb. A 5.8-Nm load torque is applied to the motor and then is reduced to 4.8 Nm. Fig-

ures 2.3 and 2.4 show the time histories of rotor speed and flux modulus along with the corresponding tracking errors: the rotor speed and flux modulus are regulated to their corresponding references as long as the load torque satisfies the inequality $T_L < \frac{\psi^{*2}(1+M\beta)}{L_r}$, while rotor speed and rotor flux modulus regulation is not achieved when the load torque is greater than $\frac{\psi^{*2}(1+M\beta)}{L_r}$. In fact, for a load torque $T_L = 4.8\,\text{Nm}$ and a constant rotor flux reference $\psi^* = 0.5\,\text{Wb}$, the origin of the error system (2.5) is unstable while the computed additional equilibrium point for (2.5) is exponentially stable. Finally, the stator currents and voltages profiles, which are within the physical saturation limits, are reported in Figures 2.5 and 2.6.

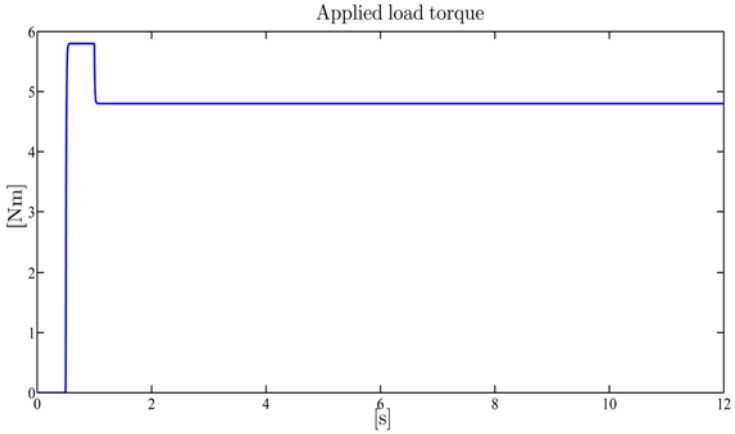

Fig. 2.2 Feedforward control: applied load torque T_L

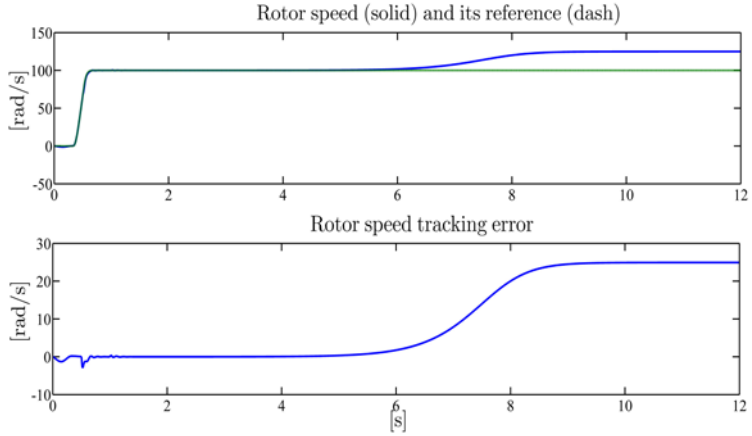

Fig. 2.3 Feedforward control: rotor speed ω and its reference ω^*; rotor speed tracking error

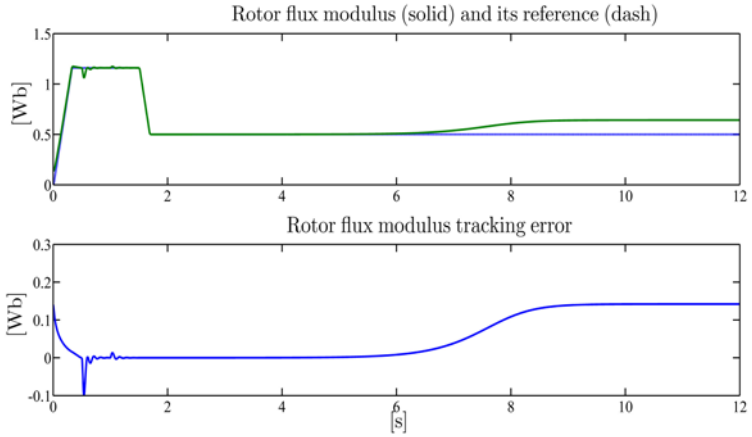

Fig. 2.4 Feedforward control: rotor flux modulus $\sqrt{\psi_{ra}^2+\psi_{rb}^2}$ and its reference ψ^*; rotor flux modulus tracking error

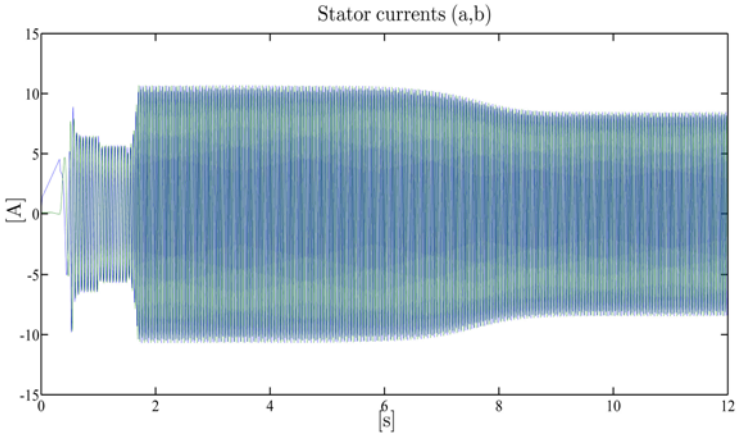

Fig. 2.5 Feedforward control: stator current vector (a,b)-components

A second simulation is performed in order to illustrate, in the particular case in which the origin of the error system (2.5) is exponentially stable according to the linear approximation Theorem A.7 in Appendix A, the effect of uncertainties in both load torque and rotor resistance. All motor initial conditions have been set equal to zero except for $\psi_{ra}(0) = \psi_{rb}(0) = 0.1\,\text{Wb}$. A 5.8-Nm load torque is applied to the motor and is reduced to 0.5 Nm as shown in Figure 2.7. The references for the speed and flux modulus are reported in Figures 2.8 and 2.9. The rotor flux modulus reference signal starts from 0.001 Wb at $t = 0\,\text{s}$ and grows up to the constant value 1.16 Wb. The speed reference is zero until $t = 0.32\,\text{s}$ and grows up to the constant

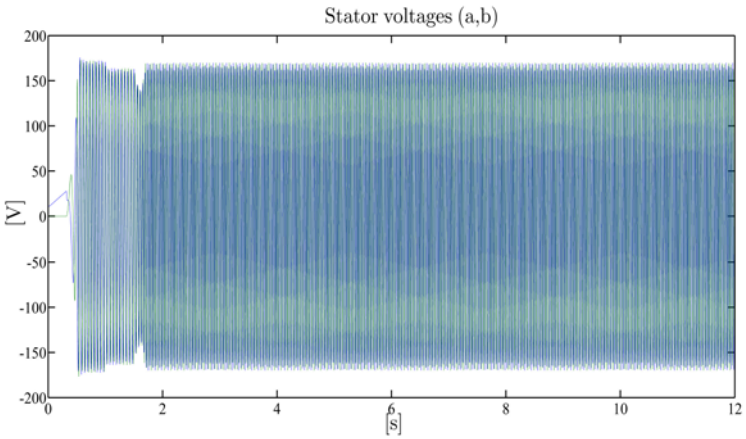

Fig. 2.6 Feedforward control: stator voltage vector (a, b)-components

value 100 rad/s; at $t = 1.5$ s the reference for the flux modulus is then reduced to 0.5 Wb. The value of the rotor resistance used by the feedforward control is 50% greater than the true value $R_r = 3.3\,\Omega$ while only a 0.2-Nm load torque is compensated by the controller for $t \geq 1$ s (see Figure 2.7). Figures 2.8 and 2.9 show the time histories of rotor speed and flux modulus along with the corresponding tracking errors: note that steady-state errors appear as expected. Finally, the stator currents and voltages profiles, which are within the physical saturation limits, are reported in Figures 2.10 and 2.11.

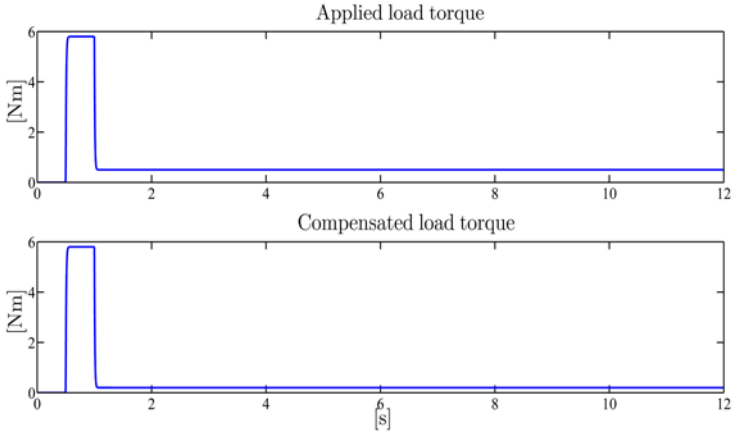

Fig. 2.7 Feedforward control with parameter uncertainties: applied load torque T_L and compensated load torque

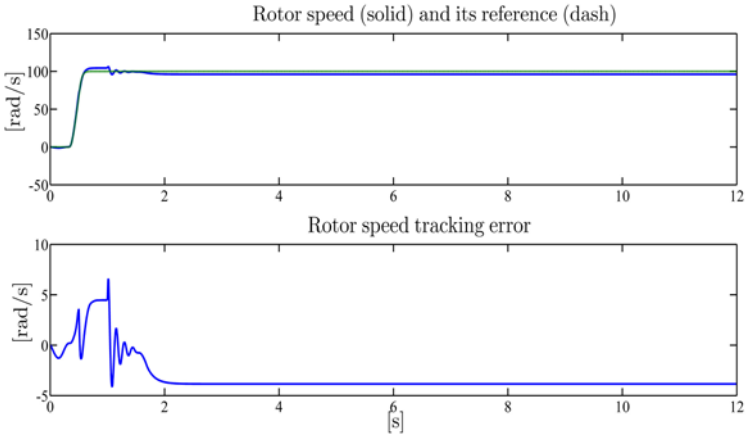

Fig. 2.8 Feedforward control with parameter uncertainties: rotor speed ω and its reference ω^*; rotor speed tracking error

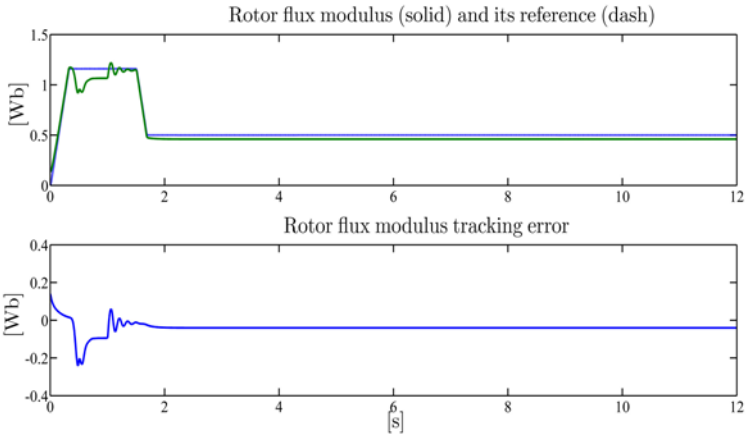

Fig. 2.9 Feedforward control with parameter uncertainties: rotor flux modulus $\sqrt{\psi_{ra}^2 + \psi_{rb}^2}$ and its reference ψ^*; rotor flux modulus tracking error

In summary, we have shown that the feedforward control (2.8), which is required to keep the motor at constant speed ω^* with a desired constant flux modulus ψ^*, does not guarantee the regulation to ω^* for any motor initial condition and may yield unstable steady-state operating conditions depending on load torque T_L, motor parameters, and desired flux modulus ψ^*, even when exact parameter values are used in (2.8). On the other hand, if the values of the critical parameters R_r and T_L used in (2.8) do not coincide with the corresponding actual values then the simulations show that steady-state tracking errors appear. Feedback is then required to guarantee asymptotically stable operating conditions for any initial condition and, at the same time, robustness with respect to uncertainties in critical motor parame-

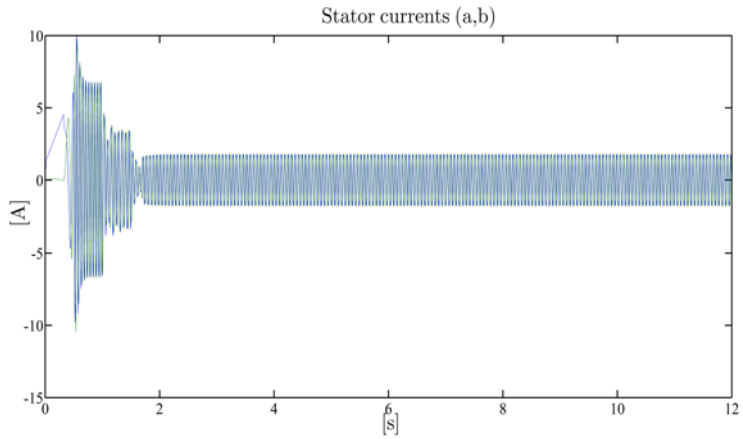

Fig. 2.10 Feedforward control with parameter uncertainties: stator current vector (a,b)-components

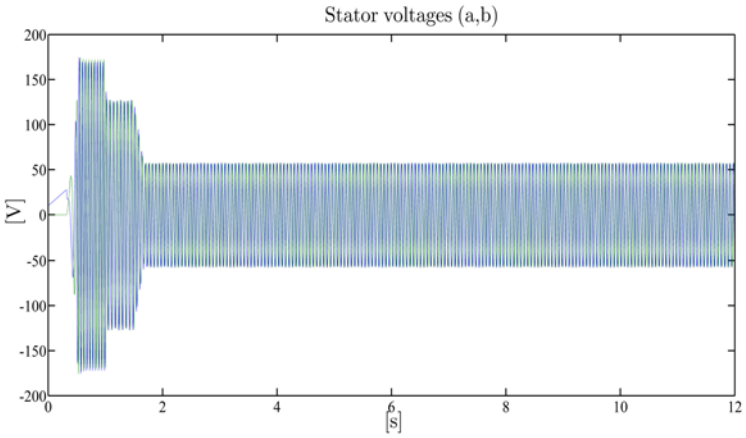

Fig. 2.11 Feedforward control with parameter uncertainties: stator voltage vector (a,b)-components

ters such as rotor resistance and load torque. This goal will be achieved in the next sections.

2.2 Direct Field-oriented Control

The purpose of this section is to illustrate the benefits of feedback control. Consider the reduced third-order model in the (d,q) frame rotating at rotor flux speed of rotation $\dot{\rho}$ and identified by the rotor flux angle ρ (see (1.39))

$$\begin{aligned}\frac{\mathrm{d}\omega}{\mathrm{d}t} &= \mu\psi_{rd}i_{sq} - \frac{T_L}{J}\\ \frac{\mathrm{d}\psi_{rd}}{\mathrm{d}t} &= -\alpha\psi_{rd} + \alpha M i_{sd}\\ \frac{\mathrm{d}\rho}{\mathrm{d}t} &= \omega + \frac{\alpha M i_{sq}}{\psi_{rd}}\end{aligned} \tag{2.9}$$

in which the pair (i_{sd}, i_{sq}) in (1.41) is viewed as the control input vector, under the assumption that the actual physical inputs (u_{sd}, u_{sq}) in (1.42) can be designed to track very quickly any desired stator current pair (i_{sd}, i_{sq}). The currents (i_{sd}, i_{sq}), which are related to the stator currents (i_{sa}, i_{sb}) in the fixed (a,b) frame attached to the stator by the nonsingular transformation (recall (1.30) with $\varepsilon_0 = \rho$ and (1.37), (1.38))

$$\begin{aligned}\cos\rho &= \frac{\psi_{ra}}{\sqrt{\psi_{ra}^2 + \psi_{rb}^2}}\\ \sin\rho &= \frac{\psi_{rb}}{\sqrt{\psi_{ra}^2 + \psi_{rb}^2}}\\ \begin{bmatrix} i_{sa}\\ i_{sb}\end{bmatrix} &= \begin{bmatrix}\cos\rho & -\sin\rho\\ \sin\rho & \cos\rho\end{bmatrix}\begin{bmatrix} i_{sd}\\ i_{sq}\end{bmatrix}\end{aligned} \tag{2.10}$$

are to be designed to track the desired signals (ω^*, ψ^*).

The structure of system (2.9) in the rotating frame is very suitable for multivariable feedback control design as the field-oriented control strategy shows. The flux modulus dynamics are linear and can be independently controlled by i_{sd} while, when the flux modulus ψ_{rd} coincides with its reference ψ^*, the rotor speed dynamics

$$\frac{\mathrm{d}\omega}{\mathrm{d}t} = \mu\psi^* i_{sq} - \frac{T_L}{J} \tag{2.11}$$

are also linear with respect to i_{sq} and can be independently controlled by i_{sq}. Since the unforced direct flux ψ_{rd} dynamics

$$\frac{\mathrm{d}\psi_{rd}}{\mathrm{d}t} = -\alpha\psi_{rd} \tag{2.12}$$

are asymptotically stable ($\alpha > 0$) when $i_{sd} = 0$, the control input i_{sd} can be designed as the following feedforward signal (recall (1.67))

$$i_{sd} = \frac{\psi^*}{M} + \frac{\dot{\psi}^*}{\alpha M} \tag{2.13}$$

which, substituted in (2.9), gives (recall that $\tilde{\psi}_{rd} = \psi_{rd} - \psi^*$)

$$\frac{\mathrm{d}\tilde{\psi}_{rd}}{\mathrm{d}t} = -\alpha\tilde{\psi}_{rd}\,. \tag{2.14}$$

On the other hand, from the first equation in (2.9), the speed error dynamics are (recall that $\tilde{\omega} = \omega - \omega^*$)

$$\begin{aligned}\frac{\mathrm{d}\tilde{\omega}}{\mathrm{d}t} &= \mu\,\psi_{rd} i_{sq} - \frac{T_L}{J} - \dot{\omega}^* \\ &= \mu\,\psi^* i_{sq} - \frac{T_L}{J} + \mu\,\tilde{\psi}_{rd} i_{sq} - \dot{\omega}^* \,. \end{aligned} \tag{2.15}$$

Define the control for i_{sq} as (k_ω is a positive control parameter)

$$i_{sq} = \frac{1}{\mu\,\psi^*}\left[-k_\omega \tilde{\omega} + \dot{\omega}^* + \frac{T_L}{J}\right] \tag{2.16}$$

and substitute it into the first equation in (2.9) or, equivalently, in (2.15) so that

$$\frac{\mathrm{d}\tilde{\omega}}{\mathrm{d}t} = -k_\omega \tilde{\omega} + \mu\,\tilde{\psi}_{rd} i_{sq} \tag{2.17}$$

in which $\tilde{\psi}_{rd}(t)$, according to (2.14), is an exponentially decaying signal for any $\psi_{rd}(0)$. According to (2.16), (2.17) may be rewritten as

$$\frac{\mathrm{d}\tilde{\omega}}{\mathrm{d}t} = -k_\omega\left[1 + \frac{\tilde{\psi}_{rd}}{\psi^*}\right]\tilde{\omega} + \frac{\tilde{\psi}_{rd}}{\psi^*}\left(\dot{\omega}^* + \frac{T_L}{J}\right) \,. \tag{2.18}$$

On the basis of (2.14) and (2.18), we conclude that $\tilde{\omega}(t)$ is bounded in the time interval $[0, t_*]$, with t_* any positive real. On the other hand, according to (2.14), for any initial condition $\psi_{rd}(0)$ and any positive real $\eta < 1$ there exists $\tilde{t}_* \geq 0$ such that, for all $t \geq \tilde{t}_*$,

$$\left|\frac{\tilde{\psi}_{rd}(t)}{\psi^*(t)}\right| \leq 1 - \eta \,.$$

Therefore, according to (2.18), $\tilde{\omega}(t)$ is an exponentially decaying signal for any initial condition $\omega(0)$. Note that in order to avoid the singularities in the controller at $\psi_{rd} = \sqrt{\psi_{ra}^2 + \psi_{rb}^2} = 0$ which appear in (2.10), according to (2.14) $\psi_{rd}(0)$ must be greater than zero so that $\psi_{rd}(t) > 0$ for all $t \geq 0$.

In conclusion: the *direct field-oriented control* (see Figure 2.12) is defined as

$$\begin{bmatrix} i_{sa} \\ i_{sb} \end{bmatrix} = \begin{bmatrix} \cos\rho & -\sin\rho \\ \sin\rho & \cos\rho \end{bmatrix} \begin{bmatrix} i_{sd} \\ i_{sq} \end{bmatrix}$$

$$i_{sd} = \frac{\psi^*}{M} + \frac{\dot{\psi}^*}{\alpha M}$$

$$i_{sq} = \frac{1}{\mu\,\psi^*}\left[-k_\omega\,(\omega - \omega^*) + \dot{\omega}^* + \frac{T_L}{J}\right]$$

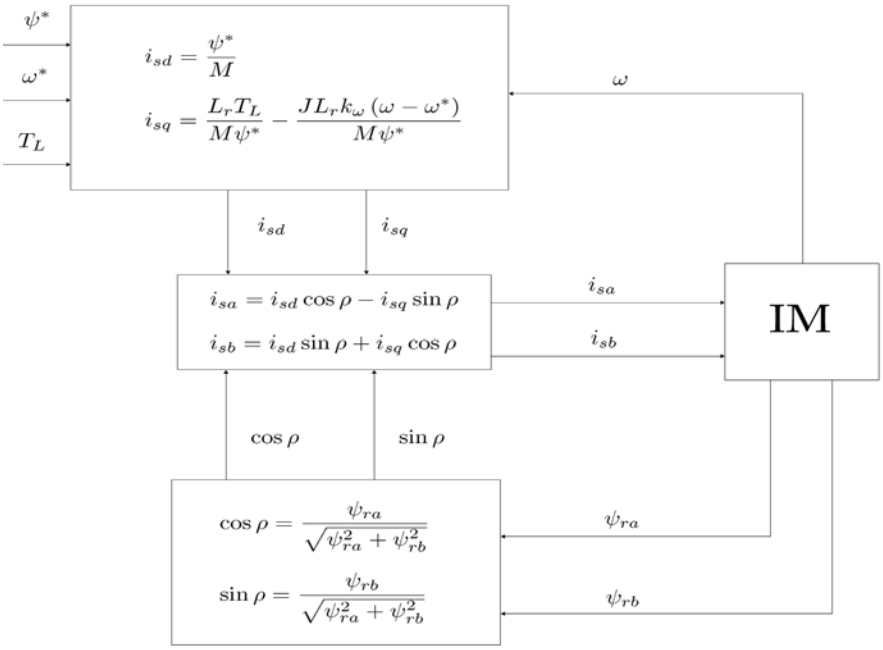

Fig. 2.12 Direct field-oriented control for current-fed motors (constant references ω^*, ψ^*)

$$\cos\rho = \frac{\psi_{ra}}{\sqrt{\psi_{ra}^2 + \psi_{rb}^2}}$$
$$\sin\rho = \frac{\psi_{rb}}{\sqrt{\psi_{ra}^2 + \psi_{rb}^2}}; \tag{2.19}$$

it is a static nonlinear feedback control algorithm which depends on the measurements of the state variables $(\omega, \psi_{ra}, \psi_{rb})$, on the reference signals (ω^*, ψ^*), on the positive control parameter k_ω, on the load torque T_L, and on the machine parameters M, R_r, L_r, J, since $\mu = \frac{M}{JL_r}$ and $\alpha = \frac{R_r}{L_r}$; it guarantees that, for any initial condition of the current-fed reduced order motor model (2.9) such that $\psi_{rd}(0) > 0$, the rotor speed and rotor flux modulus tracking errors decay exponentially to zero.

Remarks

1. The name direct field-oriented control is due to the fact that the stator current vector (i_{sa}, i_{sb}) rotates at the same speed $\dot{\rho}$ at which the rotor flux vector (ψ_{ra}, ψ_{rb}) rotates, *i.e.* it follows the orientation of the flux vector. The quadrature axis component i_{sq} of the stator current vector is responsible, according to (2.16), for the rotor speed tracking and depends on the load torque T_L, while the direct axis component i_{sd} of the stator current vector is responsible, according to (2.13), for the tracking of the rotor flux modulus.
2. The direct field-oriented control (2.19) is a static state feedback control which generates bounded currents (i_{sa}, i_{sb}) for every state value $(\omega, \psi_{rd}, \rho)$; it is not well defined at $\psi_{rd} = 0$ where (2.9) is no longer an equivalent description of the fixed frame model (1.26).
3. The measurements of (ψ_{ra}, ψ_{rb}) are required; the critical parameter R_r, which appears in i_{sd} through $\alpha = \frac{R_r}{L_r}$ when the reference ψ^* is not constant, is required only when the reference ψ^* is time-varying; if ψ^* is constant the direct field-oriented control does not depend on R_r.
4. If the flux modulus and the rotor speed are constant and equal to the desired values (ω^*, ψ^*) then the rotor flux rotates at constant speed $w = (\omega^* + \omega_s)$, with $\omega_s = \frac{\alpha M T_L}{\mu \psi^{*2}}$, and the induction motor is driven by the sinusoidal currents obtained from (2.19):

$$\begin{bmatrix} i_{sa} \\ i_{sb} \end{bmatrix} = \begin{bmatrix} \cos(\rho(0) + wt) & -\sin(\rho(0) + wt) \\ \sin(\rho(0) + wt) & \cos(\rho(0) + wt) \end{bmatrix} \begin{bmatrix} \frac{\psi^*}{M} \\ \frac{T_L}{J\mu\psi^*} \end{bmatrix}.$$

5. The direct field-oriented control (2.19) achieves asymptotic input–output feedback linearization: according to (2.14), the closed-loop dynamics for $(\psi_{rd} - \psi^*)$ are linear with a time constant equal to $\alpha^{-1} = L_r R_r^{-1}$ depending on the machine parameters; according to (2.17), once ψ_{rd} tends to its reference ψ^*, the closed-loop dynamics for $\tilde{\omega}$ tend to be linear with arbitrary time constant k_ω^{-1}. During the transient, the nonlinear term $J\mu\psi_{rd} i_{sq}$, which represents the electromagnetic torque T_e in the first equation in (2.9), makes the first two equations in (2.9) still nonlinear and coupled: for this reason the speed transients may be unsatisfactory.
6. The direct field-oriented control (2.19) can be simply modified by replacing ψ_{rd} with its reference ψ^* in the dynamic equation which generates the angle of rotation of the (d, q) reference frame, so that the indirect field-oriented control which will be discussed in the next section ($\varepsilon_0(0)$ is an arbitrary initial condition)

$$\begin{bmatrix} i_{sa} \\ i_{sb} \end{bmatrix} = \begin{bmatrix} \cos\varepsilon_0 & -\sin\varepsilon_0 \\ \sin\varepsilon_0 & \cos\varepsilon_0 \end{bmatrix} \begin{bmatrix} i_{sd} \\ i_{sq} \end{bmatrix}$$

$$\frac{\mathrm{d}\varepsilon_0}{\mathrm{d}t} = \omega_0 = \omega + \frac{\alpha M i_{sq}}{\psi^*}$$

$$i_{sd} = \frac{\psi^*}{M} + \frac{\dot{\psi}^*}{\alpha M}$$

$$i_{sq} = \frac{1}{\mu\psi^*}\left[-k_\omega(\omega-\omega^*)+\dot{\omega}^*+\frac{T_L}{J}\right] \tag{2.20}$$

is obtained. Note that (2.20) is always well defined even at $\psi_{rd}=0$ where (2.19) is, on the contrary, not well defined. Furthermore, (2.20) does not require the measurement of rotor fluxes (ψ_{ra},ψ_{rb}) but only the measurement of ω while ε_0 no longer coincides with the rotor flux angle ρ.

7. The direct field-oriented control (2.19) can be modified to obtain input–output feedback linearization (and not only asymptotic input–output feedback linearization) by using ψ_{rd} in place of ψ^* in the i_{sq} espression and by adding a feedback term in the i_{sd} espression in (2.19) as follows:

$$\begin{aligned}
\begin{bmatrix} i_{sa} \\ i_{sb} \end{bmatrix} &= \begin{bmatrix} \cos\rho & -\sin\rho \\ \sin\rho & \cos\rho \end{bmatrix}\begin{bmatrix} i_{sd} \\ i_{sq} \end{bmatrix} \\
i_{sd} &= \frac{\psi^*}{M}+\frac{\dot{\psi}^*}{\alpha M}-\frac{k_\psi(\psi_{rd}-\psi^*)}{\alpha M} \\
i_{sq} &= \frac{1}{\mu\psi_{rd}}\left[-k_\omega(\omega-\omega^*)+\dot{\omega}^*+\frac{T_L}{J}\right] \\
\psi_{rd} &= \psi_{ra}\cos\rho+\psi_{rb}\sin\rho \\
\cos\rho &= \frac{\psi_{ra}}{\sqrt{\psi_{ra}^2+\psi_{rb}^2}} \\
\sin\rho &= \frac{\psi_{rb}}{\sqrt{\psi_{ra}^2+\psi_{rb}^2}};
\end{aligned} \tag{2.21}$$

substituting (2.21) in (2.9) we have for the rotor speed and flux modulus tracking errors

$$\begin{aligned}
\frac{\mathrm{d}\tilde{\omega}}{\mathrm{d}t} &= -k_\omega\tilde{\omega} \\
\frac{\mathrm{d}\tilde{\psi}_{rd}}{\mathrm{d}t} &= -\left(\alpha+k_\psi\right)\tilde{\psi}_{rd}
\end{aligned} \tag{2.22}$$

which clarifies that the dynamics for the speed and flux modulus tracking errors are decoupled and linear with arbitrary time constants k_ω^{-1} and $\left(\alpha+k_\psi\right)^{-1}$. Note, however, that exact input–output decoupling and linearization have been achieved by the controller (2.21) at the expense of a singularity at $\psi_{rd}=0$ which, in contrast to the indirect field-oriented control (2.20), may imply very large currents (i_{sa},i_{sb}) when ψ_{rd} is close to zero.

It is instructive to compare the structures of the following four control algorithms: the feedforward control (1.74), the indirect field-oriented control (2.20), the direct field-oriented control (2.19) and the input–output feedback linearizing control (2.21). They are listed in terms of increasing complexity. In fact, the feedforward control (1.74) requires no state variable measurements but precise initialization for $\rho^*(0)$. The indirect field-oriented control (2.20) requires only rotor speed measure-

ments which are used to introduce the feedback term $-k_\omega(\omega - \omega^*)$ in the expression of i_{sq} and to replace ω^* by ω in the dynamic equation which produces the rotation angle ε_0 and can be arbitrarily initialized: the first action is the classical feedback proportional to the speed tracking error, while the second action is unconventional and is aimed to achieve the field orientation without flux measurements, as we shall see in the next section. Both the direct field-oriented control and the input–output feedback linearizing control generate the rotation matrix on the basis of rotor flux measurements (ψ_{ra}, ψ_{rb}) without computing the angles ρ^* or ε_0 by integration: they differ since the input–output linearizing control contains an additional feedback term $-k_\psi(\psi_{rd} - \psi^*)/(\alpha M)$ in the expression of i_{sd} and makes use of ψ_{rd} instead of its reference ψ^* in the expression of i_{sq}.

Illustrative Simulations

We tested the direct field-oriented control by simulations for the current-fed three-phase single pole pair 0.6-kW induction motor whose parameters have been reported in Chapter 1: stator currents dynamics have been neglected so that the stator currents (i_{sa}, i_{sb}) constitute the motor control inputs. The rotor speed initial condition has been set equal to zero while the rotor fluxes initial conditions have been set equal to $\psi_{ra}(0) = \psi_{rb}(0) = 0.1\,\text{Wb}$. The control algorithm has been tested using the control parameter (the value is in SI units) $k_\omega = 12$, which directly affects the speed tracking error dynamics. The references for the speed and flux modulus along with the applied load torque are reported in Figures 2.13–2.15. The rotor flux modulus reference signal starts from 0.001 Wb at $t = 0\,\text{s}$ and grows up to the constant value 1.16 Wb. The speed reference is zero until $t = 0.32\,\text{s}$ and grows up to the constant value 100 rad/s; at $t = 1.5\,\text{s}$ the speed is required to go up to the value 200 rad/s, while the reference for the flux modulus is reduced to 0.5 Wb. A 5.8-Nm load torque is first applied to the motor and then is reduced to 1.8 Nm. Figures 2.14 and 2.15 show the time histories of rotor speed and flux modulus along with the corresponding tracking errors: the rotor speed and flux modulus track their references tightly. As illustrated by Figure 2.16, the motor trajectories in the state space tend to two attractive limit cycles corresponding to the two constant operating conditions imposed by the reference signals. Finally, the stator currents profiles, which are within the physical saturation limits, are reported in Figure 2.17. It is very interesting to compare Figures 2.2–2.5 which illustrate the feedforward control performance with Figures 2.13–2.17 which illustrate the performance of the feedback direct field-oriented control for the same parameters and similar reference signals. The rotor speed tracking errors (see Figures 2.3 and 2.14) are two orders of magnitude smaller in the feedback case (maximum error of 5 rad/s and 0.09 rad/s, respectively). Moreover, the feedback control also achieves very precise tracking when the load torque reduces its value to 1.8 Nm. Similar improvements are obtained in rotor flux tracking (compare Figures 2.4 and 2.15).

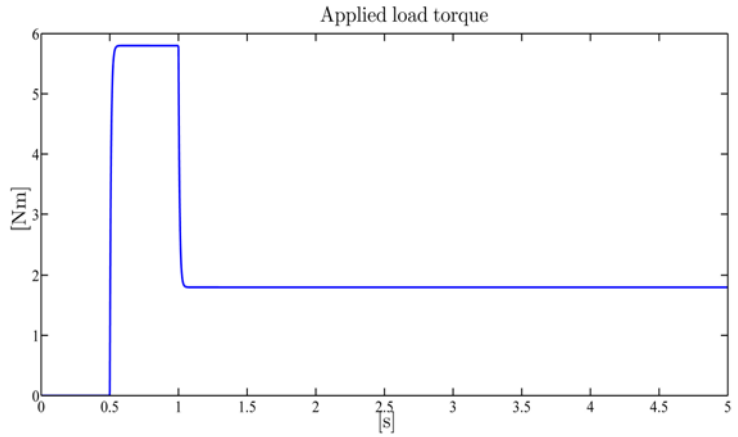

Fig. 2.13 Direct field-oriented control: applied load torque T_L

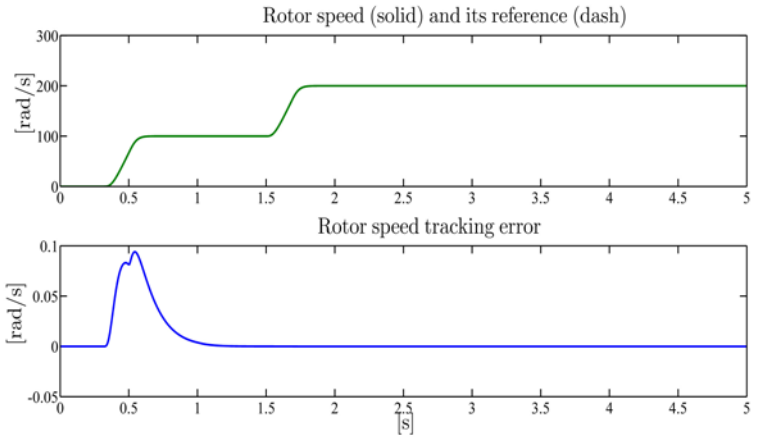

Fig. 2.14 Direct field-oriented control: rotor speed ω and its reference ω^*; rotor speed tracking error

So far we have designed the direct field-oriented control (2.19) and its variants (2.20) and (2.21) on the basis of the reduced order model (2.9) in which the stator current dynamics have been neglected, which is clearly an approximation. Reconsider now the full order model (1.39) expressed in the state coordinates (1.41) and in the control coordinates (u_{sd}, u_{sq}) which are related to the original control inputs (u_{sa}, u_{sb}) by

$$\begin{bmatrix} u_{sa} \\ u_{sb} \end{bmatrix} = \begin{bmatrix} \cos\rho & -\sin\rho \\ \sin\rho & \cos\rho \end{bmatrix} \begin{bmatrix} u_{sd} \\ u_{sq} \end{bmatrix} . \tag{2.23}$$

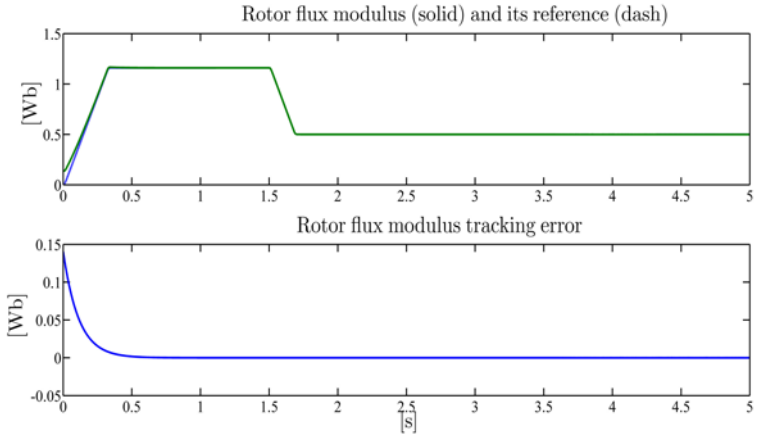

Fig. 2.15 Direct field-oriented control: rotor flux modulus $\sqrt{\psi_{ra}^2 + \psi_{rb}^2}$ and its reference ψ^*; rotor flux modulus tracking error

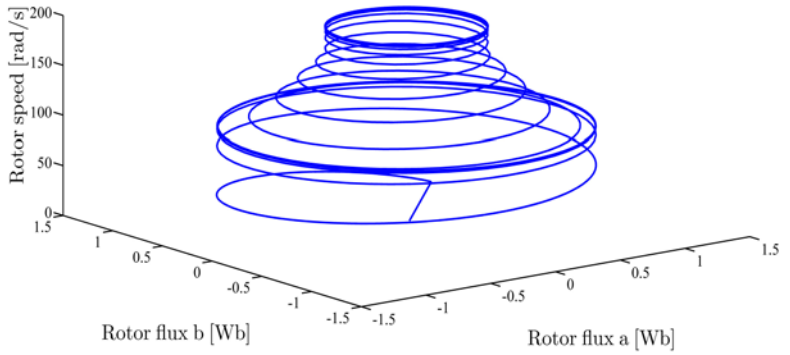

Fig. 2.16 Direct field-oriented control: $(\psi_{ra}, \psi_{rb}, \omega)$-trajectories

Let us now design (u_{sd}, u_{sq}) as state feedback controls so that the desired references (ω^*, ψ^*) are asymptotically tracked. From the last two equations in (1.39) define the state feedback control

$$\begin{aligned} u_{sd} &= \sigma\left[-\omega i_{sq} - \frac{\alpha M i_{sq}^2}{\psi_{rd}} - \beta\alpha\psi_{rd} + v_d\right] \\ u_{sq} &= \sigma\left[\omega i_{sd} + \frac{\alpha M i_{sq} i_{sd}}{\psi_{rd}} + \beta\omega\psi_{rd} + v_q\right] \end{aligned} \tag{2.24}$$

in which (v_d, v_q) are new control inputs yet to be designed. Note that the state feedback control (2.23), (2.24) introduces a singularity at $\psi_{rd} = 0$ so that very large input

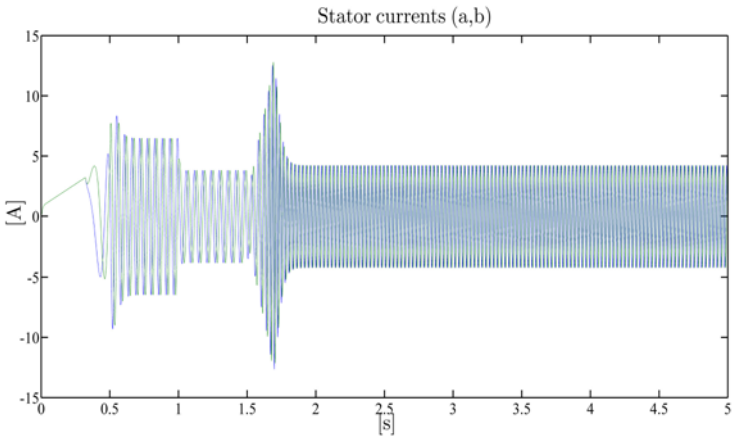

Fig. 2.17 Direct field-oriented control: stator current vector (a,b)-components (i_{sa}, i_{sb})

voltages are to be expected when the rotor flux modulus is close to zero. Substituting (2.24) in (1.39) we obtain the closed-loop system

$$\begin{aligned}
\frac{\mathrm{d}\omega}{\mathrm{d}t} &= \mu \psi_{rd} i_{sq} - \frac{T_L}{J} \\
\frac{\mathrm{d}i_{sq}}{\mathrm{d}t} &= -\gamma i_{sq} + v_q \\
\frac{\mathrm{d}\psi_{rd}}{\mathrm{d}t} &= -\alpha \psi_{rd} + \alpha M i_{sd} \\
\frac{\mathrm{d}i_{sd}}{\mathrm{d}t} &= -\gamma i_{sd} + v_d \\
\frac{\mathrm{d}\rho}{\mathrm{d}t} &= \omega + \frac{\alpha M i_{sq}}{\psi_{rd}} \,.
\end{aligned} \tag{2.25}$$

In other words, the system (1.26) is transformed into (2.25) by the state space change of coordinates (1.41) and the state feedback control (2.23), (2.24) provided that $\psi_{rd} \neq 0$, since in $\psi_{rd} = 0$ the field-oriented model (1.39) is no longer an equivalent description of the fixed frame model (1.26). The closed-loop system (2.25) has a much simpler structure than system (1.26): the flux amplitude dynamics are linear

$$\begin{aligned}
\frac{\mathrm{d}\psi_{rd}}{\mathrm{d}t} &= -\alpha \psi_{rd} + \alpha M i_{sd} \\
\frac{\mathrm{d}i_{sd}}{\mathrm{d}t} &= -\gamma i_{sd} + v_d
\end{aligned} \tag{2.26}$$

and can be independently controlled by v_d for instance via a proportional-integral (PI) controller (k_{dp} and k_{di} are positive control parameters)

$$v_d(t) = -k_{dp}(\psi_{rd}(t) - \psi^*(t)) - k_{di}\int_0^t (\psi_{rd}(\tau) - \psi^*(\tau))\mathrm{d}\tau\,. \tag{2.27}$$

Once the flux amplitude ψ_{rd} tracks its reference ψ^*, the rotor speed dynamics are also linear

$$\begin{aligned}\frac{\mathrm{d}\omega}{\mathrm{d}t} &= \mu\psi^* i_{sq} - \frac{T_L}{J}\\ \frac{\mathrm{d}i_{sq}}{\mathrm{d}t} &= -\gamma i_{sq} + v_q\end{aligned} \tag{2.28}$$

and can be independently controlled by v_q for instance via two nested loops of PI controllers (k_{qp} and k_{qi} are positive control parameters)

$$v_q(t) = -k_{qp}(T_e(t) - T_e^*(t)) - k_{qi}\int_0^t (T_e(\tau) - T_e^*(\tau))\mathrm{d}\tau \tag{2.29}$$

with (k_{Tp} and k_{Ti} are positive control parameters)

$$\begin{aligned}T_e(t) &= \mu\psi_{rd}(t) i_{sq}(t)\\ T_e^*(t) &= -k_{Tp}(\omega(t) - \omega^*(t)) - k_{Ti}\int_0^t (\omega(\tau) - \omega^*(\tau))\mathrm{d}\tau\,.\end{aligned} \tag{2.30}$$

We can then say that the state feedback control (2.23), (2.24) achieves asymptotic input–output linearization and decoupling since the first four equations in (2.25) tend to the linear ones (2.26) and (2.28) as ψ_{rd} tends to its reference ψ^*; moreover the outputs ω and ψ_{rd} can be independently controlled by the new inputs v_d and v_q, respectively. Note, however, that during flux transients the nonlinear term $J\mu\psi_{rd} i_{sq}$, which represents the electromagnetic torque T_e in the first equation in (2.25), makes the first four equations in (2.25) still nonlinear and coupled; consequently, the speed transients are difficult to evaluate and may result unacceptable when the flux undergoes a transient to improve efficiency.

2.3 Indirect Field-oriented Control

The indirect field-oriented control (2.20) is a modification of the direct field-oriented control (2.19) which uses, instead of the rotor flux angle ρ, an arbitrary rotating angle ε_0 which is generated replacing ψ_{rd} by its reference ψ^* in the differential equation defining the ε_0 dynamics, *i.e.*

$$\begin{aligned}\begin{bmatrix} i_{sa}\\ i_{sb}\end{bmatrix} &= \begin{bmatrix}\cos\varepsilon_0 & -\sin\varepsilon_0\\ \sin\varepsilon_0 & \cos\varepsilon_0\end{bmatrix}\begin{bmatrix}\frac{\psi^*}{M} + \frac{\dot\psi^*}{\alpha M}\\ \frac{1}{\mu\psi^*}\left[-k_\omega(\omega - \omega^*) + \dot\omega^* + \frac{T_L}{J}\right]\end{bmatrix}\\ \frac{\mathrm{d}\varepsilon_0}{\mathrm{d}t} &= \omega_0 = \omega + \frac{\alpha M i_{sq}}{\psi^*}\end{aligned}$$

$$= \omega + \frac{\alpha M}{\mu \psi^{*2}} \left[-k_\omega (\omega - \omega^*) + \dot{\omega}^* + \frac{T_L}{J} \right] \tag{2.31}$$

with arbitrary $\varepsilon_0(0)$.

The indirect field-oriented control (2.31) may also be designed directly on the basis of the first three equations in the rotating frame model (1.31):

$$\begin{aligned} \frac{\mathrm{d}\omega}{\mathrm{d}t} &= \mu \left(\psi_{rd} i_{sq} - \psi_{rq} i_{sd} \right) - \frac{T_L}{J} \\ \frac{\mathrm{d}\psi_{rd}}{\mathrm{d}t} &= -\alpha \psi_{rd} + (\omega_0 - \omega) \psi_{rq} + \alpha M i_{sd} \\ \frac{\mathrm{d}\psi_{rq}}{\mathrm{d}t} &= -\alpha \psi_{rq} - (\omega_0 - \omega) \psi_{rd} + \alpha M i_{sq} \,. \end{aligned} \tag{2.32}$$

Let $(\omega^*(t), \psi^*(t), 0)$ be the reference signals for $(\omega(t), \psi_{rd}(t), \psi_{rq}(t))$: (2.32) can be rewritten as ($\tilde{\omega} = \omega - \omega^*$, $\tilde{\psi}_{rd} = \psi_{rd} - \psi^*$, $\tilde{\psi}_{rq} = \psi_{rq}$)

$$\begin{aligned} \frac{\mathrm{d}\tilde{\omega}}{\mathrm{d}t} &= \mu \left(\tilde{\psi}_{rd} i_{sq} - \tilde{\psi}_{rq} i_{sd} \right) + \mu \psi^* i_{sq} - \dot{\omega}^* - \frac{T_L}{J} \\ \frac{\mathrm{d}\tilde{\psi}_{rd}}{\mathrm{d}t} &= -\alpha \tilde{\psi}_{rd} + (\omega_0 - \omega) \tilde{\psi}_{rq} - \alpha \psi^* - \dot{\psi}^* + \alpha M i_{sd} \\ \frac{\mathrm{d}\tilde{\psi}_{rq}}{\mathrm{d}t} &= -\alpha \tilde{\psi}_{rq} - (\omega_0 - \omega) \tilde{\psi}_{rd} - (\omega_0 - \omega) \psi^* + \alpha M i_{sq} \,. \end{aligned} \tag{2.33}$$

Our goal is to design a dynamic feedback control

$$\begin{aligned} \begin{bmatrix} i_{sa} \\ i_{sb} \end{bmatrix} &= \begin{bmatrix} \cos \varepsilon_0 & -\sin \varepsilon_0 \\ \sin \varepsilon_0 & \cos \varepsilon_0 \end{bmatrix} \begin{bmatrix} i_{sd} \\ i_{sq} \end{bmatrix} \\ \dot{\varepsilon}_0 &= \omega_0 \end{aligned} \tag{2.34}$$

so that the tracking errors $(\tilde{\omega}, \tilde{\psi}_{rd}, \tilde{\psi}_{rq})$ tend exponentially to zero from any initial condition. Note that by introducing a dynamic feedback we add an extra degree of freedom in the design since we can now freely choose in (2.33) three independent feedback terms (i_{sd}, i_{sq}, ω_0) in place of (i_{sd}, i_{sq}) which are at our disposal if a static feedback is designed. We design $(i_{sd}, i_{sq}, \omega_0)$ as feedback terms so that

$$\begin{aligned} \mu \psi^* i_{sq} - \dot{\omega}^* - \frac{T_L}{J} &= -k_\omega (\omega - \omega^*) \\ -\alpha \psi^* - \dot{\psi}^* + \alpha M i_{sd} &= 0 \\ -(\omega_0 - \omega) \psi^* + \alpha M i_{sq} &= 0 \end{aligned} \tag{2.35}$$

since, substituting (2.35) in (2.33), we obtain

$$\begin{aligned} \frac{\mathrm{d}\tilde{\omega}}{\mathrm{d}t} &= -k_\omega \tilde{\omega} + \mu \left(\tilde{\psi}_{rd} i_{sq} - \tilde{\psi}_{rq} i_{sd} \right) \\ \frac{\mathrm{d}\tilde{\psi}_{rd}}{\mathrm{d}t} &= -\alpha \tilde{\psi}_{rd} + (\omega_0 - \omega) \tilde{\psi}_{rq} \end{aligned}$$

$$\frac{\mathrm{d}\tilde{\psi}_{rq}}{\mathrm{d}t} = -\alpha\tilde{\psi}_{rq} - (\omega_0 - \omega)\,\tilde{\psi}_{rd}\ .$$

Solving (2.35) for $(i_{sd}, i_{sq}, \omega_0)$, we explicitly obtain the feedback terms to be used in (2.34)

$$\begin{aligned} i_{sd} &= \frac{\psi^*}{M} + \frac{\dot{\psi}^*}{\alpha M} \\ i_{sq} &= \frac{1}{\mu\psi^*}\left[-k_\omega(\omega - \omega^*) + \dot{\omega}^* + \frac{T_L}{J}\right] \\ \omega_0 &= \omega + \frac{\alpha M}{\mu\psi^{*2}}\left[-k_\omega(\omega - \omega^*) + \dot{\omega}^* + \frac{T_L}{J}\right] \end{aligned}$$

which, substituted in (2.34), gives exactly the indirect field-oriented control (2.31) in (a,b) coordinates.

The advantages of (2.31) with respect to (2.19) are:

1. while (2.19) is not well defined at $\psi_{ra}^2 + \psi_{rb}^2 = 0$, the indirect field-oriented control (2.31) is always well defined since $\psi^*(t) \geq c_\psi > 0$ for all $t \geq 0$;
2. the control (2.31) requires only the measurement of rotor speed ω while (2.19) also requires the measurement of (ψ_{ra}, ψ_{rb}) to compute $\cos\rho$ and $\sin\rho$;
3. the control (2.31) is a dynamic first order output feedback controller for the current-fed model (2.9) from rotor speed measurements while (2.19) is a static state feedback controller for the same reduced order model (2.9) from rotor speed and flux measurements.

We now substitute (2.31) in the first three equations of the fixed frame model (1.26): to evaluate the closed-loop stability it is more convenient to use directly the rotating frame model (1.31) in the (d,q) reference frame rotating at the speed

$$\frac{\mathrm{d}\varepsilon_0}{\mathrm{d}t} = \omega_0 \tag{2.36}$$

defined in (2.31). Substituting

$$\begin{aligned} i_{sd} &= \frac{\psi^*}{M} + \frac{\dot{\psi}^*}{\alpha M} \\ i_{sq} &= \frac{1}{\mu\psi^*}\left[-k_\omega\,(\omega - \omega^*) + \dot{\omega}^* + \frac{T_L}{J}\right] \end{aligned} \tag{2.37}$$

in the first three equations of model (1.31) we obtain for the second equation in (1.31)

$$\frac{\mathrm{d}\tilde{\psi}_{rd}}{\mathrm{d}t} = -\alpha\tilde{\psi}_{rd} + (\omega_0 - \omega)\,\tilde{\psi}_{rq} \tag{2.38}$$

while for the third equation in (1.31), since

$$(\omega_0 - \omega)\,\psi^* = \alpha M i_{sq}\ , \tag{2.39}$$

we have

$$\frac{\mathrm{d}\tilde{\psi}_{rq}}{\mathrm{d}t} = -\alpha\tilde{\psi}_{rq} - (\omega_0 - \omega)\,\tilde{\psi}_{rd}\ . \tag{2.40}$$

The first equation in (1.31) can be rewritten as

$$\frac{\mathrm{d}\omega}{\mathrm{d}t} = \mu\,\psi^* i_{sq} - \frac{T_L}{J} + \mu\,(\tilde{\psi}_{rd} i_{sq} - \psi_{rq} i_{sd}) \tag{2.41}$$

so that, substituting (2.37) in (2.41), we obtain

$$\frac{\mathrm{d}\tilde{\omega}}{\mathrm{d}t} = -k_\omega\tilde{\omega} + \mu\,(\tilde{\psi}_{rd} i_{sq} - \tilde{\psi}_{rq} i_{sd}) \tag{2.42}$$

which along with (2.38) and (2.40), namely

$$\begin{bmatrix} \dot{\tilde{\psi}}_{rd} \\ \dot{\tilde{\psi}}_{rq} \end{bmatrix} = \begin{bmatrix} -\alpha & (\omega_0 - \omega) \\ -(\omega_0 - \omega) & -\alpha \end{bmatrix} \begin{bmatrix} \tilde{\psi}_{rd} \\ \tilde{\psi}_{rq} \end{bmatrix}\ , \tag{2.43}$$

constitute the closed-loop linear, time-varying tracking dynamics in the (d,q) frame defined by (2.36). Consider the positive definite function

$$V = \frac{1}{2}\tilde{\psi}_{rd}^2 + \frac{1}{2}\tilde{\psi}_{rq}^2 \tag{2.44}$$

whose time derivative along the trajectories of the closed-loop system (2.43) is

$$\dot{V} = -\alpha\tilde{\psi}_{rd}^2 - \alpha\tilde{\psi}_{rq}^2 = -2\alpha V\ . \tag{2.45}$$

Since, according to (2.45),

$$V(t) = \mathrm{e}^{-2\alpha t} V(0) \tag{2.46}$$

we can establish that $\tilde{\psi}_{rd}(t)$ and $\tilde{\psi}_{rq}(t)$ exponentially tend to zero for any initial condition $(\psi_{rd}(0), \psi_{rq}(0))$. In particular, since $\psi_{rq}(t)$ tends to zero, $(\varepsilon_0(t) - \rho(t))$ tends to zero, *i.e.* the (d,q) frame rotating at speed $\omega_0(t)$ given by (2.36) will tend to have its d-axis coincident with the rotating rotor flux vector: field orientation is asymptotically achieved. According to (2.37), (2.42) may be rewritten as

$$\begin{aligned} \frac{\mathrm{d}\tilde{\omega}}{\mathrm{d}t} = &-k_\omega\left[1 + \frac{\tilde{\psi}_{rd}}{\psi^*}\right]\tilde{\omega} \\ &+ \frac{\tilde{\psi}_{rd}}{\psi^*}\left(\dot{\omega}^* + \frac{T_L}{J}\right) - \mu\,\tilde{\psi}_{rq}\left[\frac{\psi^*}{M} + \frac{\dot{\psi}^*}{\alpha M}\right]\ . \end{aligned} \tag{2.47}$$

According to (2.46) and (2.47), $\tilde{\omega}(t)$ is bounded on $[0, t_*]$ with t_* any positive real. On the other hand, according to (2.46), for any initial condition $(\psi_{rd}(0), \psi_{rq}(0))$ and any positive real $\eta < 1$ there exists $\tilde{t}_* \geq 0$ such that for all $t \geq \tilde{t}_*$

$$\left| \frac{\tilde{\psi}_{rd}(t)}{\psi^*(t)} \right| \leq 1 - \eta \ .$$

Therefore, according to (2.47), $\tilde{\omega}(t)$ is an exponentially decaying signal for any initial condition $\omega(0)$.

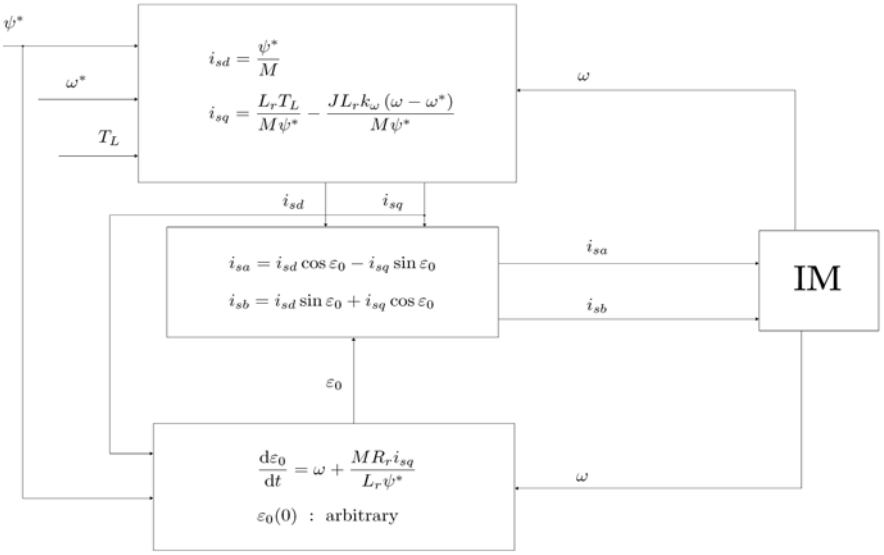

Fig. 2.18 Indirect field-oriented control for current-fed motors (constant references ω^*, ψ^*)

In conclusion: the *indirect field-oriented control* (see Figure 2.18) is defined as

$$\begin{aligned}
\begin{bmatrix} i_{sa} \\ i_{sb} \end{bmatrix} &= \begin{bmatrix} \cos\varepsilon_0 & -\sin\varepsilon_0 \\ \sin\varepsilon_0 & \cos\varepsilon_0 \end{bmatrix} \begin{bmatrix} i_{sd} \\ i_{sq} \end{bmatrix} \\
i_{sd} &= \frac{\psi^*}{M} + \frac{\dot{\psi}^*}{\alpha M} \\
i_{sq} &= \frac{1}{\mu\psi^*} \left[-k_\omega (\omega - \omega^*) + \dot{\omega}^* + \frac{T_L}{J} \right] \\
\frac{d\varepsilon_0}{dt} &= \omega + \frac{\alpha M i_{sq}}{\psi^*} \ ;
\end{aligned} \tag{2.48}$$

it is a first order dynamic control algorithm which depends on the measurements of the rotor speed ω, on the reference signals (ω^*, ψ^*), on the arbitrary initial condition $\varepsilon_0(0)$, on the positive control parameter k_ω, on the load torque

T_L, and on the machine parameters M, R_r, L_r, J, since $\mu = \frac{M}{JL_r}$ and $\alpha = \frac{R_r}{L_r}$; it guarantees that, for any $\varepsilon_0(0)$ and for any initial condition of the current-fed reduced order motor model (2.32), the rotor speed and flux modulus tracking errors decay exponentially to zero.

Remarks

1. The name indirect field-oriented control arises from the fact that it is obtained from the direct field-oriented control by using the angle ε_0 in place of the the rotor flux angle ρ: the rotor flux angle dynamics

$$\frac{\mathrm{d}\rho}{\mathrm{d}t} = \omega + \frac{\alpha M i_{sq}}{\psi_{rd}}$$

with $\rho(0) = \arctan\left(\frac{\psi_{rb}(0)}{\psi_{ra}(0)}\right)$ are replaced by

$$\frac{\mathrm{d}\varepsilon_0}{\mathrm{d}t} = \omega + \frac{\alpha M i_{sq}}{\psi^*}$$

with arbitrary $\varepsilon_0(0)$ in which the reference flux ψ^* simply replaces the unmeasured ψ_{rd}. Note that, even though ε_0 does not coincide with the rotor flux angle ρ, $[\varepsilon_0(t) - \rho(t)]$ exponentially tends to zero for every initial condition $\varepsilon_0(0)$: the remarkable fact is that field orientation is achieved for any $\varepsilon_0(0)$.
2. As in direct field-oriented control, according to (2.37), the quadrature axis component i_{sq} of the stator current vector is responsible for the rotor speed tracking and depends on T_L, while the direct axis component i_{sd} of the stator current vector is responsible for the tracking of the rotor flux modulus.
3. The critical parameter R_r is required to generate the angle ε_0 in (2.48), since $\alpha = R_r/L_r$. This feature makes the indirect field-oriented control more sensitive with respect to α than the direct field-oriented control, as the experiments reported in Section 2.8 confirm. As we shall see in Chapter 3, the online identification of α is related to the estimation of the rotor flux, so that the need for rotor flux estimation, which is seemingly eliminated by the indirect field-oriented control, reappears through the critical parameter α, whose identification is very closely related to the flux estimation.
4. The measurement of ω is always required in (2.48) even when stringent specifications on speed dynamics are not required so that the gain k_ω in i_{sq} is set equal to zero. In fact, ω is still needed to compute the angle ε_0.
5. As in direct field-oriented control, if the flux modulus and the rotor speed are constant and equal to the desired values (ω^*, ψ^*), then the rotor flux rotates at

constant speed $w = (\omega^* + \omega_s)$, with $\omega_s = \frac{\alpha M T_L}{\mu \psi^{*2}}$, and the induction motor is driven by the sinusoidal currents obtained from (2.48):

$$\begin{bmatrix} i_{sa} \\ i_{sb} \end{bmatrix} = \begin{bmatrix} \cos(\varepsilon_0(0) + wt) & -\sin(\varepsilon_0(0) + wt) \\ \sin(\varepsilon_0(0) + wt) & \cos(\varepsilon_0(0) + wt) \end{bmatrix} \begin{bmatrix} \frac{\psi^*}{M} \\ \frac{T_L}{J\mu\psi^*} \end{bmatrix}.$$

6. According to (2.47), once ψ_{rd} tends to its reference ψ^* and ψ_{rq} tends to zero, the closed-loop dynamics for $\tilde{\omega}$ tend to be linear with arbitrary time constant k_ω^{-1}. During the transient, the nonlinear term $J\mu\,(\psi_{rd} i_{sq} - \psi_{rq} i_{sd})$, which represents the electromagnetic torque T_e in the first equation in (1.31), makes the first two equations in (1.31) still nonlinear and coupled: for this reason the speed transients may be unsatisfactory, for instance when the flux modulus is adjusted to improve power efficiency.

Illustrative Simulations

We tested the indirect field-oriented control by simulations for the current-fed, three-phase, single pole pair 0.6-kW induction motor whose parameters have been reported in Chapter 1: stator currents dynamics have been neglected so that the stator currents (i_{sa}, i_{sb}) constitute the motor control inputs. The rotor speed initial condition has been set equal to zero while the rotor fluxes initial conditions have been set equal to $\psi_{ra}(0) = \psi_{rb}(0) = 0.1\,\text{Wb}$. The control algorithm has been tested with the control parameter (the value is in SI units) $k_\omega = 12$, which directly affects the speed tracking error dynamics, and the initial condition $\varepsilon_0(0) = 0$. The references for the speed and flux modulus along with the applied load torque are reported in Figures 2.19–2.21. The rotor flux modulus reference signal starts from 0.001 Wb at $t = 0\,\text{s}$ and grows up to the constant value 1.16 Wb. The speed reference is zero until $t = 0.32\,\text{s}$ and grows up to the constant value 100 rad/s; at $t = 1.5\,\text{s}$ the speed is required to go up to the value 200 rad/s, while the reference for the flux modulus is reduced to 0.5 Wb. A 5.8-Nm load torque is applied to the motor at $t = 0.5\,\text{s}$ and is reduced to 1.8 Nm at $t = 1\,\text{s}$. Figures 2.20 and 2.21 show the time histories of rotor speed and flux modulus along with the corresponding tracking errors: both the rotor speed and the flux modulus track their references tightly. As illustrated by Figure 2.22 the motor trajectories in the state space tend to two attractive limit cycles corresponding to the two constant operating conditions imposed by the reference signals. Finally, the stator currents profiles, which are within physical saturation limits, are reported in Figure 2.23. We now compare the performance of the direct field-oriented control illustrated in Figures 2.13–2.17 with the performance obtained by the indirect field-oriented control illustrated in Figures 2.19–2.23 for the same motor, same initial conditions, same motor parameters, same control parameters ($k_\omega = 12$), and same reference signals. While the stator current inputs can be hardly distinguished (compare Figures 2.17 and 2.23) and the state space trajectories are very similar (compare Figures 2.16 and 2.22), the only difference is in

the transient behavior of the speed errors (compare Figures 2.14 and 2.20), which shows a worse speed transient during the time interval $[0, 1]$ s in which the rotor flux error is different from zero (see Figure 2.21) when the indirect field-oriented control is used.

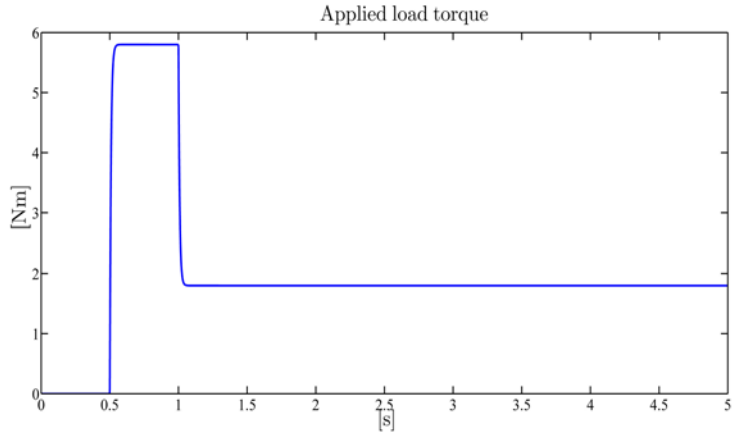

Fig. 2.19 Indirect field-oriented control: applied load torque T_L

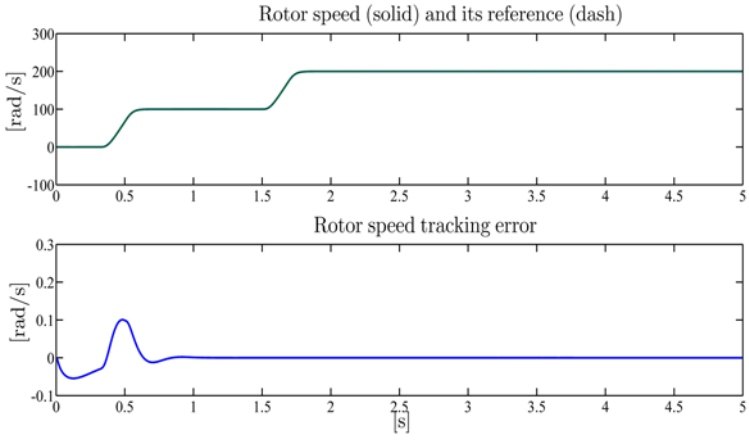

Fig. 2.20 Indirect field-oriented control: rotor speed ω and its reference ω^*; rotor speed tracking error

So far we have designed the indirect field-oriented control (2.48) on the basis of the reduced order model (2.9). If the full order model (1.31), expressed in the

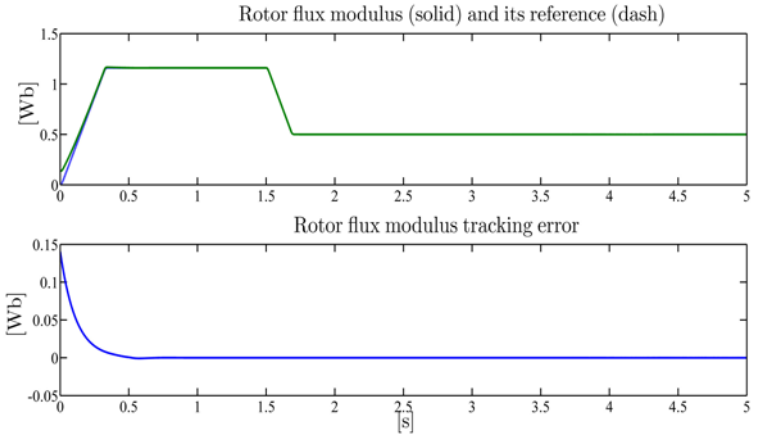

Fig. 2.21 Indirect field-oriented control: rotor flux modulus $\sqrt{\psi_{ra}^2+\psi_{rb}^2}$ and its reference ψ^*; rotor flux modulus tracking error

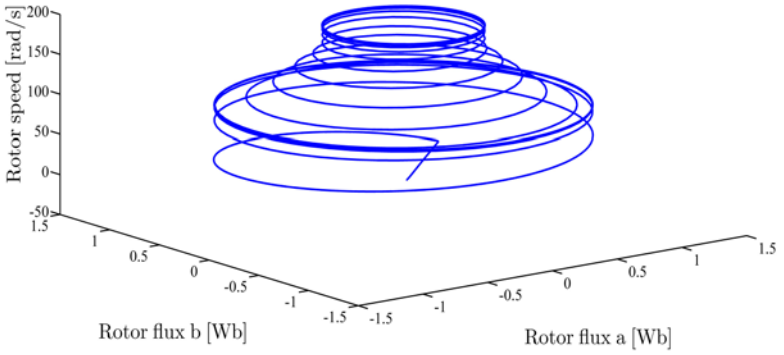

Fig. 2.22 Indirect field-oriented control: $(\psi_{ra}, \psi_{rb}, \omega)$-trajectories

state and control coordinates (1.30), is considered, then (u_{sd}, u_{sq}) are to be designed as state feedback controls so that the reference signals (ω^*, ψ^*) are asymptotically tracked. This can actually be achieved by defining the speed of the rotating (d,q) frame and the reference signals for the stator current vector (d,q) components as

$$\begin{aligned}\frac{\mathrm{d}\varepsilon_0}{\mathrm{d}t} &= \omega_0 = \omega + \frac{\alpha M i_{sq}}{\psi^*}\\ i_{sd}^* &= \frac{\psi^*}{M} + \frac{\dot{\psi}^*}{\alpha M}\\ i_{sq}^* &= \frac{1}{\mu\psi^*}\left[-k_\omega(\omega-\omega^*) + \dot{\omega}^* + \frac{T_L}{J}\right]\end{aligned} \tag{2.49}$$

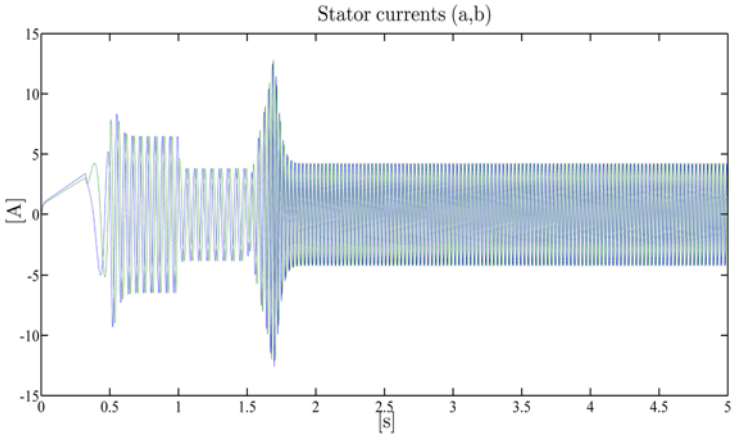

Fig. 2.23 Indirect field-oriented control: stator current vector (a,b)-components (i_{sa}, i_{sb})

and the stator voltages (u_{sd}, u_{sq}) in the (d,q) frame rotating at speed ω_0 as (k_i is a positive control parameter)

$$
\begin{aligned}
u_{sd} &= \sigma\left[\gamma i^*_{sd} - \omega_0 i_{sq} - \beta\alpha\psi_{rd} - \beta\omega\psi_{rq} + \frac{\mathrm{d}i^*_{sd}}{\mathrm{d}t} - k_i\left(i_{sd} - i^*_{sd}\right) - \alpha M\left(\psi_{rd} - \psi^*\right)\right] \\
u_{sq} &= \sigma\left[\gamma i^*_{sq} + \omega_0 i_{sd} - \beta\alpha\psi_{rq} + \beta\omega\psi_{rd} + \frac{\mathrm{d}i^*_{sq}}{\mathrm{d}t} - k_i\left(i_{sq} - i^*_{sq}\right)\right]
\end{aligned}
\tag{2.50}
$$

in which, according to (2.49) and the first equation in (1.31), the time derivatives of i^*_{sd} and i^*_{sq} are given by

$$
\begin{aligned}
\frac{\mathrm{d}i^*_{sd}}{\mathrm{d}t} &= \frac{\dot{\psi}^*}{M} + \frac{\ddot{\psi}^*}{\alpha M} \\
\frac{\mathrm{d}i^*_{sq}}{\mathrm{d}t} &= \frac{1}{\mu\psi^*}\left[-k_\omega\left(\dot{\omega} - \dot{\omega}^*\right) + \ddot{\omega}^*\right] - \frac{\dot{\psi}^*}{\mu\psi^{*2}}\left[-k_\omega\left(\omega - \omega^*\right) + \dot{\omega}^* + \frac{T_L}{J}\right] \\
&= \frac{1}{\mu\psi^*}\left[-k_\omega\left[\mu\left(\psi_{rd} i_{sq} - \psi_{rq} i_{sd}\right) - \frac{T_L}{J} - \dot{\omega}^*\right] + \ddot{\omega}^*\right] \\
&\quad - \frac{\dot{\psi}^*}{\mu\psi^{*2}}\left[-k_\omega\left(\omega - \omega^*\right) + \dot{\omega}^* + \frac{T_L}{J}\right].
\end{aligned}
\tag{2.51}
$$

Exponential rotor speed and flux modulus tracking can be proved for any motor initial condition (see Problem 2.6). However, as in the current-fed case, the rate of convergence depends on α, according to (2.46).

2.4 Input–Output Feedback Linearizing Control

The input–output feedback linearizing control (2.21) for current-fed induction motors has the structure given in Figure 2.24 (compare with Figures 2.1 and 2.12). In this section we design an input–output feedback linearizing control both for the field-oriented model (1.39) and for the fixed frame model (1.26). The direct field-

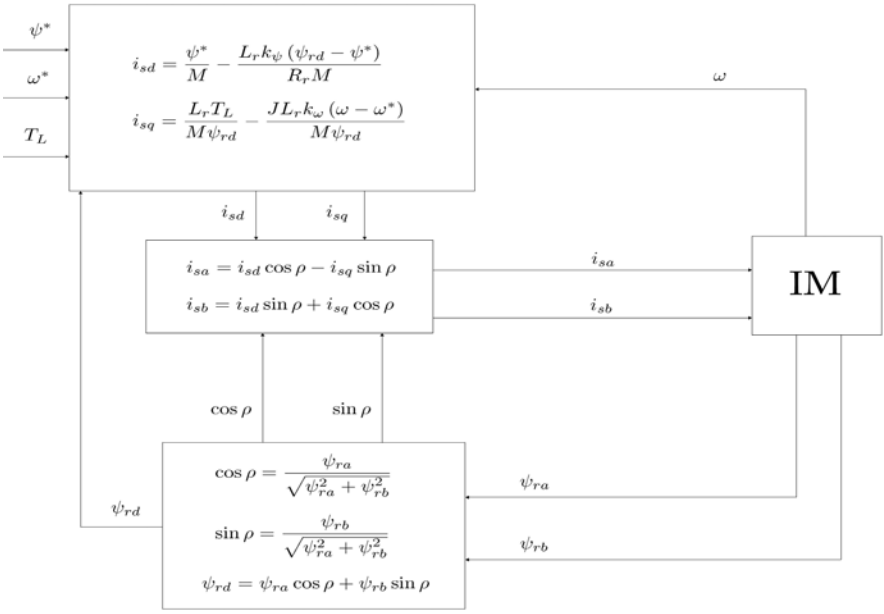

Fig. 2.24 Input–output feedback linearizing control for current-fed motors (constant references ω^*, ψ^*)

oriented control design which led us to the state feedback control (2.23), (2.24) can be improved by designing the additional control input v_q so that the first two equations in (2.25) are made linear by state feedback and input–output feedback linearization and decoupling are achieved: to this end, introduce the rotor angular acceleration

$$a = \mu \psi_{rd} i_{sq} - \frac{T_L}{J} \tag{2.52}$$

in place of i_{sq} as a new state variable so that the first two equations in (2.25) become (recall that T_L is assumed to be constant)

$$\frac{\mathrm{d}\omega}{\mathrm{d}t} = a$$

$$\begin{aligned}\frac{\mathrm{d}a}{\mathrm{d}t} &= \mu\frac{\mathrm{d}\psi_{rd}}{\mathrm{d}t}i_{sq} + \mu\psi_{rd}\frac{\mathrm{d}i_{sq}}{\mathrm{d}t} \\ &= -\mu\alpha\psi_{rd}i_{sq} + \mu\alpha M i_{sd}i_{sq} - \gamma\mu\psi_{rd}i_{sq} + \mu\psi_{rd}v_q \,. \end{aligned} \tag{2.53}$$

Define the additional state feedback term

$$v_q = \alpha i_{sq} + \gamma i_{sq} - \frac{\alpha M i_{sd} i_{sq}}{\psi_{rd}} + \frac{1}{\mu\psi_{rd}}v_q' \tag{2.54}$$

in which v_q' is an additional control input. Substituting (2.54) in (2.53), the closed-loop system (2.25), (2.54) becomes

$$\begin{aligned}\frac{\mathrm{d}\omega}{\mathrm{d}t} &= a \\ \frac{\mathrm{d}a}{\mathrm{d}t} &= v_q' \\ \frac{\mathrm{d}\psi_{rd}}{\mathrm{d}t} &= -\alpha\psi_{rd} + \alpha M i_{sd} \\ \frac{\mathrm{d}i_{sd}}{\mathrm{d}t} &= -\gamma i_{sd} + v_d \\ \frac{\mathrm{d}\rho}{\mathrm{d}t} &= \omega + \frac{\alpha M i_{sq}}{\psi_{rd}} \,. \end{aligned} \tag{2.55}$$

The first four equations in (2.55) are linear and decoupled since the dynamics of ω and ψ_{rd} are independent and can be independently controlled by the control inputs v_q' and v_d, respectively. If we compare the closed-loop dynamics (2.25) with (2.55) we note that while rotor speed ω transients in (2.55) are not influenced by rotor flux ψ_{rd} transients, this is not so in (2.25). We can then conclude that the state feedback control (2.23), (2.24), and (2.54) improves the direct field-oriented control since it achieves input–output feedback linearization and decoupling as shown by the closed-loop dynamics (2.55). To design v_d in (2.26), introduce the time derivative of ψ_{rd}

$$v_{\psi d} = -\alpha\psi_{rd} + \alpha M i_{sd}$$

so that (2.26) is transformed into

$$\begin{aligned}\frac{\mathrm{d}\psi_{rd}}{\mathrm{d}t} &= v_{\psi d} \\ \frac{\mathrm{d}v_{\psi d}}{\mathrm{d}t} &= -\alpha(\alpha M i_{sd} - \alpha\psi_{rd}) + \alpha M(-\gamma i_{sd} + v_d) \,. \end{aligned}$$

Define

$$v_d = \gamma i_{sd} - \frac{\alpha\psi_{rd}}{M} + \alpha i_{sd} + v_d' \tag{2.56}$$

so that we can write

$$\begin{aligned}\frac{\mathrm{d}\omega}{\mathrm{d}t} &= a\\ \frac{\mathrm{d}a}{\mathrm{d}t} &= v'_q\\ \frac{\mathrm{d}\psi_{rd}}{\mathrm{d}t} &= v_{\psi d}\\ \frac{\mathrm{d}v_{\psi d}}{\mathrm{d}t} &= v'_d\,.\end{aligned}$$

In order to track the desired references ω^* and ψ^* for ω and ψ_{rd}, the input signals (v'_d, v'_q) are designed as

$$\begin{aligned}v'_d(t) &= -k_{\psi p}\left(\psi_{rd}(t)-\psi(t)\right)-k_{\psi d}\left(v_{\psi d}(t)-\dot{\psi}^*(t)\right)+\ddot{\psi}^*(t)\\ v'_q(t) &= -k_{\omega p}\left(\omega(t)-\omega^*(t)\right)-k_{\omega d}\left(a(t)-\dot{\omega}^*(t)\right)+\ddot{\omega}^*(t)\end{aligned}\tag{2.57}$$

where $k_{\psi p}$, $k_{\psi d}$, $k_{\omega p}$ and $k_{\omega d}$ are positive constant design parameters to be determined in order to make the decoupled, linear, time-invariant, second order systems $(\tilde{\omega}=\omega-\omega^*,\ \tilde{\psi}_{rd}=\psi_{rd}-\psi^*)$

$$\begin{aligned}\frac{\mathrm{d}^2\tilde{\omega}}{\mathrm{d}t^2} &= -k_{\omega p}\tilde{\omega}-k_{\omega d}\frac{\mathrm{d}\tilde{\omega}}{\mathrm{d}t}\\ \frac{\mathrm{d}^2\tilde{\psi}_{rd}}{\mathrm{d}t^2} &= -k_{\psi p}\tilde{\psi}_{rd}-k_{\psi d}\frac{\mathrm{d}\tilde{\psi}_{rd}}{\mathrm{d}t}\end{aligned}$$

exponentially stable and to shape their dynamics.

Note that the same result can be achieved directly in fixed (a,b) coordinates without introducing any rotating frame at all. It is enough to perform the following state space change of coordinates $z=\varphi(\omega,\psi_{ra},\psi_{rb},i_{sa},i_{sb})$ with $z=[z_1,\ldots,z_5]$ and

$$\begin{aligned}z_1 &= \omega\\ z_2 &= a=\mu\left(\psi_{ra}i_{sb}-\psi_{rb}i_{sa}\right)-\frac{T_L}{J}\\ z_3 &= \psi_{ra}^2+\psi_{rb}^2\\ z_4 &= \frac{\mathrm{d}\left(\psi_{ra}^2+\psi_{rb}^2\right)}{\mathrm{d}t}=-2\alpha\left(\psi_{ra}^2+\psi_{rb}^2\right)+2\alpha M\left(\psi_{ra}i_{sa}+\psi_{rb}i_{sb}\right)\\ z_5 &= \rho=\arctan\left(\frac{\psi_{rb}}{\psi_{ra}}\right)\,.\end{aligned}\tag{2.58}$$

According to the Inverse Function Theorem B.1 in Appendix B, for any point $p=(\omega,\psi_{ra},\psi_{rb},i_{sa},i_{sb})$ satisfying $\psi_{ra}^2+\psi_{rb}^2\neq 0$ there exists an open neighborhood U of p such that $\varphi(p)=(z_1(p),\ldots,z_n(p)):U\to\varphi(U)$ is a diffeomorphism, that is a bijection with $\varphi(\cdot)$ and $\varphi^{-1}(\cdot)$ smooth maps. In the new z-coordinates, system (1.26) becomes

$$\begin{bmatrix} \dot{z}_1 \\ \dot{z}_2 \\ \dot{z}_3 \\ \dot{z}_4 \\ \dot{z}_5 \end{bmatrix} = \begin{bmatrix} z_2 \\ \Gamma_1 \\ z_4 \\ \Gamma_2 \\ \omega + \dfrac{\alpha M \left(\psi_{ra} i_{sb} - \psi_{rb} i_{sa}\right)}{\left(\psi_{ra}^2 + \psi_{rb}^2\right)} \end{bmatrix} + \begin{bmatrix} 0 & 0 \\ 1 & 0 \\ 0 & 0 \\ 0 & 1 \\ 0 & 0 \end{bmatrix} \begin{bmatrix} -\dfrac{\mu \psi_{rb}}{\sigma} & \dfrac{\mu \psi_{ra}}{\sigma} \\ \dfrac{2\alpha M \psi_{ra}}{\sigma} & \dfrac{2\alpha M \psi_{rb}}{\sigma} \end{bmatrix} \begin{bmatrix} u_{sa} \\ u_{sb} \end{bmatrix} \tag{2.59}$$

in which the nonlinear terms

$$\begin{aligned} \Gamma_1(\omega, \psi_{ra}, \psi_{rb}, i_{sa}, i_{sb}) &= -\mu\beta\omega\left(\psi_{ra}^2 + \psi_{rb}^2\right) - \mu\left(\alpha + \gamma\right)\left(\psi_{ra} i_{sb} - \psi_{rb} i_{sa}\right) \\ &\quad -\mu\omega\left(\psi_{ra} i_{sa} + \psi_{rb} i_{sb}\right) \\ \Gamma_2(\omega, \psi_{ra}, \psi_{rb}, i_{sa}, i_{sb}) &= \left(4\alpha^2 + 2\alpha^2\beta M\right)\left(\psi_{ra}^2 + \psi_{rb}^2\right) + 2\alpha M\omega\left(\psi_{ra} i_{sb} - \psi_{rb} i_{sa}\right) \\ &\quad -\left(6\alpha^2 M + 2\alpha\gamma M\right)\left(\psi_{ra} i_{sa} + \psi_{rb} i_{sb}\right) + 2\alpha^2 M^2\left(i_{sa}^2 + i_{sb}^2\right) \end{aligned}$$

appear and the decoupling matrix

$$D(\psi_{ra}, \psi_{rb}) = \begin{bmatrix} -\dfrac{\mu \psi_{rb}}{\sigma} & \dfrac{\mu \psi_{ra}}{\sigma} \\ \dfrac{2\alpha M \psi_{ra}}{\sigma} & \dfrac{2\alpha M \psi_{rb}}{\sigma} \end{bmatrix}$$

whose determinant is

$$\det\left[D\right](\psi_{ra}, \psi_{rb}) = -\frac{2\mu\alpha M}{\sigma^2}\left(\psi_{ra}^2 + \psi_{rb}^2\right)$$

is nonsingular provided that $\left(\psi_{ra}^2 + \psi_{rb}^2\right) \neq 0$: hence, Theorem B.10 in Appendix B applies with control characteristic indices $\rho_1 = 2$, $\rho_2 = 2$. As a matter of fact, Theorem B.10 applies directly to the induction motor fixed frame model (1.26) with outputs ω and $\psi_{ra}^2 + \psi_{rb}^2$ and decoupling indices $\rho_1 = 2$, $\rho_2 = 2$. The input–output state feedback linearizing control is

$$\begin{bmatrix} u_{sa} \\ u_{sb} \end{bmatrix} = D(\psi_{ra}, \psi_{rb})^{-1} \begin{bmatrix} -\Gamma_1 + v_a \\ -\Gamma_2 + v_b \end{bmatrix} \tag{2.60}$$

which substituted in (2.59) gives

$$\begin{bmatrix} \dot{z}_1 \\ \dot{z}_2 \\ \dot{z}_3 \\ \dot{z}_4 \\ \dot{z}_5 \end{bmatrix} = \begin{bmatrix} z_2 \\ v_a \\ z_4 \\ v_b \\ \omega + \dfrac{\alpha M \left(\psi_{ra} i_{sb} - \psi_{rb} i_{sa}\right)}{\left(\psi_{ra}^2 + \psi_{rb}^2\right)} \end{bmatrix}$$

$$= \begin{bmatrix} z_2 \\ v_a \\ z_4 \\ v_b \\ z_1 + \dfrac{\alpha M \left(z_2 + \frac{T_L}{J}\right)}{\mu z_3} \end{bmatrix} = \begin{bmatrix} z_2 \\ v_a \\ z_4 \\ v_b \\ z_1 + \dfrac{R_r \left(J z_2 + T_L\right)}{z_3} \end{bmatrix}. \tag{2.61}$$

The last equation in (2.61) represents the dynamics which have been made unobservable from the outputs ω and $(\psi_{ra}^2 + \psi_{rb}^2)$ by the state feedback control (2.60). The same interpretation can be given to the last equation in (2.55).

Remarks

1. The closed-loop system (2.61) is input–output decoupled and linear: the input–output map consists of a pair of second order linear time-invariant systems. This allows for an independent tracking of the outputs so that transient responses can be decoupled: this is an improvement with respect to both the direct and the indirect field-oriented controls. Note however that the exact input–output decoupling and linearization have been achieved by the controller (2.60) at the expense of a singularity at $(\psi_{ra}^2 + \psi_{rb}^2) = 0$ introduced by the inversion of the decoupling matrix

$$D(\psi_{ra}, \psi_{rb})^{-1} = \left[\det [D] (\psi_{ra}, \psi_{rb})\right]^{-1} \begin{bmatrix} \frac{2\alpha M \psi_{rb}}{\sigma} & -\frac{\mu \psi_{ra}}{\sigma} \\ -\frac{2\alpha M \psi_{ra}}{\sigma} & -\frac{\mu \psi_{rb}}{\sigma} \end{bmatrix}$$

$$= \left[-\frac{2\mu\alpha M}{\sigma^2} \left(\psi_{ra}^2 + \psi_{rb}^2\right)\right]^{-1} \begin{bmatrix} \frac{2\alpha M \psi_{rb}}{\sigma} & -\frac{\mu \psi_{ra}}{\sigma} \\ -\frac{2\alpha M \psi_{ra}}{\sigma} & -\frac{\mu \psi_{rb}}{\sigma} \end{bmatrix} \tag{2.62}$$

in (2.60) which, in contrast to the indirect field-oriented control, may imply very large voltages (u_{sa}, u_{sb}) when $(\psi_{ra}^2 + \psi_{rb}^2)$ is close to zero. Recall that the direct field-oriented control also cannot operate when the rotor flux modulus is zero. Note that (2.62) can be rewritten as

$$D(\psi_{ra}, \psi_{rb})^{-1} = \begin{bmatrix} -\sin\rho & \cos\rho \\ \cos\rho & \sin\rho \end{bmatrix} \begin{bmatrix} \frac{\sigma}{\mu \sqrt{\psi_{ra}^2 + \psi_{rb}^2}} & 0 \\ 0 & \frac{\sigma}{2\alpha M \sqrt{\psi_{ra}^2 + \psi_{rb}^2}} \end{bmatrix}$$

with $\sin\rho = \psi_{rb}/\sqrt{\psi_{ra}^2+\psi_{rb}^2}$ and $\cos\rho = \psi_{ra}/\sqrt{\psi_{ra}^2+\psi_{rb}^2}$. The rotation matrix has been reobtained without introducing any rotating frame from the beginning.
2. Measurements of the state variables are required both by the control (2.60) and by the direct field-oriented control.
3. While the indirect field-oriented control is a first order output feedback (from ω) dynamic control, the control (2.60) is a static state feedback control law.
4. Since it has been previously shown that the induction motor model (1.26) is not feedback linearizable and that the largest feedback linearizable subsystem has dimension 4, the control (2.60) provides the largest linearizable subsystem in the closed-loop.

We now design the input signals v_a and v_b in (2.60) in order to track the desired references ω^* and ψ^{*2} for the rotor speed $z_1 = \omega$ and $z_3 = (\psi_{ra}^2+\psi_{rb}^2)$. Similarly to the design of v_d' and v_q', we choose

$$\begin{aligned}
v_a &= -k_{\omega p}(z_1-\omega^*) - k_{\omega d}(\dot z_1 - \dot\omega^*) + \ddot\omega^* \\
&= -k_{\omega p}(\omega-\omega^*) - k_{\omega d}\left(\mu(\psi_{ra}i_{sb}-\psi_{rb}i_{sa}) - \frac{T_L}{J} - \dot\omega^*\right) + \ddot\omega^* \\
v_b &= -k_{\psi p}\left(z_3-\psi^{*2}\right) - k_{\psi d}(\dot z_3 - 2\psi^*\dot\psi^*) + 2\dot\psi^{*2} + 2\psi^*\ddot\psi^* \\
&= -k_{\psi p}\left[\left(\psi_{ra}^2+\psi_{rb}^2\right) - \psi^{*2}\right] \\
&\quad -k_{\psi d}\left[-2\alpha\left(\psi_{ra}^2+\psi_{rb}^2\right) + 2\alpha M(\psi_{ra}i_{sa}+\psi_{rb}i_{sb}) - 2\psi^*\dot\psi^*\right] \\
&\quad +2\dot\psi^{*2} + 2\psi^*\ddot\psi^*
\end{aligned}$$

where $k_{\omega p}, k_{\omega d}, k_{\psi p}, k_{\psi d}$ are constant design parameters to be determined in order to make the decoupled, linear, time-invariant, second order systems ($\tilde\Psi = \psi_{ra}^2+\psi_{rb}^2-\psi^{*2}$)

$$\begin{aligned}
\frac{\mathrm{d}^2\tilde\omega}{\mathrm{d}t^2} &= -k_{\omega p}\tilde\omega - k_{\omega d}\frac{\mathrm{d}\tilde\omega}{\mathrm{d}t} \\
\frac{\mathrm{d}^2\tilde\Psi}{\mathrm{d}t^2} &= -k_{\psi p}\tilde\Psi - k_{\psi d}\frac{\mathrm{d}\tilde\Psi}{\mathrm{d}t}
\end{aligned} \tag{2.63}$$

exponentially stable and to shape their dynamics.

In conclusion: the *input–output feedback linearizing control* is defined as

$$\begin{bmatrix} u_{sa} \\ u_{sb} \end{bmatrix} = \left[-\frac{2\mu\alpha M}{\sigma^2}\left(\psi_{ra}^2+\psi_{rb}^2\right)\right]^{-1} \begin{bmatrix} \dfrac{2\alpha M\psi_{rb}}{\sigma} & -\dfrac{\mu\psi_{ra}}{\sigma} \\ -\dfrac{2\alpha M\psi_{ra}}{\sigma} & -\dfrac{\mu\psi_{rb}}{\sigma} \end{bmatrix} \begin{bmatrix} -\Gamma_1 + v_a \\ -\Gamma_2 + v_b \end{bmatrix}$$

$$\begin{aligned}
\Gamma_1 &= -\mu\beta\omega\left(\psi_{ra}^2+\psi_{rb}^2\right) - \mu(\alpha+\gamma)(\psi_{ra}i_{sb}-\psi_{rb}i_{sa}) \\
&\quad -\mu\omega(\psi_{ra}i_{sa}+\psi_{rb}i_{sb})
\end{aligned}$$

$$
\begin{aligned}
\Gamma_2 &= \left(4\alpha^2 + 2\alpha^2\beta M\right)\left(\psi_{ra}^2 + \psi_{rb}^2\right) + 2\alpha M\omega\left(\psi_{ra} i_{sb} - \psi_{rb} i_{sa}\right) \\
&\quad - \left(6\alpha^2 M + 2\alpha\gamma M\right)\left(\psi_{ra} i_{sa} + \psi_{rb} i_{sb}\right) + 2\alpha^2 M^2\left(i_{sa}^2 + i_{sb}^2\right) \\
v_a &= -k_{\omega p}\left(\omega - \omega^*\right) - k_{\omega d}\left(\mu\left(\psi_{ra} i_{sb} - \psi_{rb} i_{sa}\right) - \frac{T_L}{J} - \dot{\omega}^*\right) + \ddot{\omega}^* \\
v_b &= -k_{\psi p}\left[\left(\psi_{ra}^2 + \psi_{rb}^2\right) - \psi^{*2}\right] \\
&\quad - k_{\psi d}\left[-2\alpha\left(\psi_{ra}^2 + \psi_{rb}^2\right) + 2\alpha M\left(\psi_{ra} i_{sa} + \psi_{rb} i_{sb}\right) - 2\psi^*\dot{\psi}^*\right] \\
&\quad + 2\dot{\psi}^{*2} + 2\psi^*\ddot{\psi}^*;
\end{aligned}
\tag{2.64}
$$

it is a static nonlinear feedback control algorithm which depends on the measurements of the state variables $(\omega, \psi_{ra}, \psi_{rb}, i_{sa}, i_{sb})$, on the reference signals (ω^*, ψ^*), on the positive control parameters $k_{\omega p}$, $k_{\omega d}$, $k_{\psi p}$, $k_{\psi d}$, on the load torque T_L and on the machine parameters M, R_r, L_r, J, R_s, L_s, since $\mu = \dfrac{M}{JL_r}$, $\alpha = \dfrac{R_r}{L_r}$, $\sigma = L_s\left(1 - \dfrac{M^2}{L_s L r}\right)$, $\beta = \dfrac{M}{\sigma L_r}$, $\gamma = \dfrac{R_s}{\sigma} + \beta\alpha M$; it guarantees that, for suitable motor initial conditions such that $\psi_{ra}^2(t) + \psi_{rb}^2(t) \geq c_\psi > 0$ for all $t \geq 0$, the rotor speed and flux modulus tracking errors have decoupled dynamics and decay exponentially to zero according to (2.63).

Illustrative Simulations

We tested the input–output feedback linearizing control by simulations for the three-phase single pole pair 0.6-kW induction motor whose parameters have been reported in Chapter 1. All the motor initial conditions have been set equal to zero except for $\psi_{ra}(0) = \psi_{rb}(0) = 0.1\,\text{Wb}$. The control algorithm has been tested with the control parameters (all the values are in SI units) $k_{\omega p} = 8100$, $k_{\omega d} = 180$, $k_{\psi p} = 8100$, $k_{\psi d} = 180$; real coincident eigenvalues are assigned to the matrices associated with the decoupled, linear time-invariant second order systems (2.63). The references for the speed and flux modulus along with the applied load torque are reported in Figures 2.25–2.27. The rotor flux modulus reference signal starts from 0.001 Wb at $t = 0\,\text{s}$ and grows up to the constant value 1.16 Wb. The speed reference is zero until $t = 0.32\,\text{s}$ and grows up to the constant value 100 rad/s; at $t = 1.5\,\text{s}$ the speed is required to go up to the value 200 rad/s, while the reference for the flux modulus is reduced to 0.5 Wb. A 5.8-Nm load torque is applied to the motor and is reduced to 1.8 Nm. Figures 2.26 and 2.27 show the time histories of rotor speed and flux modulus along with the corresponding tracking errors: the rotor speed and flux modulus track tightly their references. Note that there is no coupling between rotor speed tracking and rotor flux modulus tracking at $t = 0.5\,\text{s}$ and $t = 1\,\text{s}$ when rotor speed is perturbed by the uncompensated load torque time derivative. Finally, the

stator current and voltages profiles, which are within the physical saturation limits, are reported in Figures 2.28 and 2.29.

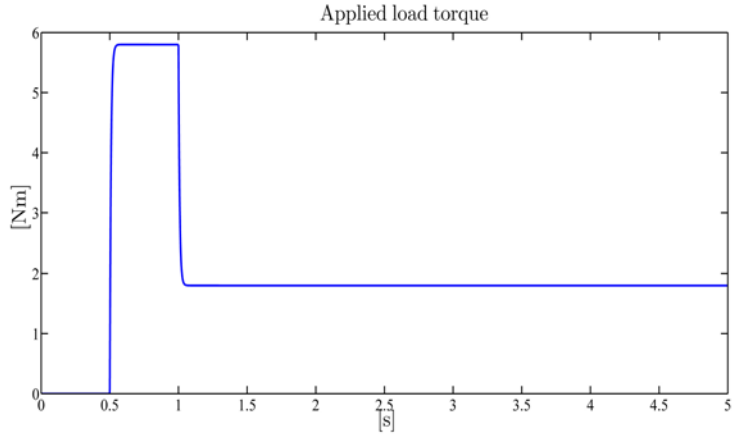

Fig. 2.25 Input–output feedback linearizing control: applied load torque T_L

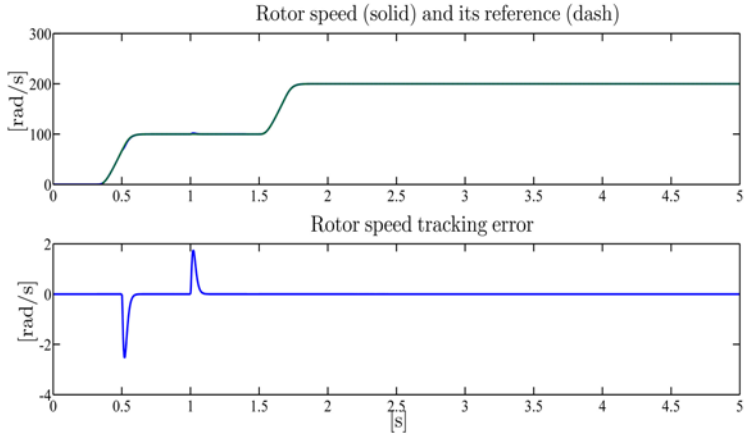

Fig. 2.26 Input–output feedback linearizing control: rotor speed ω and its reference ω^*; rotor speed tracking error

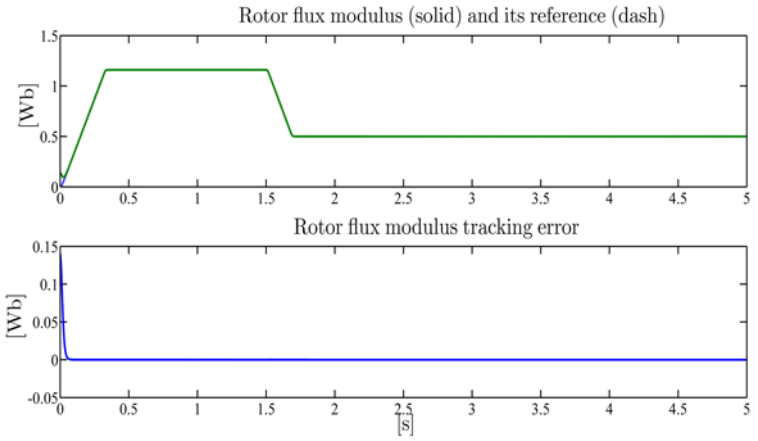

Fig. 2.27 Input–output feedback linearizing control: rotor flux modulus $\sqrt{\psi_{ra}^2 + \psi_{rb}^2}$ and its reference ψ^*; rotor flux modulus tracking error

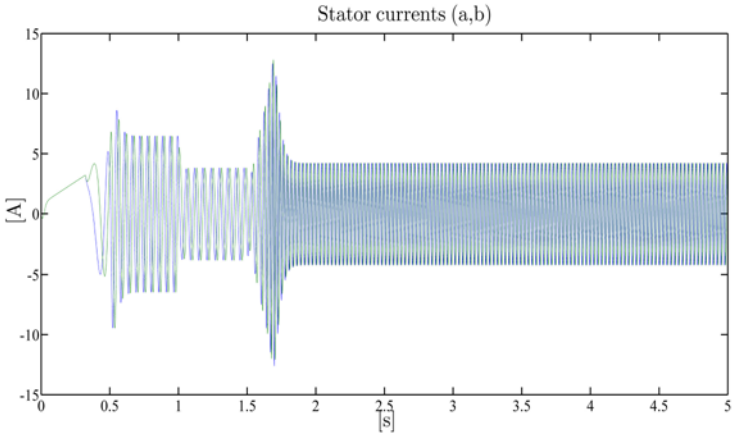

Fig. 2.28 Input–output feedback linearizing control: stator current vector (a,b)-components (i_{sa}, i_{sb})

2.5 Adaptive Input–Output Feedback Linearizing Control

So far we have designed the state feedback control algorithms by assuming the knowledge of the rotor resistance R_r and of the load torque T_L. While the load torque depends on applications, the rotor resistance may vary up to 100% during operations due to rotor heating: thus they constitute typically uncertain parameters. Experiments reported in Section 2.8 will show how critical the rotor resistance parameter is for the control design. In this section we shall estimate its value online along with the load torque.

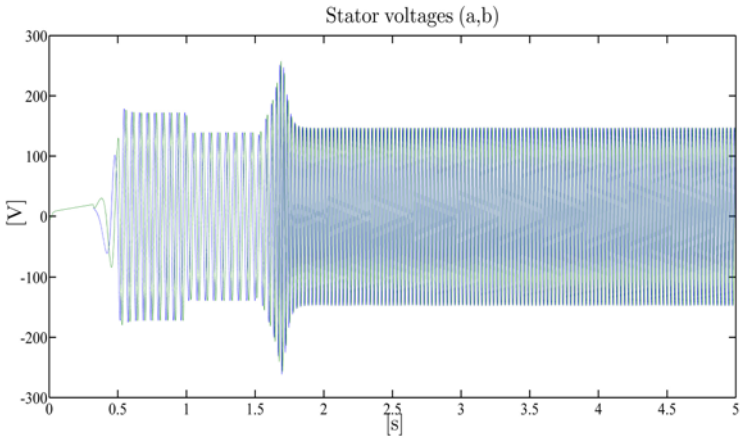

Fig. 2.29 Input–output feedback linearizing control: stator voltage vector (a,b)-components (u_{sa}, u_{sb})

Reconsider the state feedback input–output linearizing control (2.23), (2.24), (2.54) and (2.56); note that (u_{sd}, u_{sq}) defined in (2.24) are linear with respect to the unknown parameter $\alpha = R_r L_r^{-1}$. Hence, the controller (2.23), (2.24), (2.54) and (2.56) constitutes a good starting point to design an adaptation with respect to α. To this end, let us denote by $\hat{\alpha}$ the estimate of the parameter α and by

$$\tilde{\alpha} = \alpha - \hat{\alpha}$$

the corresponding estimation error. Recalling (2.24), define (u_{sd}, u_{sq}) as

$$\begin{aligned} u_{sd} &= \sigma \left[\frac{R_s}{\sigma} i_{sd} - \omega i_{sq} - \frac{\hat{\alpha} M i_{sq}^2}{\psi_{rd}} - \hat{\alpha}\beta\psi_{rd} + \hat{\alpha} M \beta i_{sd} + v_d \right] \\ u_{sq} &= \sigma \left[\frac{R_s}{\sigma} i_{sq} + \omega i_{sd} + \frac{\hat{\alpha} M i_{sq} i_{sd}}{\psi_{rd}} + \beta\omega\psi_{rd} + \hat{\alpha} M \beta i_{sq} + v_q \right] \end{aligned} \tag{2.65}$$

in which (v_d, v_q) are additional control inputs to be designed. Substituting (2.65) in (1.39) we obtain

$$\begin{aligned} \frac{\mathrm{d}\omega}{\mathrm{d}t} &= \mu \psi_{rd} i_{sq} - \frac{T_L}{J} \\ \frac{\mathrm{d}i_{sq}}{\mathrm{d}t} &= -\left(\frac{M i_{sq} i_{sd}}{\psi_{rd}} + M\beta i_{sq} \right) \tilde{\alpha} + v_q \\ \frac{\mathrm{d}\psi_{rd}}{\mathrm{d}t} &= -\alpha\psi_{rd} + \alpha M i_{sd} \\ \frac{\mathrm{d}i_{sd}}{\mathrm{d}t} &= \left(\frac{M i_{sq}^2}{\psi_{rd}} + \beta\psi_{rd} - M\beta i_{sd} \right) \tilde{\alpha} + v_d \end{aligned}$$

$$\frac{\mathrm{d}\rho}{\mathrm{d}t} = \omega + \frac{\alpha M i_{sq}}{\psi_{rd}} \,. \tag{2.66}$$

Let us denote by $\hat{T}_L$ the estimate of the load torque T_L and by

$$\tilde{T}_L = T_L - \hat{T}_L$$

the corresponding estimation error. Since the load torque appears additively in the rotor speed dynamics given by the first equation in (1.31), we design the load torque estimate $\hat{T}_L$ as the output of a linear time-invariant one-dimensional system

$$\begin{aligned} \dot{\xi} &= -\lambda\xi + \lambda J\mu\psi_{rd} i_{sq} + \lambda^2 J\omega - v_T \\ \hat{T}_L &= \xi - \lambda J\omega \end{aligned} \tag{2.67}$$

in which the term v_T is yet to be defined. The above choice is justified by the fact that, according to (2.67), $\dot{\hat{T}}_L$ satisfies

$$\begin{aligned} \dot{\hat{T}}_L &= -\lambda J\mu\psi_{rd} i_{sq} + \lambda T_L + \dot{\xi} \\ &= \lambda T_L - \lambda(\xi - \lambda J\omega) - v_T \\ &= \lambda(T_L - \hat{T}_L) - v_T \end{aligned} \tag{2.68}$$

and therefore

$$\dot{\tilde{T}}_L = -\lambda\tilde{T}_L + v_T \tag{2.69}$$

which will be useful in the overall stability analysis. Introduce two new state variables: the estimated rotor angular acceleration

$$\hat{a} = \mu\psi_{rd} i_{sq} - \frac{\hat{T}_L}{J} \tag{2.70}$$

and the estimated time derivative of the rotor flux direct component ψ_{rd}

$$\hat{v}_{\psi d} = -\hat{\alpha}\psi_{rd} + \hat{\alpha} M i_{sd} \,. \tag{2.71}$$

In new state coordinates $(\omega, \hat{a}, \psi_{rd}, \hat{v}_{\psi d}, \rho)$, (2.66) are rewritten as (recall (2.53))

$$\begin{aligned} \frac{\mathrm{d}\omega}{\mathrm{d}t} &= \hat{a} - \frac{\tilde{T}_L}{J} \\ \frac{\mathrm{d}\hat{a}}{\mathrm{d}t} &= \mu(-\alpha\psi_{rd} + \alpha M i_{sd}) i_{sq} - \mu\tilde{\alpha} M i_{sq} i_{sd} + \mu\psi_{rd} v_q - \mu\tilde{\alpha}\psi_{rd}\beta M i_{sq} \\ &\quad - \frac{\lambda}{J}\tilde{T}_L + \frac{v_T}{J} \\ \frac{\mathrm{d}\psi_{rd}}{\mathrm{d}t} &= \hat{v}_{\psi d} + (M i_{sd} - \psi_{rd})\tilde{\alpha} \\ \frac{\mathrm{d}\hat{v}_{\psi d}}{\mathrm{d}t} &= \dot{\hat{\alpha}}(M i_{sd} - \psi_{rd}) - \hat{\alpha}(\alpha M i_{sd} - \alpha\psi_{rd}) \end{aligned}$$

$$+\hat{\alpha}M\left[\left(\frac{Mi_{sq}^2}{\psi_{rd}}+\beta\psi_{rd}-M\beta i_{sd}\right)\tilde{\alpha}+v_d\right]$$

$$\frac{\mathrm{d}\rho}{\mathrm{d}t}=\omega+\alpha M\left(\frac{\hat{a}}{\mu\psi_{rd}^2}+\frac{\hat{T}_L}{J\mu\psi_{rd}^2}\right). \tag{2.72}$$

Define

$$\begin{aligned}
v_q &= \hat{\alpha}i_{sq}-\frac{\hat{\alpha}Mi_{sd}i_{sq}}{\psi_{rd}}-\frac{v_T}{J\mu\psi_{rd}}\\
&\quad+\frac{1}{\mu\psi_{rd}}\left[-k_{\omega p}(\omega-\omega^*)-k_{\omega d}(\hat{a}-\dot{\omega}^*)+\ddot{\omega}^*\right]\\
v_d &= -\frac{\hat{\alpha}\psi_{rd}}{M}+\hat{\alpha}i_{sd}+\frac{1}{\hat{\alpha}M}\Bigg[-\dot{\hat{\alpha}}(Mi_{sd}-\psi_{rd})\\
&\quad-k_{\psi p}(\psi_{rd}-\psi^*)-k_{\psi d}(\hat{v}_{\psi d}-\dot{\psi}^*)+\ddot{\psi}^*\Bigg]
\end{aligned} \tag{2.73}$$

which substituted in (2.72) give

$$\begin{aligned}
\frac{\mathrm{d}\omega}{\mathrm{d}t} &= \hat{a}-\frac{\tilde{T}_L}{J}\\
\frac{\mathrm{d}\hat{a}}{\mathrm{d}t} &= -k_{\omega p}(\omega-\omega^*)-k_{\omega d}(\hat{a}-\dot{\omega}^*)+\ddot{\omega}^*-\mu\tilde{\alpha}(1+\beta M)\psi_{rd}i_{sq}-\frac{\lambda}{J}\tilde{T}_L\\
\frac{\mathrm{d}\psi_{rd}}{\mathrm{d}t} &= \hat{v}_{\psi d}+(Mi_{sd}-\psi_{rd})\tilde{\alpha}\\
\frac{\mathrm{d}\hat{v}_{\psi d}}{\mathrm{d}t} &= -k_{\psi p}(\psi_{rd}-\psi^*)-k_{\psi d}(\hat{v}_{\psi d}-\dot{\psi}^*)+\ddot{\psi}^*\\
&\quad+\tilde{\alpha}\left[-\hat{\alpha}M(1+\beta M)i_{sd}+\hat{\alpha}(1+\beta M)\psi_{rd}+\frac{\hat{\alpha}M^2i_{sq}^2}{\psi_{rd}}\right]\\
\frac{\mathrm{d}\rho}{\mathrm{d}t} &= \omega+\alpha M\left(\frac{\hat{a}}{\mu\psi_{rd}^2}+\frac{\hat{T}_L}{J\mu\psi_{rd}^2}\right).
\end{aligned} \tag{2.74}$$

Let P_ω and P_ψ be the positive definite solutions of the Lyapunov matrix equations (see Theorem A.6 in Appendix A)

$$\begin{bmatrix}0 & -k_{\omega p}\\ 1 & -k_{\omega d}\end{bmatrix}P_\omega+P_\omega\begin{bmatrix}0 & 1\\ -k_{\omega p} & -k_{\omega d}\end{bmatrix}=-I_2 \tag{2.75}$$

$$\begin{bmatrix}0 & -k_{\psi p}\\ 1 & -k_{\psi d}\end{bmatrix}P_\psi+P_\psi\begin{bmatrix}0 & 1\\ -k_{\psi p} & -k_{\psi d}\end{bmatrix}=-I_2 \tag{2.76}$$

in which I_2 is the 2×2 identity matrix. Define the tracking errors

$$\tilde{\omega}=\omega-\omega^*$$

$$\tilde{a} = \hat{a} - \dot{\omega}^*$$
$$\tilde{\psi}_{rd} = \psi_{rd} - \psi^*$$
$$\tilde{v}_{\psi d} = \hat{v}_{\psi d} - \dot{\psi}^*$$

and introduce the error vectors

$$w_1 = [\tilde{\omega}, \tilde{a}]^{\mathrm{T}}$$
$$w_2 = [\tilde{\psi}_{rd}, \tilde{v}_{\psi d}]^{\mathrm{T}} .$$

Consider the Lyapunov function

$$V = w_1^{\mathrm{T}} P_\omega w_1 + w_2^{\mathrm{T}} P_\psi w_2 + \tilde{T}_L^2 + \frac{\tilde{\alpha}^2}{\lambda_\alpha} \tag{2.77}$$

in which λ_α is a positive control parameter. The time derivative of function V along the trajectories of the closed-loop system (2.74) is

$$\begin{aligned}\dot{V} = &-\|w_1\|^2 - \|w_2\|^2 - 2\lambda \tilde{T}_L^2 + \tilde{T}_L \left(2v_T + 2w_1^{\mathrm{T}} P_\omega \left[-\frac{1}{J}, -\frac{\lambda}{J} \right]^{\mathrm{T}} \right) \\ &+ \tilde{\alpha} \Bigg(2\lambda_\alpha^{-1} \dot{\hat{\alpha}} + 2w_1^{\mathrm{T}} P_\omega \left[0, -(1+M\beta)\mu \psi_{rd} i_{sq} \right]^{\mathrm{T}} \\ &+ 2w_2^{\mathrm{T}} P_\psi \left[M i_{sd} - \psi_{rd}, -(1+M\beta)\hat{\alpha} M i_{sd} + (1+M\beta)\hat{\alpha}\psi_{rd} + \frac{\hat{\alpha} M^2 i_{sq}^2}{\psi_{rd}} \right]^{\mathrm{T}} \Bigg) .\end{aligned} \tag{2.78}$$

If we design the yet undefined term v_T and the estimation law for $\hat{\alpha}$ as

$$v_T = -w_1^{\mathrm{T}} P_\omega \left[-\frac{1}{J}, -\frac{\lambda}{J} \right]^{\mathrm{T}}$$
$$\begin{aligned}\dot{\hat{\alpha}} = \lambda_\alpha \Bigg(&w_1^{\mathrm{T}} P_\omega \left[0, -(1+M\beta)\mu \psi_{rd} i_{sq} \right]^{\mathrm{T}} \\ &+ w_2^{\mathrm{T}} P_\psi \left[M i_{sd} - \psi_{rd}, -(1+M\beta)\hat{\alpha} M i_{sd} + (1+M\beta)\hat{\alpha}\psi_{rd} + \frac{\hat{\alpha} M^2 i_{sq}^2}{\psi_{rd}} \right]^{\mathrm{T}} \Bigg)\end{aligned}$$

then from (2.78) we obtain

$$\dot{V} = -\|w_1\|^2 - \|w_2\|^2 - 2\lambda \tilde{T}_L^2 . \tag{2.79}$$

Since the previous equation implies that for all $t \geq 0$

$$V(t) \leq V(0)$$

then we can restrict the initial conditions for the tracking and the estimation errors such that $V(0)$ is sufficiently small to guarantee $\psi_{rd}(t) \geq c_1 > 0$ and $\hat{\alpha}(t) \geq c_2 > 0$ for all $t \geq 0$. On the other hand, from (2.77) and (2.79) we can establish that $w_1(t)$, $w_2(t)$, $\tilde{T}_L(t)$, and $\tilde{\alpha}(t)$ are bounded functions on $[0,\infty)$ and therefore, according to (2.70) and (2.71), $\mu\psi_{rd}(t)i_{sq}(t)$ and $(Mi_{sd}(t) - \psi_{rd}(t))$ are bounded functions on $[0,\infty)$. Since $\psi_{rd}(t)$ is a bounded function on $[0,\infty)$, it follows that $i_{sd}(t)$ and $i_{sq}(t)$ are bounded functions on $[0,\infty)$. Therefore $\dot{\omega}(t)$, $\dot{\psi}_{rd}(t)$, $\dot{\hat{T}}_L(t)$, and $\dot{\hat{a}}(t)$ are bounded functions on $[0,\infty)$ so that $\tilde{\omega}(t)$, $\tilde{\psi}_{rd}(t)$, and $\tilde{T}_L(t)$ are uniformly continuous functions on $[0,\infty)$. Since for any $t \geq 0$

$$\int_0^t (\tilde{\omega}^2(\tau) + \tilde{\psi}_{rd}^2(\tau) + \tilde{a}^2(\tau) + 2\lambda\tilde{T}_L^2(\tau))\mathrm{d}\tau \leq V(0) - V(t) \leq V(0) \quad (2.80)$$

which implies

$$\lim_{t\to\infty} \int_0^t [\tilde{\omega}^2(\tau) + \tilde{\psi}_{rd}^2(\tau) + \tilde{a}^2(\tau) + 2\lambda\tilde{T}_L^2(\tau)]\mathrm{d}\tau \leq V(0) \quad (2.81)$$

by applying Barbalat's Lemma A.2 in Appendix A, we have

$$\begin{aligned} \lim_{t\to\infty} \tilde{\omega}(t) &= 0 \\ \lim_{t\to\infty} \tilde{\psi}_{rd}(t) &= 0 \\ \lim_{t\to\infty} \tilde{a}(t) &= 0 \\ \lim_{t\to\infty} \tilde{T}_L(t) &= 0\,. \end{aligned} \quad (2.82)$$

Hence, asymptotic rotor speed and flux modulus tracking of the reference signals ω^* and ψ^* is achieved along with estimation of the unknown load torque.

On the other hand, since $\ddot{\tilde{a}}(t)$ is a bounded function on $[0,\infty)$, $\dot{\tilde{a}}(t)$ is a uniformly continuous function on $[0,\infty)$ so that, by Barbalat's Lemma A.2,

$$\lim_{t\to\infty} \dot{\tilde{a}}(t) = 0\,.$$

Since from (2.74) we have

$$\begin{aligned} \dot{\tilde{a}} &= -k_{\omega p}\tilde{\omega} - k_{\omega d}\tilde{a} - \tilde{\alpha}(1+\beta M)\left(\hat{a} + \frac{\hat{T}_L}{J}\right) - \frac{\lambda}{J}\tilde{T}_L \\ &= -k_{\omega p}\tilde{\omega} - k_{\omega d}\tilde{a} - \tilde{\alpha}(1+\beta M)\left(\tilde{a} - \frac{\tilde{T}_L}{J}\right) - \frac{\lambda}{J}\tilde{T}_L - \tilde{\alpha}(1+\beta M)\left(\dot{\omega}^* + \frac{T_L}{J}\right)\,, \end{aligned}$$

according to (2.82) we can finally establish that

$$\lim_{t\to\infty} \left[\left(\dot{\omega}^*(t) + \frac{T_L}{J}\right)\tilde{\alpha}(t)\right] = 0 \quad (2.83)$$

which implies that $\tilde{\alpha}(t)$ asymptotically converges to zero provided that $\dot{\omega}^*(t)+T_L/J$ is different from zero for all $t \geq 0$. A stronger result is obtained since, if there exist two positive reals T_p and c_p such that

$$\int_t^{t+T_p} \left[\left(\dot{\omega}^*(\tau) + \frac{T_L}{J} \right)^2 \right] \mathrm{d}\tau \geq c_p, \quad \forall t \geq 0\,, \tag{2.84}$$

then exponential convergence to zero of the rotor speed and rotor flux modulus tracking errors is guaranteed, for sufficiently small initial conditions, along with exponential estimation of both the uncertain parameters α and T_L.

In conclusion: the *adaptive input–output feedback linearizing control* is defined as

$$\begin{bmatrix} u_{sa} \\ u_{sb} \end{bmatrix} = \begin{bmatrix} \cos\rho & -\sin\rho \\ \sin\rho & \cos\rho \end{bmatrix} \begin{bmatrix} u_{sd} \\ u_{sq} \end{bmatrix}$$

$$u_{sd} = \sigma \left[\frac{R_s}{\sigma} i_{sd} - \omega i_{sq} - \frac{\hat{\alpha} M i_{sq}^2}{\psi_{rd}} - \hat{\alpha}\beta\psi_{rd} + \hat{\alpha} M \beta i_{sd} + v_d \right]$$

$$u_{sq} = \sigma \left[\frac{R_s}{\sigma} i_{sq} + \omega i_{sd} + \frac{\hat{\alpha} M i_{sq} i_{sd}}{\psi_{rd}} + \beta\omega\psi_{rd} + \hat{\alpha} M \beta i_{sq} + v_q \right]$$

$$v_d = -\frac{\hat{\alpha}\psi_{rd}}{M} + \hat{\alpha} i_{sd} + \frac{1}{\hat{\alpha} M} \left[-\dot{\hat{\alpha}}(M i_{sd} - \psi_{rd}) \right.$$

$$\left. -k_{\psi p}(\psi_{rd} - \psi^*) - k_{\psi d}(\hat{v}_{\psi d} - \dot{\psi}^*) + \ddot{\psi}^* \right]$$

$$v_q = \hat{\alpha} i_{sq} - \frac{\hat{\alpha} M i_{sd} i_{sq}}{\psi_{rd}} - \frac{v_T}{J\mu\psi_{rd}}$$

$$+ \frac{1}{\mu\psi_{rd}} \left[-k_{\omega p}(\omega - \omega^*) - k_{\omega d}(\hat{a} - \dot{\omega}^*) + \ddot{\omega}^* \right]$$

$$\psi_{rd} = \psi_{ra}\cos\rho + \psi_{rb}\sin\rho$$

$$\begin{bmatrix} i_{sd} \\ i_{sq} \end{bmatrix} = \begin{bmatrix} \cos\rho & \sin\rho \\ -\sin\rho & \cos\rho \end{bmatrix} \begin{bmatrix} i_{sa} \\ i_{sb} \end{bmatrix}$$

$$-I_2 = \begin{bmatrix} 0 & -k_{\omega p} \\ 1 & -k_{\omega d} \end{bmatrix} P_\omega + P_\omega \begin{bmatrix} 0 & 1 \\ -k_{\omega p} & -k_{\omega d} \end{bmatrix}$$

$$-I_2 = \begin{bmatrix} 0 & -k_{\psi p} \\ 1 & -k_{\psi d} \end{bmatrix} P_\psi + P_\psi \begin{bmatrix} 0 & 1 \\ -k_{\psi p} & -k_{\psi d} \end{bmatrix}$$

$$\dot{\xi} = -\lambda\xi + \lambda J \mu \psi_{rd} i_{sq} + \lambda^2 J \omega - v_T$$

$$\hat{T}_L = \xi - \lambda J \omega$$

$$v_T = w_1^{\mathrm{T}} P_\omega \left[\frac{1}{J}, \frac{\lambda}{J}\right]^{\mathrm{T}}$$

$$\dot{\hat{\alpha}} = \lambda_\alpha \left(w_1^{\mathrm{T}} P_\omega \left[0, -(1+M\beta)\mu\psi_{rd} i_{sq}\right]^{\mathrm{T}} + w_2^{\mathrm{T}} P_\psi \left[M i_{sd} - \psi_{rd}, \right.\right.$$

$$\left.\left. -(1+M\beta)\hat{\alpha} M i_{sd} + (1+M\beta)\hat{\alpha}\psi_{rd} + \frac{\hat{\alpha} M^2 i_{sq}^2}{\psi_{rd}} \right]^{\mathrm{T}} \right); \quad (2.85)$$

it is a second order dynamic nonlinear feedback control algorithm which depends on the measurements of the state variables $(\omega, \psi_{ra}, \psi_{rb}, i_{sa}, i_{sb})$, on the reference signals (ω^*, ψ^*), on the positive control parameters $k_{\omega p}$, $k_{\omega d}$, $k_{\psi p}$, $k_{\psi d}$, λ, λ_α, and on the machine parameters M, L_r, J, R_s, L_s since $\mu = \dfrac{M}{JL_r}$, $\alpha = \dfrac{R_r}{L_r}$, $\sigma = L_s\left(1 - \dfrac{M^2}{L_s Lr}\right)$, $\beta = \dfrac{M}{\sigma L_r}$; it guarantees that, for any initial condition such that $\psi_{rd}(t) \geq c_1 > 0$ and $\hat{\alpha}(t) \geq c_2 > 0$ for all $t \geq 0$, the rotor speed and flux modulus tracking errors tend asymptotically to zero; moreover, the rotor speed and flux modulus tracking errors along with the rotor resistance and load torque estimation errors decay exponentially to zero provided that there exist two positive reals T_p and c_p such that the persistency of excitation condition (2.84) is satisfied.

Remarks

1. Note that even for constant speed and zero load torque, that is when the rotor resistance estimate is not guaranteed to converge to the true value, both the rotor speed and the rotor flux modulus tracking errors asymptotically converge to zero.
2. When both the critical parameters T_L and α are known, so that we can set $\hat{T}_L \equiv T_L$ and $\hat{\alpha} \equiv \alpha$, the controller (2.85) reduces to the input–output feedback linearizing controller designed in the first part of Section 2.4.
3. When the critical parameter α is known, so that we can set $\hat{\alpha} = \alpha$, the controller (2.85) guarantees exponential rotor speed and flux modulus tracking along with exponential load torque estimation.
4. The resulting controller (2.85) shows singularities at $\psi_{rd} = 0$ and $\hat{\alpha} = 0$ which can imply very large voltages when ψ_{rd} and $\hat{\alpha}$ are close to zero.

Illustrative Simulations

We tested the adaptive input–output feedback linearizing control by simulations for the three-phase single pole pair 0.6-kW induction motor whose parameters have been reported in Chapter 1. All the motor initial conditions have been set equal to zero except for $\psi_{ra}(0) = \psi_{rb}(0) = 0.1\,\text{Wb}$. The control algorithm has been tested with the control parameters (all the values are in SI units): $k_{\omega p} = 8100$, $k_{\omega d} = 180$, $k_{\psi p} = 8100$, $k_{\psi d} = 180$. Real coincident eigenvalues are assigned to the matrices associated with the decoupled, linear, time-invariant, second order systems describing the dynamics of the rotor speed and tracking errors when the estimates of the unknown parameters are equal to the corresponding true parameter values. Those values are the same as those used for the nonadaptive version of the previous section. The parameters λ and λ_α, which are the adaptation gains for the estimates of the load torque T_L and of the parameter α, have been set equal to $\lambda = 120$ and $\lambda_\alpha = 0.09$. The initial condition $\hat{T}_L(0)$ has been set equal to zero while the initial condition for the estimate of α has been set equal to $\hat{\alpha}(0) = 13.2\,\text{s}^{-1}$ which is 50% greater than the true parameter value $\alpha = 8.8\ \text{s}^{-1}$. The references for the speed and flux modulus along with the applied load torque are reported in Figures 2.30–2.32. The rotor flux modulus reference signal starts from 0.001 Wb at $t = 0\,\text{s}$ and grows up to the constant value 1.16 Wb. The speed reference is zero until $t = 0.32\,\text{s}$ and grows up to the constant value 100 rad/s; at $t = 1.5\,\text{s}$ the speed is required to go up to the value 200 rad/s, while the reference for the flux modulus is reduced to 0.5 Wb. A 5.8-Nm load torque is applied to the motor and is reduced to 1.8 Nm. Figures 2.30 and 2.31 show the time histories of rotor speed and flux modulus along with the corresponding tracking errors: the rotor speed tracks its reference tightly even though load torque sharply changes since, according to Figure 2.32, the load torque estimate quickly recovers the applied unknown load torque. The rotor flux modulus tracks its reference: there is, however, a coupling with rotor speed tracking at $t = 0.5\,\text{s}$ and $t = 1\,\text{s}$ when the rotor speed tracking error is perturbed by the unknown load torque. Also the estimate of α quickly converges, according to Figure 2.33, to the true value (unknown to the controller). Stator currents and voltages are within the saturation limits, as illustrated by Figures 2.34 and 2.35.

2.6 Dynamic Feedback Linearizing Control

The key idea of field-oriented control is to use the direct current component i_{sd} to control the flux modulus ψ_{rd} and the quadrature current component i_{sq} to control the speed ω in (1.39): there is no concern on controlling the dynamics of the remaining state variable in (2.9). However, while the dynamics of ψ_{rd} are linear and the dynamics of ω tend to be linear if ψ_{rd} tends to be constant, the dynamics of ρ in (2.9) remain nonlinear in terms of the states (ω, ψ_{rd}) and of the control input i_{sq} in (2.9). Similarly, the input–output feedback linearizing control (2.23), (2.24), (2.54), (2.56) aims at controlling linearly and independently ω and ψ_{rd} while leaving the

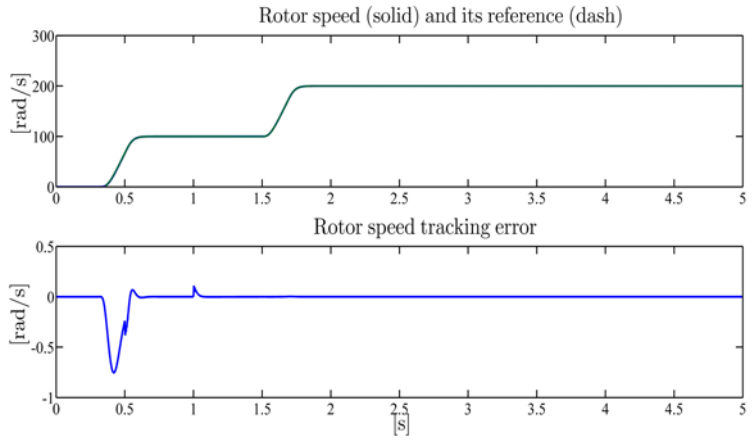

Fig. 2.30 Adaptive input–output feedback linearizing control: rotor speed ω and its reference ω^*; rotor speed tracking error

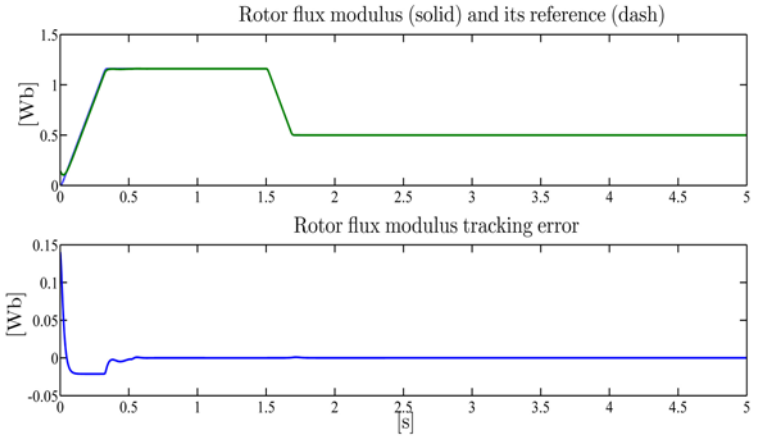

Fig. 2.31 Adaptive input–output feedback linearizing control: rotor flux modulus $\sqrt{\psi_{ra}^2 + \psi_{rb}^2}$ and its reference ψ^*; rotor flux modulus tracking error

dynamics of ρ nonlinearly dependent on the state variables $(\omega, \psi_{rd}, i_{sq})$ in (2.55). For this reason the state feedback control (2.23), (2.24), (2.54), (2.56) linearizes the input–output behavior from (v_d, v_q') to (ω, ψ_{rd}) but fails to make the controlled system dynamics (2.55) linear since the dynamics of ρ remain nonlinear.

On the other hand, if the goal of the control is to make the system, in suitable state coordinates, linear by state feedback, then it is convenient to consider the four equations in (1.39)

$$\frac{\mathrm{d}\omega}{\mathrm{d}t} = \mu \psi_{rd} i_{sq} - \frac{T_L}{J}$$

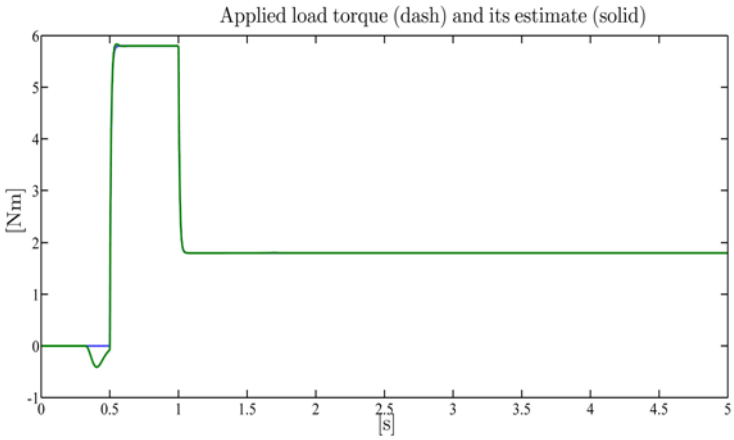

Fig. 2.32 Adaptive input–output feedback linearizing control: applied load torque T_L and its estimate $\hat{T}_L$

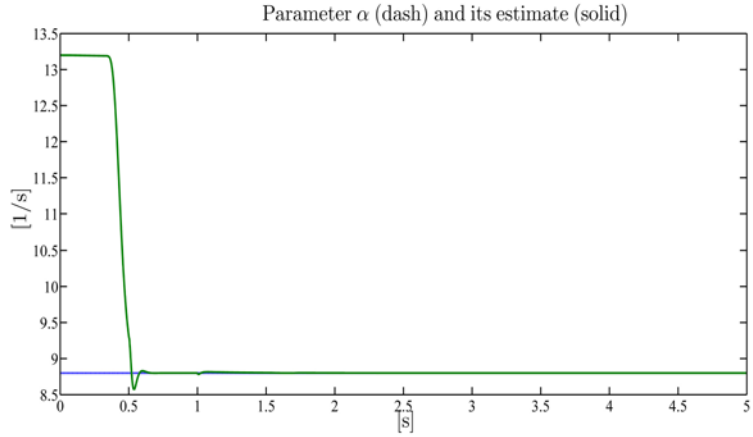

Fig. 2.33 Adaptive input–output feedback linearizing control: parameter α and its estimate $\hat{\alpha}$

$$\begin{aligned}
\frac{\mathrm{d}i_{sq}}{\mathrm{d}t} &= -\gamma i_{sq} - \omega i_{sd} - \frac{\alpha M i_{sq} i_{sd}}{\psi_{rd}} - \beta\,\omega\,\psi_{rd} + \frac{u_{sq}}{\sigma} \\
\frac{\mathrm{d}\rho}{\mathrm{d}t} &= \omega + \frac{\alpha M i_{sq}}{\psi_{rd}} \\
\frac{\mathrm{d}\psi_{rd}}{\mathrm{d}t} &= -\alpha\,\psi_{rd} + \alpha M i_{sd}
\end{aligned} \tag{2.86}$$

in which u_{sq} and i_{sd} are viewed as the control inputs.

Consider the state space change of coordinates from $(\omega, i_{sq}, \rho, \psi_{rd})$ to $(\omega, \dot{\omega}, \rho, \dot{\rho})$, which is nonsingular provided that $\psi_{rd} \neq 0$ and $i_{sq} \neq 0$ since from

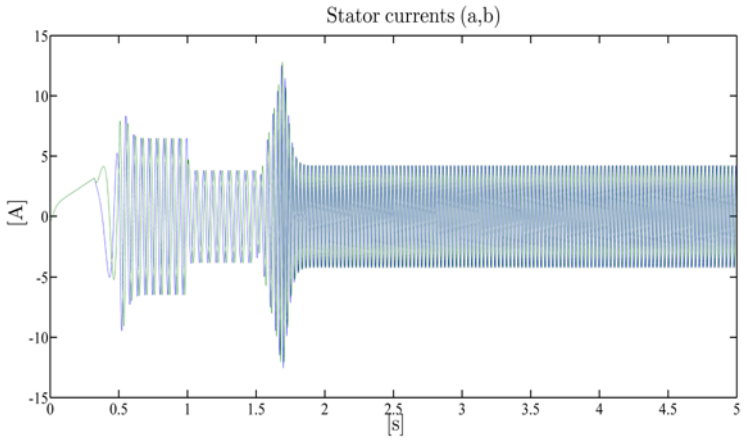

Fig. 2.34 Adaptive input–output feedback linearizing control: stator current vector (a,b)-components (i_{sa}, i_{sb})

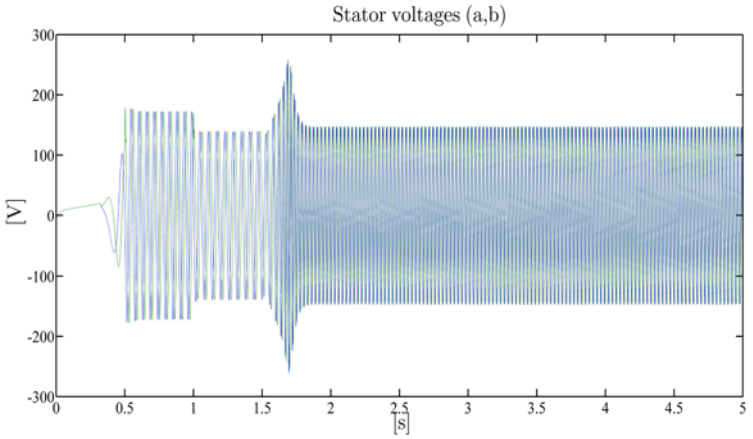

Fig. 2.35 Adaptive input–output feedback linearizing control: stator voltage vector (a,b)-components (u_{sa}, u_{sb})

$$\dot{\rho} - \omega = \frac{\alpha M i_{sq}}{\psi_{rd}} = \frac{\alpha M}{\mu \psi_{rd}^2} \left(\dot{\omega} + \frac{T_L}{J} \right)$$

we can solve for ψ_{rd} obtaining (if $i_{sq} \neq 0$)

$$\psi_{rd} = \sqrt{\frac{\alpha M \left(\dot{\omega} + \frac{T_L}{J} \right)}{\mu (\dot{\rho} - \omega)}} \tag{2.87}$$

while

$$i_{sq} = \frac{\left(\dot{\omega} + \frac{T_L}{J}\right)}{\mu \psi_{rd}} = \sqrt{\frac{\left(\dot{\omega} + \frac{T_L}{J}\right)(\dot{\rho} - \omega)}{\mu \alpha M}} \,. \tag{2.88}$$

In new coordinates $(\omega, \dot{\omega}, \rho, \dot{\rho})$ the dynamics become

$$\begin{aligned}
\begin{bmatrix} \ddot{\omega} \\ \ddot{\rho} \end{bmatrix} &= \begin{bmatrix} -\mu(\gamma+\alpha)\psi_{rd} i_{sq} - \mu\beta\omega\psi_{rd}^2 \\ \mu\psi_{rd} i_{sq} - \frac{T_L}{J} + \frac{\alpha M(\alpha-\gamma) i_{sq}}{\psi_{rd}} - \alpha M \beta \omega \end{bmatrix} \\
&\quad + \begin{bmatrix} \frac{\mu\psi_{rd}}{\sigma} & -\mu\omega\psi_{rd} \\ \frac{\alpha M}{\sigma\psi_{rd}} & -\frac{2\alpha^2 M^2 i_{sq}}{\psi_{rd}^2} - \frac{\alpha M \omega}{\psi_{rd}} \end{bmatrix} \begin{bmatrix} u_{sq} \\ i_{sd} \end{bmatrix} \\
&\triangleq \begin{bmatrix} -\mu(\gamma+\alpha)\psi_{rd} i_{sq} - \mu\beta\omega\psi_{rd}^2 \\ \mu\psi_{rd} i_{sq} - \frac{T_L}{J} + \frac{\alpha M(\alpha-\gamma) i_{sq}}{\psi_{rd}} - \alpha M \beta \omega \end{bmatrix} + D_d \begin{bmatrix} u_{sq} \\ i_{sd} \end{bmatrix} \,.
\end{aligned} \tag{2.89}$$

Since

$$\det[D_d] = -\frac{2\mu\alpha^2 M^2 i_{sq}}{\sigma\psi_{rd}} \,,$$

provided that $\psi_{rd} \neq 0$ and $i_{sq} \neq 0$, the signals u_{sq} and i_{sd} can be uniquely expressed in terms of $(\omega, \dot{\omega}, \ddot{\omega}, \rho, \dot{\rho}, \ddot{\rho})$ from (2.87), (2.88) and (2.89) as

$$\begin{bmatrix} u_{sq} \\ i_{sd} \end{bmatrix} = D_d^{-1} \begin{bmatrix} \ddot{\omega} + \mu(\gamma+\alpha)\psi_{rd} i_{sq} + \mu\beta\omega\psi_{rd}^2 \\ \ddot{\rho} - \mu\psi_{rd} i_{sq} + \frac{T_L}{J} - \frac{\alpha M(\alpha-\gamma) i_{sq}}{\psi_{rd}} + \alpha M \beta \omega \end{bmatrix} \tag{2.90}$$

with ψ_{rd} and i_{sq} given by (2.87) and (2.88). Hence, if a new input v_{sq} is defined as

$$\frac{\mathrm{d}u_{sq}}{\mathrm{d}t} = \frac{v_{sq}}{\sigma} \tag{2.91}$$

so that the variable u_{sq} becomes an additional state, (1.39) together with (2.91) become

$$\begin{aligned}
\frac{\mathrm{d}\omega}{\mathrm{d}t} &= \mu\psi_{rd} i_{sq} - \frac{T_L}{J} \\
\frac{\mathrm{d}i_{sq}}{\mathrm{d}t} &= -\gamma i_{sq} - \omega i_{sd} - \frac{\alpha M i_{sd} i_{sq}}{\psi_{rd}} - \beta\omega\psi_{rd} + \frac{u_{sq}}{\sigma} \\
\frac{\mathrm{d}u_{sq}}{\mathrm{d}t} &= \frac{v_{sq}}{\sigma} \\
\frac{\mathrm{d}\rho}{\mathrm{d}t} &= \omega + \frac{\alpha M i_{sq}}{\psi_{rd}}
\end{aligned}$$

$$\begin{aligned}\frac{\mathrm{d}\psi_{rd}}{\mathrm{d}t} &= -\alpha\psi_{rd} + \alpha M i_{sd} \\ \frac{\mathrm{d}i_{sd}}{\mathrm{d}t} &= -\gamma i_{sd} + \omega i_{sq} + \frac{\alpha M i_{sq}^2}{\psi_{rd}} + \beta\alpha\psi_{rd} + \frac{u_{sd}}{\sigma}\end{aligned} \tag{2.92}$$

in which $(\omega, i_{sq}, u_{sq}, \rho, \psi_{rd}, i_{sd})$ are the state variables and (v_{sq}, u_{sd}) are the control input variables. From (2.87), (2.88), and (2.90) it follows that $(\omega, \dot{\omega}, \ddot{\omega}, \rho, \dot{\rho}, \ddot{\rho})$ defined in (2.86) and (2.89) constitute an equivalent set of state variables if $\psi_{rd} \neq 0$ and $i_{sq} \neq 0$ since $(\omega, i_{sq}, u_{sq}, \rho, \psi_{rd}, i_{sd})$ can be uniquely expressed in terms of $(\omega, \dot{\omega}, \ddot{\omega}, \rho, \dot{\rho}, \ddot{\rho})$. Hence, differentiating (2.89) with respect to time we can express the dynamics (2.92) in new coordinates $(\omega, \dot{\omega}, \ddot{\omega}, \rho, \dot{\rho}, \ddot{\rho})$ as follows

$$\begin{bmatrix}\dddot{\omega} \\ \dddot{\rho}\end{bmatrix} = \begin{bmatrix}\Phi_\omega \\ \Phi_\rho\end{bmatrix} + \frac{D_d}{\sigma}\begin{bmatrix}v_{sq} \\ u_{sd}\end{bmatrix}$$

with

$$\begin{aligned}\Phi_\omega &= -\mu(\gamma+\alpha)[\Delta_1 i_{sq} + \Delta_2\psi_{rd}] - \mu\beta[\Delta_3\psi_{rd}^2 + 2\omega\psi_{rd}\Delta_1] \\ &\quad + \frac{\mu\Delta_1 u_{sq}}{\sigma} - \mu\Delta_1\omega i_{sd} - \mu\omega\psi_{rd}\Delta_4 - \mu\Delta_3\psi_{rd} i_{sd} \\ \Phi_\rho &= \mu\Delta_1 i_{sq} + \mu\psi_{rd}\Delta_2 + \frac{\alpha M(\alpha-\gamma)\Delta_2}{\psi_{rd}} - \frac{\alpha M(\alpha-\gamma) i_{sq}\Delta_1}{\psi_{rd}^2} - \alpha M\beta\Delta_3 \\ &\quad - \frac{\alpha M\Delta_1 u_{sq}}{\sigma\psi_{rd}^2} - \frac{\alpha M\Delta_3 i_{sd}}{\psi_{rd}} + \frac{\alpha M\omega\Delta_1 i_{sd}}{\psi_{rd}^2} - \frac{2\alpha^2 M^2\Delta_2 i_{sd}}{\psi_{rd}^2} \\ &\quad + \frac{4\alpha^2 M^2 i_{sq} i_{sd}\Delta_1}{\psi_{rd}^3} - \left(\frac{2\alpha^2 M^2 i_{sq}}{\psi_{rd}^2} + \frac{\alpha M\omega}{\psi_{rd}}\right)\Delta_4\end{aligned}$$

and

$$\begin{aligned}\Delta_1 &= -\alpha\psi_{rd} + \alpha M i_{sd} \\ \Delta_2 &= -\gamma i_{sq} - \omega i_{sd} - \frac{\alpha M i_{sd} i_{sq}}{\psi_{rd}} - \beta\omega\psi_{rd} + \frac{u_{sq}}{\sigma} \\ \Delta_3 &= \mu\psi_{rd} i_{sq} - \frac{T_L}{J} \\ \Delta_4 &= -\gamma i_{sd} + \omega i_{sq} + \frac{\alpha M i_{sq}^2}{\psi_{rd}} + \beta\alpha\psi_{rd}\,.\end{aligned}$$

By defining the state feedback control law

$$\begin{bmatrix}v_{sq} \\ u_{sd}\end{bmatrix} = \sigma D_d^{-1}\begin{bmatrix}-\Phi_\omega - k_{\omega 1}(\omega-\omega^*) - k_{\omega 2}(\dot{\omega}-\dot{\omega}^*) - k_{\omega 3}(\ddot{\omega}-\ddot{\omega}^*) + \dddot{\omega}^* \\ -\Phi_\rho - k_{\rho 1}(\rho-\rho^*) - k_{\rho 2}(\dot{\rho}-\dot{\rho}^*) - k_{\rho 3}(\ddot{\rho}-\ddot{\rho}^*) + \dddot{\rho}^*\end{bmatrix}$$

the closed-loop linear dynamics are obtained

$$\begin{aligned}\frac{\mathrm{d}^3\tilde{\omega}}{\mathrm{d}t^3} &= -k_{\omega 1}\tilde{\omega} - k_{\omega 2}\frac{\mathrm{d}\tilde{\omega}}{\mathrm{d}t} - k_{\omega 3}\frac{\mathrm{d}^2\tilde{\omega}}{\mathrm{d}t^2}\\ \frac{\mathrm{d}^3\tilde{\rho}}{\mathrm{d}t^3} &= -k_{\rho 1}\tilde{\rho} - k_{\rho 2}\frac{\mathrm{d}\tilde{\rho}}{\mathrm{d}t} - k_{\rho 3}\frac{\mathrm{d}^2\tilde{\rho}}{\mathrm{d}t^2}\end{aligned} \tag{2.93}$$

with $\tilde{\omega} = \omega - \omega^*$, $\tilde{\rho} = \rho - \rho^*$, ρ^* defined in (1.70) and $k_{\omega 1}, k_{\omega 2}, k_{\omega 3}, k_{\rho 1}, k_{\rho 2}, k_{\rho 3}$ positive control parameters such that all the roots of the polynomials

$$\begin{aligned}\pi_\omega(s) &= s^3 + k_{\omega 3}s^2 + k_{\omega 2}s + k_{\omega 1}\\ \pi_\rho(s) &= s^3 + k_{\rho 3}s^2 + k_{\rho 2}s + k_{\rho 1}\end{aligned}$$

have negative real parts.

In conclusion: the *dynamic feedback linearizing control* is defined as

$$\begin{bmatrix} u_{sa}\\ u_{sb}\end{bmatrix} = \begin{bmatrix}\cos\rho & -\sin\rho\\ \sin\rho & \cos\rho\end{bmatrix}\begin{bmatrix} u_{sd}\\ u_{sq}\end{bmatrix}$$

$$\frac{\mathrm{d}u_{sq}}{\mathrm{d}t} = \frac{v_{sq}}{\sigma}$$

$$\begin{bmatrix} v_{sq}\\ v_{sd}\end{bmatrix} = \sigma D_d^{-1}\begin{bmatrix} -\Phi_\omega - k_{\omega 1}(\omega-\omega^*) - k_{\omega 2}(\dot{\omega}-\dot{\omega}^*) - k_{\omega 3}(\ddot{\omega}-\ddot{\omega}^*) + \dddot{\omega}^*\\ -\Phi_\rho - k_{\rho 1}(\rho-\rho^*) - k_{\rho 2}(\dot{\rho}-\dot{\rho}^*) - k_{\rho 3}(\ddot{\rho}-\ddot{\rho}^*) + \dddot{\rho}^*\end{bmatrix}$$

$$\dot{\rho} = \omega + \frac{\alpha M i_{sq}}{\psi_{rd}}$$

$$\dot{\rho}^* = \omega^* + \frac{\alpha M T_L}{\mu J \psi^{*2}},\quad \rho^*(0) = \arctan\left(\frac{\psi_{rb}(0)}{\psi_{ra}(0)}\right)$$

$$\psi_{rd} = \psi_{ra}\cos\rho + \psi_{rb}\sin\rho$$

$$\begin{bmatrix} i_{sd}\\ i_{sq}\end{bmatrix} = \begin{bmatrix}\cos\rho & \sin\rho\\ -\sin\rho & \cos\rho\end{bmatrix}\begin{bmatrix} i_{sa}\\ i_{sb}\end{bmatrix}$$

$$\begin{aligned}\Phi_\omega = {} & -\mu(\gamma+\alpha)[\Delta_1 i_{sq} + \Delta_2\psi_{rd}] - \mu\beta[\Delta_3\psi_{rd}^2 + 2\omega\psi_{rd}\Delta_1]\\ & + \frac{\mu\Delta_1 u_{sq}}{\sigma} - \mu\Delta_1\omega i_{sd} - \mu\omega\psi_{rd}\Delta_4 - \mu\Delta_3\psi_{rd}i_{sd}\end{aligned}$$

$$\begin{aligned}\Phi_\rho = {} & \mu\Delta_1 i_{sq} + \mu\psi_{rd}\Delta_2 + \frac{\alpha M(\alpha-\gamma)\Delta_2}{\psi_{rd}} - \frac{\alpha M(\alpha-\gamma)i_{sq}\Delta_1}{\psi_{rd}^2} - \alpha M\beta\Delta_3\\ & - \frac{\alpha M\Delta_1 u_{sq}}{\sigma\psi_{rd}^2} - \frac{\alpha M\Delta_3 i_{sd}}{\psi_{rd}} + \frac{\alpha M\omega\Delta_1 i_{sd}}{\psi_{rd}^2} - \frac{2\alpha^2M^2\Delta_2 i_{sd}}{\psi_{rd}^2}\\ & + \frac{4\alpha^2M^2 i_{sq}i_{sd}\Delta_1}{\psi_{rd}^3} - \left(\frac{2\alpha^2M^2 i_{sq}}{\psi_{rd}^2} + \frac{\alpha M\omega}{\psi_{rd}}\right)\Delta_4\end{aligned}$$

$$\Delta_1 = -\alpha\psi_{rd} + \alpha M i_{sd}$$

$$\Delta_2 = -\gamma i_{sq} - \omega i_{sd} - \frac{\alpha M i_{sd}i_{sq}}{\psi_{rd}} - \beta\omega\psi_{rd} + \frac{u_{sq}}{\sigma}$$

$$\Delta_3 = \mu \psi_{rd} i_{sq} - \frac{T_L}{J}$$
$$\Delta_4 = -\gamma i_{sd} + \omega i_{sq} + \frac{\alpha M i_{sq}^2}{\psi_{rd}} + \beta \alpha \psi_{rd} \; ; \tag{2.94}$$

it is a third order dynamic nonlinear feedback control algorithm which depends on the measurements of the state variables $(\omega, \psi_{ra}, \psi_{rb}, i_{sa}, i_{sb})$, on the reference signals (ω^*, ψ^*), on the positive control parameters $k_{\omega 1}$, $k_{\omega 2}$, $k_{\omega 3}$, $k_{\rho 1}$, $k_{\rho 2}$, $k_{\rho 3}$, on the load torque T_L, and on the machine parameters M, R_r, L_r, J, R_s, L_s, since $\mu = \dfrac{M}{JL_r}$, $\alpha = \dfrac{R_r}{L_r}$, $\sigma = L_s \left(1 - \dfrac{M^2}{L_s Lr}\right)$, $\beta = \dfrac{M}{\sigma L_r}$, $\gamma = \dfrac{R_s}{\sigma} + \beta \alpha M$; it guarantees that, for suitable initial and operating conditions such that $\psi_{rd}(t) \geq c_1 > 0$ and $i_{sq}(t) \geq c_2 > 0$ for all $t \geq 0$, the rotor speed and flux angle tracking errors have decoupled dynamics and decay exponentially to zero according to (2.93), with c_1 and c_2 depending on the initial tracking errors.

Illustrative Simulations

We tested the dynamic feedback linearizing control by simulations for the three-phase single pole pair 0.6-kW induction motor whose parameters have been reported in Chapter 1. All the motor initial conditions have been set equal to zero except for $\psi_{ra}(0) = \psi_{rb}(0) = 0.1\,\text{Wb}$. The motor is driven by the feedforward control until $t = 0.7\,\text{s}$ in order to avoid the singularities appearing in the dynamic feedback linearizing control; at $t = 0.7\,\text{s}$ the dynamic feedback linearizing control is applied. The control parameters used in the simulation are (all the values are in SI units): $k_{\omega 1} = 10^6$, $k_{\omega 2} = 3 \times 10^4$, $k_{\omega 3} = 3 \times 10^2$, $k_{\rho 1} = 10^6$, $k_{\rho 2} = 3 \times 10^4$, $k_{\rho 3} = 3 \times 10^2$; real coincident eigenvalues are assigned to the matrices associated to the decoupled, linear time-invariant third order systems (2.93). The controller initial condition has been set equal to $u_{sq}(0) = 171.46922\,\text{V}$ in order to avoid discontinuities at the switching time $t = 0.7\,\text{s}$. The references for the speed and flux modulus along with the applied load torque are reported in Figures 2.36–2.38. The rotor flux modulus reference signal starts from 0.001 Wb at $t = 0\,\text{s}$ and grows up to the constant value 1.16 Wb. The speed reference is zero until $t = 0.32\,\text{s}$ and grows up to the constant value 100 rad/s. A 5.8-Nm load torque is applied to the motor and is reduced to 4.8 Nm. Figures 2.37 and 2.38 show the time histories of the rotor speed and rotor flux modulus along with the corresponding tracking errors: the rotor speed and rotor flux modulus track their references. Note that at $t = 1.5\,\text{s}$ the speed and flux modulus tracking errors are perturbed by the uncompensated load torque time derivatives.

Finally, the stator current and voltages profiles, which are within the physical saturation limits, are reported in Figures 2.39 and 2.40.

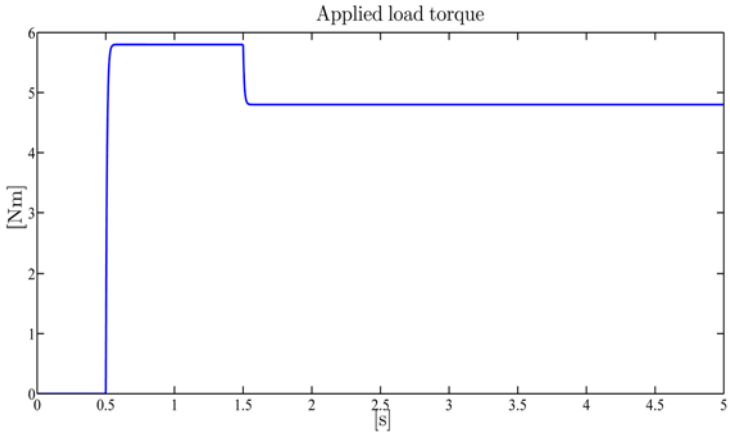

Fig. 2.36 Dynamic feedback linearizing control: applied load torque T_L

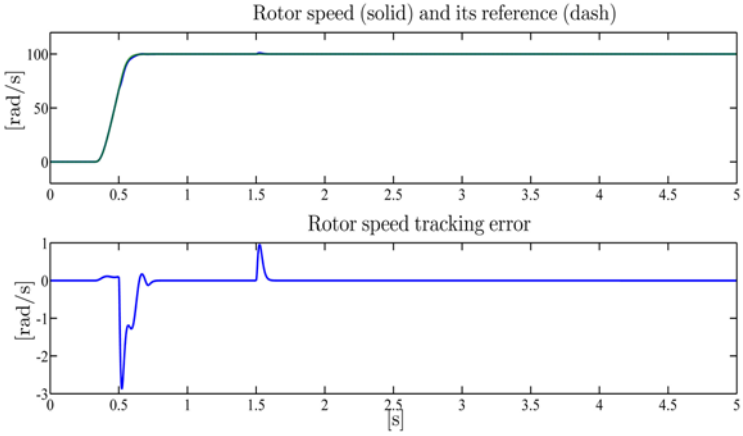

Fig. 2.37 Dynamic feedback linearizing control: rotor speed ω and its reference ω^*; rotor speed tracking error

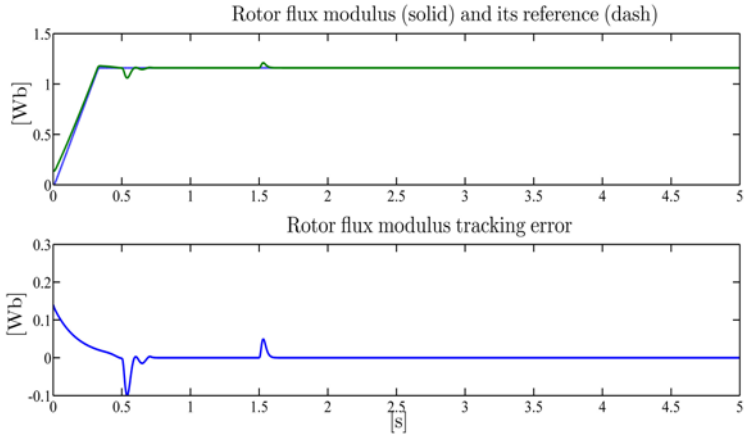

Fig. 2.38 Dynamic feedback linearizing control: rotor flux modulus $\sqrt{\psi_{ra}^2 + \psi_{rb}^2}$ and its reference ψ^*; rotor flux modulus tracking error

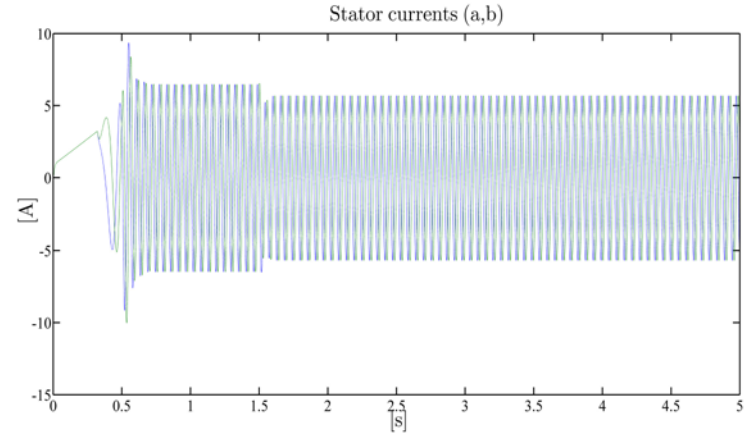

Fig. 2.39 Dynamic feedback linearizing control: stator current vector (a,b)-components (i_{sa}, i_{sb})

2.7 Global Control with Arbitrary Rate of Convergence

The goal of this section is to improve the indirect field-oriented control presented in Section 2.3, which has the advantage of allowing for any motor initial condition but has the drawback of not guaranteeing exponential tracking of reference signals $(\omega^*(t), \psi^*(t))$ with arbitrary rate of convergence. On the other hand, we have seen in Section 2.4 that it is possible to design a state feedback control which achieves exponential tracking with arbitrary rate from sufficiently small initial errors. We would like to bridge the gap between these two control schemes. To this end, we reconsider the control algorithm (2.48) and modify the reference for the stator current

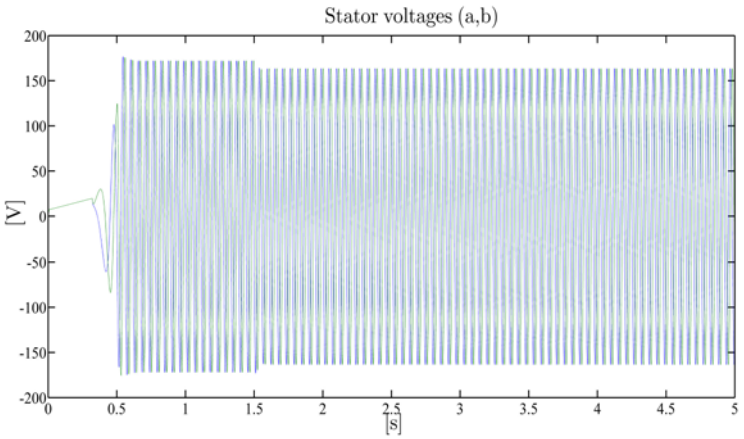

Fig. 2.40 Dynamic feedback linearizing control: stator voltage vector (a,b)-components (u_{sa}, u_{sb})

vector d-component and the speed of the rotating (d,q) frame as follows:

$$\begin{aligned} i_{sd}^{*} &= \frac{\psi^{*}}{M} + \frac{\dot{\psi}^{*}}{\alpha M} + \frac{\eta_d}{\alpha M} \\ \omega_0 &= \omega + \frac{\alpha M i_{sq}}{\psi^{*}} - \frac{\eta_q}{\psi^{*}} , \end{aligned} \tag{2.95}$$

i.e. by adding two feedback terms η_d and η_q which will be designed in the following. The reference for the stator current vector q-component remains the same as in (2.48), *i.e.*

$$i_{sq}^{*} = \frac{1}{\mu \psi^{*}} \left[-k_\omega (\omega - \omega^{*}) + \dot{\omega}^{*} + \frac{T_L}{J} \right] . \tag{2.96}$$

Introduce the tracking errors

$$\begin{aligned} \tilde{\omega} &= \omega - \omega^{*} \\ \tilde{\psi}_{rd} &= \psi_{rd} - \psi^{*} \\ \tilde{\psi}_{rq} &= \psi_{rq} \\ \tilde{i}_{sd} &= i_{sd} - i_{sd}^{*} \\ \tilde{i}_{sq} &= i_{sq} - i_{sq}^{*} \end{aligned}$$

for the rotor speed, rotor flux vector (d,q)-components and stator current vector (d,q)-components, respectively. The dynamics for $\tilde{\omega}$, $\tilde{\psi}_{rd}$, and $\tilde{\psi}_{rq}$ are given by

$$\begin{aligned} \dot{\tilde{\omega}} &= -k_\omega \tilde{\omega} + \mu (\tilde{\psi}_{rd} i_{sq} - \tilde{\psi}_{rq} i_{sd}) + \mu \psi^{*} \tilde{i}_{sq} \\ \dot{\tilde{\psi}}_{rd} &= -\alpha \tilde{\psi}_{rd} + (\omega_0 - \omega) \tilde{\psi}_{rq} + \alpha M \tilde{i}_{sd} + \eta_d \\ \dot{\tilde{\psi}}_{rq} &= -\alpha \tilde{\psi}_{rq} - (\omega_0 - \omega) \tilde{\psi}_{rd} + \eta_q . \end{aligned} \tag{2.97}$$

In order to design the additional undetermined terms η_d and η_q in (2.95), we introduce the positive control parameter λ and consider the Lyapunov function

$$W = \frac{1}{2}\left(\lambda\tilde{\omega}^2 + \tilde{\psi}_{rd}^2 + \tilde{\psi}_{rq}^2\right) \tag{2.98}$$

whose time derivative along the trajectories of (2.97) is

$$\begin{aligned}\dot{W} = &-\lambda k_\omega \tilde{\omega}^2 + \lambda\mu(\tilde{\psi}_{rd} i_{sq} - \tilde{\psi}_{rq} i_{sd})\tilde{\omega} + \lambda\mu\psi^* \tilde{i}_{sq}\tilde{\omega} \\ &-\alpha(\tilde{\psi}_{rd}^2 + \tilde{\psi}_{rq}^2) + \alpha M \tilde{i}_{sd}\tilde{\psi}_{rd} + \eta_d\tilde{\psi}_{rd} + \eta_q\tilde{\psi}_{rq}\,.\end{aligned} \tag{2.99}$$

Since $i_{sq} = \tilde{i}_{sq} + i_{sq}^*$, we define the additive feedback terms in (2.95) as

$$\begin{aligned}\eta_d &= -k_\psi(\psi_{rd} - \psi^*) - \lambda\mu i_{sq}^*\tilde{\omega} \\ \eta_q &= -k_\psi\psi_{rq} + \lambda\mu i_{sd}\tilde{\omega}\end{aligned} \tag{2.100}$$

in which k_ψ is a positive control parameter and (ψ_{rd}, ψ_{rq}) are the measured rotor flux vector components in the (d,q) frame which is identified by the rotating angle ε_0, whose dynamics are

$$\frac{\mathrm{d}\varepsilon_0}{\mathrm{d}t} = \omega_0 = \omega + \frac{\alpha M i_{sq}}{\psi^*} + \frac{k_\psi\psi_{rq}}{\psi^*} - \frac{\lambda\mu i_{sd}\tilde{\omega}}{\psi^*}$$

with arbitrary initial condition $\varepsilon_0(0)$. Recall that

$$\begin{bmatrix}\psi_{rd}\\ \psi_{rq}\end{bmatrix} = \begin{bmatrix}\cos\varepsilon_0 & \sin\varepsilon_0\\ -\sin\varepsilon_0 & \cos\varepsilon_0\end{bmatrix}\begin{bmatrix}\psi_{ra}\\ \psi_{rb}\end{bmatrix}$$
$$\begin{bmatrix}i_{sd}\\ i_{sq}\end{bmatrix} = \begin{bmatrix}\cos\varepsilon_0 & \sin\varepsilon_0\\ -\sin\varepsilon_0 & \cos\varepsilon_0\end{bmatrix}\begin{bmatrix}i_{sa}\\ i_{sb}\end{bmatrix}.$$

By substituting (2.100) in (2.99) we obtain

$$\dot{W} = -\lambda k_\omega\tilde{\omega}^2 - (\alpha + k_\psi)(\tilde{\psi}_{rd}^2 + \tilde{\psi}_{rq}^2) + \lambda\mu\psi_{rd}\tilde{i}_{sq}\tilde{\omega} + \alpha M\tilde{i}_{sd}\tilde{\psi}_{rd}\,. \tag{2.101}$$

Note that the feedback terms depending on the arbitrary control parameter k_ψ introduced in (2.100) are beneficial since k_ψ is added to the given motor parameter α in (2.101). The influence of the last two terms in (2.101) will then be compensated by a suitable choice of the stator voltages (u_{sd}, u_{sq}). To this end, let us compute

$$\frac{\mathrm{d}i_{sq}^*}{\mathrm{d}t} = \Gamma_q \tag{2.102}$$

in which the term Γ_q depending on known signals is

$$\Gamma_q = \frac{1}{\mu\psi^*}\left[k_\omega^2\tilde{\omega} - k_\omega\mu\psi^*\tilde{i}_{sq} + \ddot{\omega}^*\right] - \frac{\dot{\psi}^*}{\mu\psi^{*2}}\left[-k_\omega\tilde{\omega} + \frac{T_L}{J} + \dot{\omega}^*\right]$$

$$-\frac{k_\omega i_{sq}}{\psi^*}\tilde{\psi}_{rd}+\frac{k_\omega i_{sd}}{\psi^*}\tilde{\psi}_{rq}\,. \tag{2.103}$$

Similarly, let us compute

$$\frac{\mathrm{d}i^*_{sd}}{\mathrm{d}t}=\Gamma_d \tag{2.104}$$

in which the term Γ_d depending on known signals is

$$\begin{aligned}\Gamma_d=&\frac{\dot{\psi}^*}{M}+\frac{\ddot{\psi}^*}{\alpha M}-\frac{\lambda\mu^2\psi^*\tilde{i}_{sq}i^*_{sq}}{\alpha M}-\frac{\lambda\mu\Gamma_q\tilde{\omega}}{\alpha M}+\frac{\lambda\mu k_\omega\tilde{\omega}i^*_{sq}}{\alpha M}+\frac{k_\psi\dot{\psi}^*}{\alpha M}\\&-\frac{k_\psi}{\alpha M}\left[-\alpha\psi_{rd}+(\omega_0-\omega)\psi_{rq}+\alpha M i_{sd}\right]\\&-\frac{\lambda\mu^2\tilde{\psi}_{rd}i_{sq}i^*_{sq}}{\alpha M}+\frac{\lambda\mu^2\tilde{\psi}_{rq}i_{sd}i^*_{sq}}{\alpha M}\,.\end{aligned} \tag{2.105}$$

On the basis of (2.102) and (2.104) the dynamics for the stator currents tracking errors $\tilde{i}_{sd}$ and $\tilde{i}_{sq}$ can be computed as follows

$$\begin{aligned}\frac{\mathrm{d}\tilde{i}_{sd}}{\mathrm{d}t}&=-\gamma i_{sd}+\omega_0 i_{sq}+\alpha\beta\psi_{rd}+\beta\omega\psi_{rq}+\frac{u_{sd}}{\sigma}-\Gamma_d\\\frac{\mathrm{d}\tilde{i}_{sq}}{\mathrm{d}t}&=-\gamma i_{sq}-\omega_0 i_{sd}+\alpha\beta\psi_{rq}-\beta\omega\psi_{rd}+\frac{u_{sq}}{\sigma}-\Gamma_q\,.\end{aligned} \tag{2.106}$$

Design the control inputs (u_{sd},u_{sq}) as

$$\begin{aligned}u_{sd}&=\sigma\left[\gamma i^*_{sd}-\omega_0 i_{sq}-\alpha\beta\psi_{rd}-\beta\omega\psi_{rq}+\Gamma_d-k_i\tilde{i}_{sd}+v_d\right]\\u_{sq}&=\sigma\left[\gamma i^*_{sq}+\omega_0 i_{sd}-\alpha\beta\psi_{rq}+\beta\omega\psi_{rd}+\Gamma_q-k_i\tilde{i}_{sq}+v_q\right]\end{aligned} \tag{2.107}$$

where v_d and v_q are yet to be designed and k_i is a positive control parameter, so that (2.106) becomes

$$\begin{aligned}\frac{\mathrm{d}\tilde{i}_{sd}}{\mathrm{d}t}&=-(\gamma+k_i)\tilde{i}_{sd}+v_d\\\frac{\mathrm{d}\tilde{i}_{sq}}{\mathrm{d}t}&=-(\gamma+k_i)\tilde{i}_{sq}+v_q\,.\end{aligned} \tag{2.108}$$

In order to choose the undefined terms v_d and v_q, consider the Lyapunov function for the overall tracking error dynamics

$$V=W+\frac{1}{2}\left(\tilde{i}^2_{sd}+\tilde{i}^2_{sq}\right) \tag{2.109}$$

whose time derivative along the trajectories of the closed-loop system (2.97), (2.106) and (2.107) satisfies

$$\dot{V}=-\lambda k_\omega\tilde{\omega}^2-\left(\alpha+k_\psi\right)\left(\tilde{\psi}^2_{rd}+\tilde{\psi}^2_{rq}\right)+\lambda\mu\psi_{rd}\tilde{i}_{sq}\tilde{\omega}+\alpha M\tilde{i}_{sd}\tilde{\psi}_{rd}$$

$$-(\gamma+k_i)(\tilde{i}_{sd}^2+\tilde{i}_{sq}^2)+v_d\tilde{i}_{sd}+v_q\tilde{i}_{sq}\,. \tag{2.110}$$

If we design the yet undefined terms v_d and v_q as

$$\begin{aligned} v_d &= -\alpha M\tilde{\psi}_{rd} \\ v_q &= -\lambda\mu\psi_{rd}\tilde{\omega} \end{aligned} \tag{2.111}$$

then from (2.110) we obtain

$$\begin{aligned} \dot{V} &\le -\lambda k_\omega\tilde{\omega}^2-\left(\alpha+k_\psi\right)\left(\tilde{\psi}_{rd}^2+\tilde{\psi}_{rq}^2\right)-(\gamma+k_i)(\tilde{i}_{sd}^2+\tilde{i}_{sq}^2) \\ &\le -2\min\{k_\omega,\alpha+k_\psi,\gamma+k_i\}V\,. \end{aligned} \tag{2.112}$$

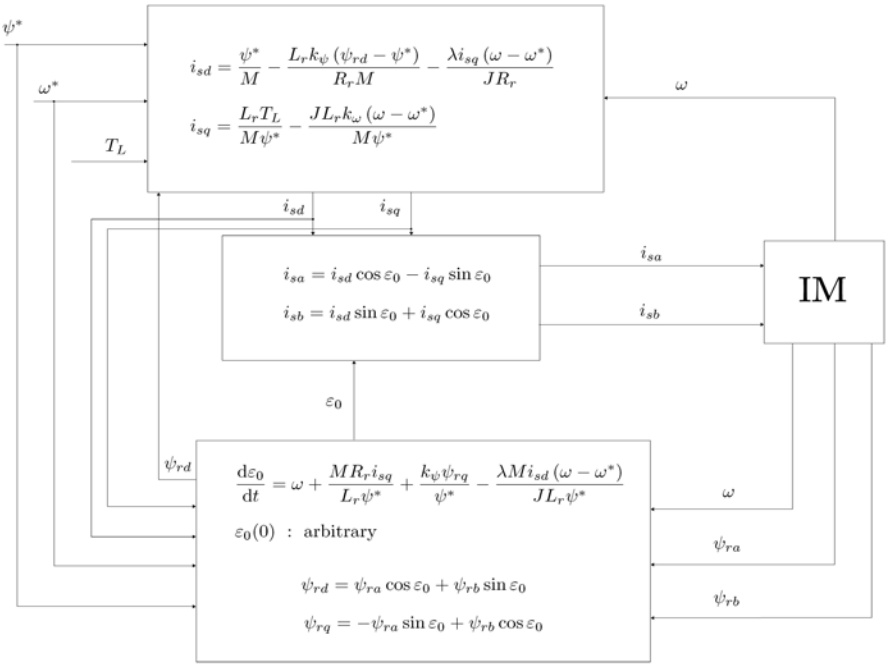

Fig. 2.41 Global control with arbitrary rate of convergence for current-fed motors (constant references ω^*, ψ^*)

In conclusion, the first order nonlinear state feedback *global control with arbitrary rate of convergence* (see Figure 2.41)

$$
\begin{aligned}
u_{sd} &= \sigma\left[\gamma i_{sd}^{*} - \omega_0 i_{sq} - \alpha\beta\psi_{rd} - \beta\omega\psi_{rq} + \Gamma_d - k_i(i_{sd} - i_{sd}^{*}) + v_d\right] \\
u_{sq} &= \sigma\left[\gamma i_{sq}^{*} + \omega_0 i_{sd} - \alpha\beta\psi_{rq} + \beta\omega\psi_{rd} + \Gamma_q - k_i(i_{sq} - i_{sq}^{*}) + v_q\right] \\
v_d &= -\alpha M(\psi_{rd} - \psi^{*}) \\
v_q &= -\lambda\mu\psi_{rd}(\omega - \omega^{*})
\end{aligned}
\tag{2.113}
$$

with Γ_d and Γ_q given in (2.105) and (2.103) and

$$
\begin{aligned}
\begin{bmatrix} u_{sa} \\ u_{sb} \end{bmatrix} &= \begin{bmatrix} \cos\varepsilon_0 & -\sin\varepsilon_0 \\ \sin\varepsilon_0 & \cos\varepsilon_0 \end{bmatrix} \begin{bmatrix} u_{sd} \\ u_{sq} \end{bmatrix} \\
i_{sd}^{*} &= \frac{\psi^{*}}{M} + \frac{\dot{\psi}^{*}}{\alpha M} + \frac{\eta_d}{\alpha M} \\
i_{sq}^{*} &= \frac{1}{\mu\psi^{*}}\left[-k_\omega(\omega - \omega^{*}) + \dot{\omega}^{*} + \frac{T_L}{J}\right] \\
\frac{\mathrm{d}\varepsilon_0}{\mathrm{d}t} = \omega_0 &= \omega + \frac{\alpha M i_{sq}}{\psi^{*}} - \frac{\eta_q}{\psi^{*}} \\
\eta_d &= -k_\psi(\psi_{rd} - \psi^{*}) - \lambda\mu i_{sq}^{*}(\omega - \omega^{*}) \\
\eta_q &= -k_\psi\psi_{rq} + \lambda\mu i_{sd}(\omega - \omega^{*}) \\
\begin{bmatrix} i_{sd} \\ i_{sq} \end{bmatrix} &= \begin{bmatrix} \cos\varepsilon_0 & \sin\varepsilon_0 \\ -\sin\varepsilon_0 & \cos\varepsilon_0 \end{bmatrix} \begin{bmatrix} i_{sa} \\ i_{sb} \end{bmatrix} \\
\begin{bmatrix} \psi_{rd} \\ \psi_{rq} \end{bmatrix} &= \begin{bmatrix} \cos\varepsilon_0 & \sin\varepsilon_0 \\ -\sin\varepsilon_0 & \cos\varepsilon_0 \end{bmatrix} \begin{bmatrix} \psi_{ra} \\ \psi_{rb} \end{bmatrix}
\end{aligned}
\tag{2.114}
$$

with (k_ω, k_ψ, k_i) arbitrary positive design parameters, is such that $(\omega - \omega^{*})$, $(\psi_{rd} - \psi^{*})$, ψ_{rq}, $(i_{sd} - i_{sd}^{*})$, $(i_{sq} - i_{sq}^{*})$ tend exponentially to zero from any initial condition with arbitrary rate of convergence $\min\{k_\omega, \alpha + k_\psi, \gamma + k_i\}$.

As we shall see, in Chapter 4 a global adaptive version of the controller (2.114) will be presented which does not rely on rotor flux measurements and is adaptive with respect to both critical parameters T_L and α: no arbitrary exponential rate of convergence will, however, be obtained when the parameters T_L and α are uncertain.

Illustrative Simulations

We tested the global control with arbitrary rate of convergence by simulations for the three-phase single pole pair 0.6-kW induction motor whose parameters have been reported in Chapter 1. All the motor and controller initial conditions have been set to zero except for $\psi_{ra}(0) = \psi_{rb}(0) = 0.1\,\mathrm{Wb}$. The control parameters are (all values are in SI units) $\lambda = 0.005$, $k_\omega = 450$, $k_i = 800$, $k_\psi = 12$. The references for the speed and flux modulus along with the applied load torque are reported in

Figures 2.42–2.44. The rotor flux modulus reference signal starts from 0.01 Wb at $t = 0$ s and grows up to the constant value 1.16 Wb. The speed reference is zero until $t = 0.32$ s and grows up to the constant value 100 rad/s; at $t = 1.5$ s the speed is required to go up to the value 200 rad/s, while the reference for the flux modulus is reduced to 0.5 Wb. A 5.8-Nm load torque is applied to the motor and is reduced to 1.8 Nm. Figures 2.43 and 2.44 show the time histories of the rotor speed and the flux modulus along with the corresponding tracking errors: the rotor speed and the flux modulus track their references tightly. Finally, the stator current and voltages profiles (which are within physical saturation limits) are reported in Figures 2.45 and 2.46.

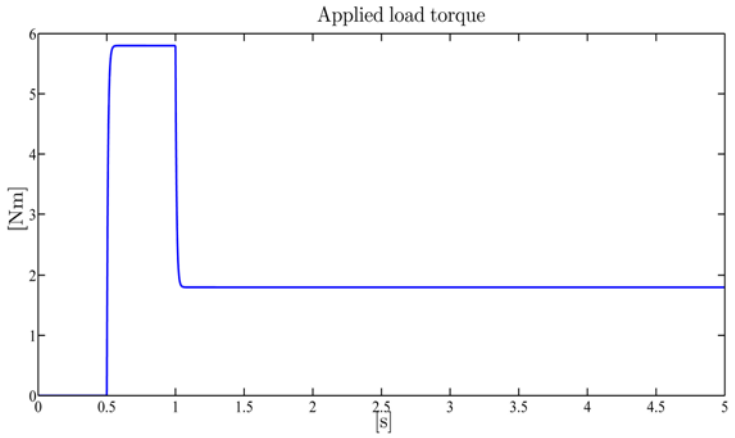

Fig. 2.42 Global control with arbitrary rate of convergence: applied load torque T_L

2.8 Experimental Results

Two experiments have been performed in order to test how critical the parameter α is in practice. The indirect field-oriented control (2.49) has been tested with u_{sd} and u_{sq} in (2.50) simplified by PI controls on the current errors $i_{sd} - i_{sd}^*$ and $i_{sq} - i_{sq}^*$ and T_L replaced by its estimate (2.115) (see Problem 2.5), in which in place of the true value of α a constant estimate $\hat{\alpha}$ has been used. The reference signals for speed and rotor flux modulus in the experiments are reported in Figure 2.47: the flux modulus is first required to reach its desired value of 1.16 Wb before 0.5 s when the rotor speed is then required to reach its desired value of 100 rad/s. After start-up, a constant load torque of 5.8 Nm is applied. In the first experiment $\hat{\alpha}$ underestimates the correct value of α, *i.e.* $\hat{\alpha}/\alpha = 0.7$, while in the second one α is overestimated, *i.e.* $\hat{\alpha}/\alpha = 1.5$. The following control parameters and initial conditions have been used: $k_\omega = 300$, $k_T = 187$, $\hat{T}_L(0) = 0$, $\varepsilon_0(0) = 0$. The gains k_P and k_I of the PI controllers

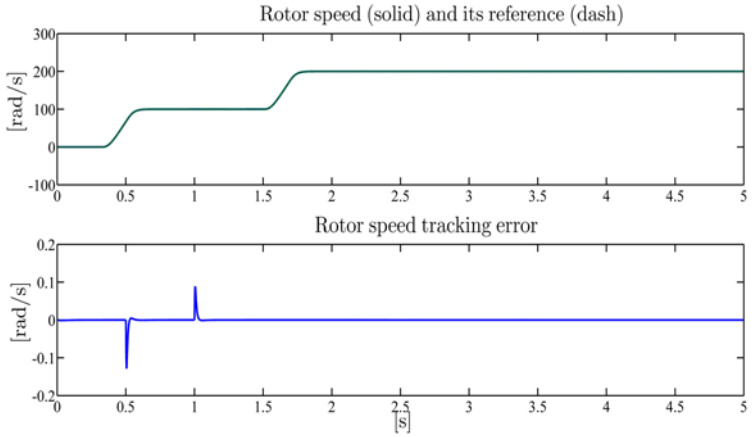

Fig. 2.43 Global control with arbitrary rate of convergence: rotor speed ω and its reference ω^*; rotor speed tracking error

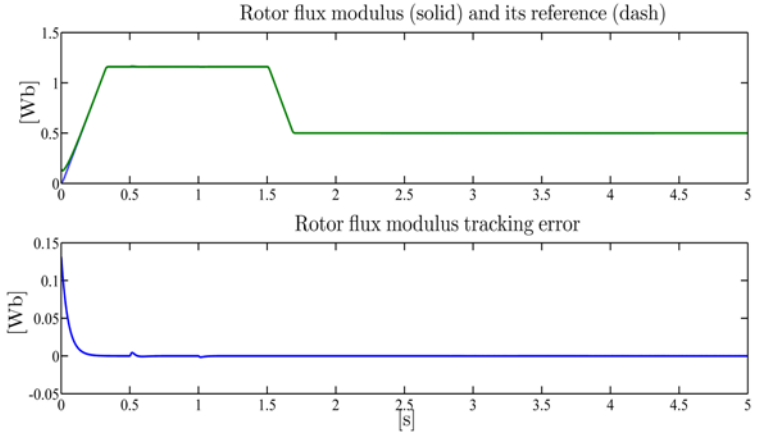

Fig. 2.44 Global control with arbitrary rate of convergence: rotor flux modulus $\sqrt{\psi_{ra}^2 + \psi_{rb}^2}$ and its reference ψ^*; rotor flux modulus tracking error

for the voltages (u_{sd}, u_{sq}) are chosen so that a unit step reference is tracked with a settling time of about 2.5 ms. The flux is estimated by the open-loop rotor flux observer (3.8) which will be given in Section 3.1.1 (converging outside the magnetic saturation region), which makes use of the true value of α. The performance achieved by the controller in the two cases are reported in Figures 2.48 and 2.49: while the speed error is still satisfactory, the flux modulus is above the reference rated value when $\hat{\alpha}/\alpha = 0.7$ and below when $\hat{\alpha}/\alpha = 1.5$ and, therefore, the power efficiency degrades. In both cases higher i_q currents (when compared with the corresponding i_q obtained in simulations) are required to produce the rated torque: this is

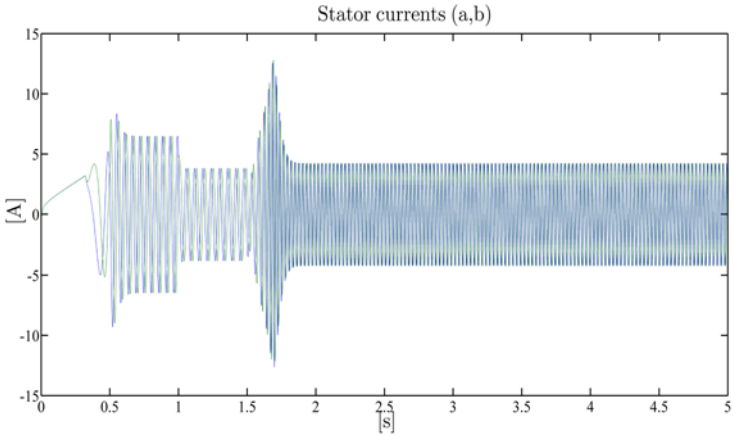

Fig. 2.45 Global control with arbitrary rate of convergence: stator current vector (a,b)-components (i_{sa}, i_{sb})

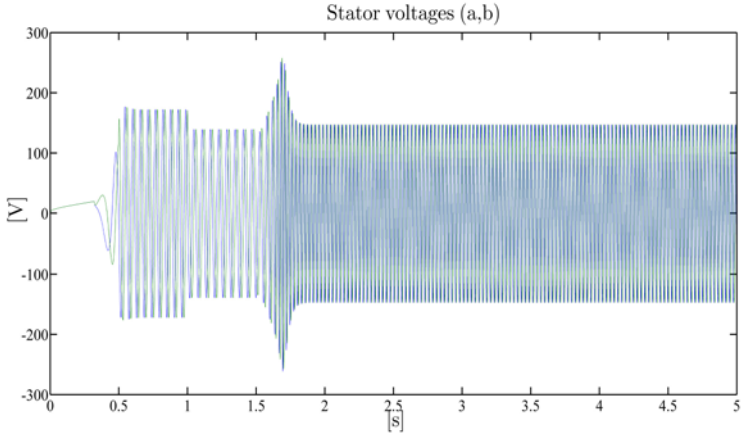

Fig. 2.46 Global control with arbitrary rate of convergence: stator voltage vector (a,b)-components (u_{sa}, u_{sb})

due to the magnetic saturation when $\hat{\alpha}/\alpha = 0.7$ and to the low flux modulus when $\hat{\alpha}/\alpha = 1.5$.

2.9 Conclusions

In this chapter the potentiality of feedback control for induction motors has been fully explored under the assumption that all the state variables are available for feedback. The motivation for introducing feedback actions in the controller comes

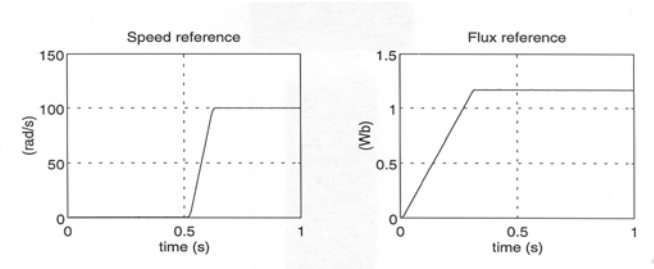

Fig. 2.47 Reference signals in the experiments

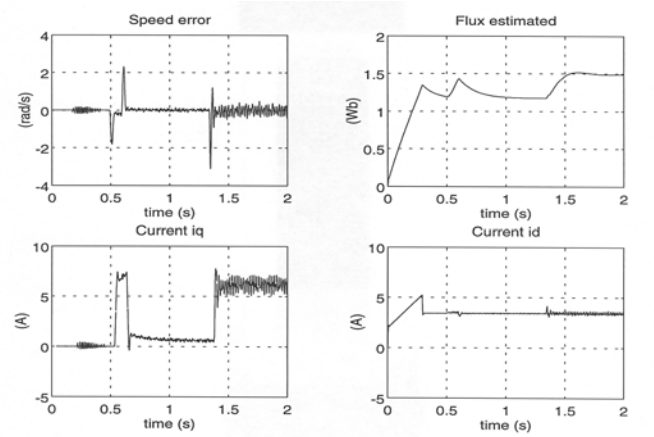

Fig. 2.48 Experimental results with the indirect field-oriented control and underestimated rotor resistance

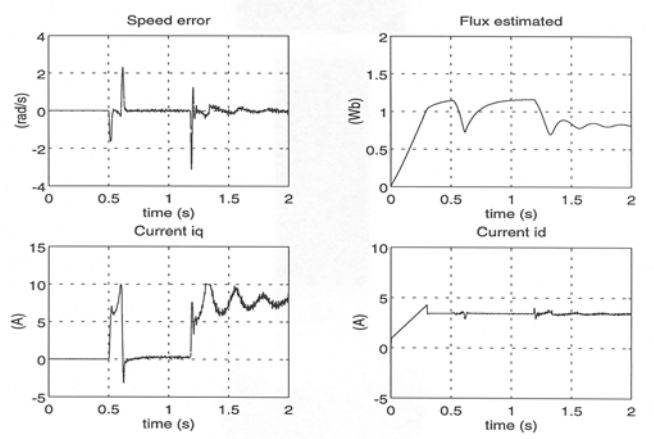

Fig. 2.49 Experimental results with the indirect field-oriented control and overestimated rotor resistance

from the analysis in Section 2.1 of the motor driven by the feedforward control which, when the initial conditions are compatible and the parameters values are exact, forces the motor to follow the desired rotor speed and flux modulus reference signals as shown in Chapter 1. In Section 2.1 the existence of constant rotor speed and flux modulus references and nonzero load torque is shown such that the origin of the error system is not globally attractive. In fact, an additional nonzero equilibrium point exists so that rotor speed tracking is not achieved for any motor initial condition. Moreover, the stability of the origin of the error system critically depends on the load torque which turns an asymptotically stable operating condition into an unstable one by crossing a critical value. Hence, the main goal of the feedback control is to make the desired operating condition attractive for any motor initial condition, for any value of the load torque, and robust with respect to motor parameter variations. The simplest way to achieve this goal is to modify the feedforward control by including a feedback action from the rotor speed as in the indirect field-oriented control presented in Section 2.3. This control is a modification of the original, historically important, direct field-oriented control, which requires rotor flux measurements and has a distinctive drawback: a singularity when the rotor flux modulus is zero requires the motor to start from nonzero rotor flux modulus initial conditions, in order to achieve exponential tracking of rotor speed reference signals for any load torque. If one is willing to accept singularities in the control law and to rely on rotor flux measurements with the aim of improving the closed-loop motor performance, then the input–output feedback linearizing control presented in Section 2.4 achieves an independent exponential tracking of rotor speed and flux modulus reference signals. For instance, the rotor flux modulus reference can be independently adjusted to minimize the power losses, as discussed in Chapter 1, without affecting the speed tracking: this feature is very appealing in electric traction applications. This control strategy can be rendered adaptive with respect to uncertainties in the load torque and rotor resistance by the adaptive input–output feedback linearizing control which is presented in Section 2.5. This control involves estimates of both parameters: assuming that either the load torque is different from zero or the rotor speed is not constant, the convergence of the rotor resistance estimator is achieved while the load torque estimator is always convergent to the true value. The online estimation of critical parameters constitutes a strong motivation for the use of feedback control and leads to an improved efficiency. In Section 2.6 it is shown that a dynamic third order state feedback control, the dynamic feedback linearizing control, can render the closed-loop motor linear so that the rotor speed and rotor flux angle can independently track their desired reference signals. However the control shows singularities when either the rotor flux modulus is zero or the stator current vector quadrature component is zero and it works only when the initial tracking errors are sufficiently small. Finally, in Section 2.7 the indirect field-oriented control introduced in Section 2.4 is generalized to obtain a global control that has several important features: it works for any motor initial condition and for any load torque; it achieves exponential tracking of desired reference signals $(\omega^*(t), \psi^*(t))$ with arbitrary rate of convergence; it is linear with respect to the rotor fluxes, the load torque, and the rotor resistance, so that, as we shall see in Chapter 4, rotor flux observers and uncertain parameter es-

timators can be incorporated. An indirect field-oriented control, which is the only implementable since it does not require flux measurements, has been experimentally tested in Section 2.8 to evaluate how critical the exact knowledge of the rotor resistance is. It turns out that an uncertain rotor resistance causes errors in the flux regulation so that power efficiency degrades. Many control algorithms presented in this chapter require flux measurements and exact parameter values. It will be discussed in Chapter 3 how to design rotor flux observers, adaptive observers, and parameter estimators for load torque and rotor resistance. The global control with arbitrary rate of convergence presented in Section 2.7 will be the starting point in Chapter 4 to design control algorithms which achieve rotor speed and flux modulus tracking for any initial condition, without the need of rotor flux measurements and of load torque and rotor resistance exact values.

Problems

2.1. Given any positive constant rotor speed and flux modulus reference values (ω^*, ψ^*), show that, in the case of zero load torque, exponential rotor speed and flux modulus tracking are guaranteed for any motor initial condition by the feedforward control (2.8). *Suggestion: use the positive definite function* $V = \gamma_1(\omega - \omega^*)^2 + \gamma_2(\psi_{rd} - \psi^*)^2 + \gamma_2\psi_{rq}^2 + \gamma_3(i_{sd} - i_{sd}^*)^2 + \gamma_3(i_{sq} - i_{sq}^*)^2$ *with* $\gamma_1\mu = \gamma_2 M = \gamma_3\beta$ *and* γ_1, γ_2, γ_3 *positive reals.*

2.2. Show that the constant rotor flux modulus reference minimizing the power losses given by (1.51) in Chapter 1 makes the origin of the error system exponentially stable.

2.3. Show that exponential rotor speed and flux modulus tracking along with exponential load torque estimation can be achieved for current-fed motors by both the direct and the indirect field-oriented controls (2.19) and (2.48) with the load torque estimate (k_T is a positive control parameter)

$$\hat{T}_L(t) = \hat{T}_L(0) - k_T \int_0^t (\omega(\tau) - \omega^*(\tau))\mathrm{d}\tau \tag{2.115}$$

in place of T_L. *Suggestion: follow the analysis performed for the nonadaptive case.*

2.4. Design a modified version of the indirect field-oriented control (2.48) for current-fed motors which guarantees, for any motor initial condition using rotor speed measurements only, exponential rotor speed and flux modulus tracking with a rate of decay which depends on α. *Suggestion: use the positive definite function* $V = \lambda(\omega - \omega^*)^2 + (\psi_{rd} - \psi^*)^2 + \psi_{rq}^2$ *with* λ *a positive real.*

2.5. Consider the indirect field-oriented control algorithm (2.48) with $\hat{T}_L$ given in Problem 2.3 in place of T_L

$$\begin{bmatrix} i_{sa}^* \\ i_{sb}^* \end{bmatrix} = \begin{bmatrix} \cos\varepsilon_0 & -\sin\varepsilon_0 \\ \sin\varepsilon_0 & \cos\varepsilon_0 \end{bmatrix} \begin{bmatrix} i_{sd}^* \\ i_{sq}^* \end{bmatrix}$$

$$i_{sd}^* = \frac{\psi^*}{M} + \frac{\dot{\psi}^*}{\alpha M}$$

$$i_{sq}^* = \frac{1}{\mu\psi^*}\left[-k_\omega(\omega-\omega^*) + \dot{\omega}^* + \frac{\hat{T}_L}{J}\right]$$

$$\dot{\varepsilon}_0 = \omega_0 = \omega + \frac{\alpha M i_{sq}}{\psi^*}$$

$$\hat{T}_L(t) = \hat{T}_L(0) - k_T \int_0^t [\omega(\tau) - \omega^*(\tau)]\mathrm{d}\tau$$

and the PI control inputs

$$u_{sa}(t) = -k_P[i_{sa}(t) - i_{sa}^*(t)] - k_I \int_0^t [i_{sa}(\tau) - i_{sa}^*(\tau)]\mathrm{d}\tau$$

$$u_{sb}(t) = -k_P[i_{sb}(t) - i_{sb}^*(t)] - k_I \int_0^t [i_{sb}(\tau) - i_{sb}^*(\tau)]\mathrm{d}\tau$$

to drive the stator current tracking errors $(i_{sa} - i_{sa}^*)$ and $(i_{sb} - i_{sb}^*)$ quickly to zero. Simulate the closed-loop performance and compare with the experimental results given in Section 2.8.

2.6. Show that exponential rotor speed and flux modulus tracking is guaranteed for any initial condition of the full order model by the indirect field-oriented control (2.49)–(2.51). *Suggestion: follow the analysis performed for the third-order model.*

2.7. Design a modified version of the indirect field-oriented control (2.49)–(2.51) which is global (*i.e.* it works for any motor initial condition) and adaptive with respect to the critical parameters T_L (load torque) and R_r (rotor resistance). *Suggestion: use the positive definite function* $V = \gamma_1(\omega-\omega^*)^2 + \gamma_2(\psi_{rd}-\psi^*)^2 + \gamma_2\psi_{rq}^2 + (i_{sd}-i_{sd}^*)^2 + (i_{sq}-i_{sq}^*)^2 + \gamma_3(T_L-\hat{T}_L)^2 + \gamma_4(\alpha-\hat{\alpha})^2$ *with* γ_1, γ_2, γ_3, *and* γ_4 *positive reals.*

2.8. Design a modified version of the input–output feedback linearizing control (2.85) which is adaptive with respect to the load torque T_L and both rotor and stator resistances R_r, R_s. *Suggestion: follow, in the control design, steps similar to those presented in Section 2.5.*

2.9. By following the ideas presented in Section 2.6, design a dynamic feedback linearizing control by choosing $\left(\psi_{rd}, \omega - \frac{\mu\psi_{rd}^2\rho}{\alpha M}\right)$ in place of (ω, ρ).

2.10. Analyze the closed-loop behavior of the full order motor model (1.39) controlled by the algorithm (2.24), (2.27), (2.29), and (2.30) when ω^* and ψ^* are constant while T_L and α are constant uncertain parameters. What happens if the feedback terms $-\alpha M i_{sq}^2/\psi_{rd}$ and $\alpha M i_{sq} i_{sd}/\psi_{rd}$ are dropped in (2.24)?

2.11. Rewrite the input–output feedback linearizing control (2.64) as

$$\begin{bmatrix} u_{sa} \\ u_{sb} \end{bmatrix} = \begin{bmatrix} \cos\rho & -\sin\rho \\ \sin\rho & \cos\rho \end{bmatrix} \begin{bmatrix} v_{sd} \\ v_{sq} \end{bmatrix}$$

with $\cos\rho = \psi_{ra}/\sqrt{\psi_{ra}^2+\psi_{rb}^2}$, $\sin\rho = \psi_{rb}/\sqrt{\psi_{ra}^2+\psi_{rb}^2}$ and compare (v_{sd}, v_{sq}) with (u_{sd}, u_{sq}) in (2.24), (2.54), (2.56), and (2.57).

2.12. Show that if the condition (2.84) holds, then the control (2.85) guarantees for suitable initial conditions exponential convergence to zero of the rotor speed and the rotor flux modulus tracking errors and of the estimation errors as well. *Suggestion: use the Persistency of Excitation Lemma A.3 in Appendix A.*

2.13. Design an adaptive version of the global control with arbitrary rate of convergence (2.113) when the load torque T_L is unknown: replace T_L with its estimate $\hat{T}_L$ and then design an adaptation law for $\hat{T}_L$ using the function [recall (2.98) and (2.109)]

$$V_T = V + \frac{1}{2\lambda_T}(T_L - \hat{T}_L)^2$$

with λ_T a positive real design parameter. Compare the resulting controller with that obtained by setting $\hat{\alpha} = \alpha$ in (2.85).

2.14. Simulate the adaptive control

$$\begin{aligned}
\begin{bmatrix} u_{sa} \\ u_{sb} \end{bmatrix} &= \begin{bmatrix} \cos\rho & -\sin\rho \\ \sin\rho & \cos\rho \end{bmatrix} \begin{bmatrix} u_{sd} \\ u_{sq} \end{bmatrix} \\
u_{sd} &= \sigma\left[\gamma i_{sd}^* - \left(\omega + \frac{\alpha M i_{sq}}{\psi_{rd}}\right) i_{sq} - \alpha\beta\psi_{rd} + \Gamma_d - k_i\tilde{i}_{sd} - \alpha M\tilde{\psi}_{rd}\right] \\
u_{sq} &= \sigma\left[\gamma i_{sq}^* + \left(\omega + \frac{\alpha M i_{sq}}{\psi_{rd}}\right) i_{sd} + \beta\omega\psi_{rd} + \Gamma_q - k_i\tilde{i}_{sq} - \mu\tilde{\omega}\tilde{\psi}_{rd}\right] \\
i_{sd}^* &= \frac{\psi^*}{M} + \frac{\dot{\psi}^*}{\alpha M} - \frac{k_\psi\tilde{\psi}_{rd}}{\alpha M} \\
i_{sq}^* &= \frac{1}{\mu\psi_{rd}}\left(-k_\omega\tilde{\omega} + \frac{\hat{T}_L}{J} + \dot{\omega}^*\right) \\
\hat{T}_L &= \xi - \lambda J\omega \\
\dot{\xi} &= -\lambda\xi + \lambda J\mu\psi_{rd} i_{sq} + \lambda^2 J\omega - v_T \\
v_T &= \frac{(k_\omega + \lambda)}{J\mu\psi_{rd}}\tilde{i}_{sq} + \frac{\tilde{\omega}}{J} \\
\Gamma_d &= \frac{\dot{\psi}^*}{M} + \frac{\ddot{\psi}^*}{\alpha M} - \frac{k_\psi}{\alpha M}(-\alpha\psi_{rd} + \alpha M i_{sd} - \dot{\psi}^*) \\
\Gamma_q &= \frac{1}{\mu\psi_{rd}}\left[-k_\omega\left(\mu\psi_{rd} i_{sq} - \frac{\hat{T}_L}{J} - \dot{\omega}^*\right) - \frac{v_T}{J} + \ddot{\omega}^*\right]
\end{aligned}$$

$$-\frac{1}{\mu\psi_{rd}^2}\left(-k_\omega\tilde{\omega}+\frac{\hat{T}_L}{J}+\dot{\omega}^*\right)(-\alpha\psi_{rd}+\alpha M i_{sd})$$

$$\psi_{rd} = \psi_{ra}\cos\rho+\psi_{rb}\sin\rho$$

$$\begin{bmatrix} i_{sd} \\ i_{sq} \end{bmatrix} = \begin{bmatrix} \cos\rho & \sin\rho \\ -\sin\rho & \cos\rho \end{bmatrix}\begin{bmatrix} i_{sa} \\ i_{sb} \end{bmatrix}$$

by choosing the control parameters $(k_i, k_\psi, k_\omega, \lambda)$; compare the results with those obtained by (2.85) with $\hat{\alpha}=\alpha$ and $k_{\omega p}=8,100$, $k_{\omega d}=180$, $k_{\psi p}=8,100$, $k_{\psi d}=180$, $\lambda=120$.

2.15. Consider the current-fed model (2.32) in an arbitrary rotating frame and the dynamic feedback control (2.34): design $(i_{sd}, i_{sq}, \omega_0)$ assuming that $(\omega, \psi_{rd}, \psi_{rq})$ are measured so that the closed-loop system (2.32), (2.34) becomes linear and decoupled (k_ω, k_d, and k_q are positive reals)

$$\dot{\tilde{\omega}} = -k_\omega\tilde{\omega}$$
$$\dot{\tilde{\psi}}_{rd} = -k_d\tilde{\psi}_{rd}$$
$$\dot{\tilde{\psi}}_{rq} = -k_q\tilde{\psi}_{rq}$$

provided that $\psi_{rd}^2(t)+\psi_{rq}^2(t)\geq c>0$ for all $t\geq 0$.

2.16. Design an adaptive version of the global control with arbitrary rate of convergence (2.113) which is adaptive with respect to all model parameters and guarantees the asymptotic tracking of both rotor speed and flux modulus references from any motor initial conditions. *Suggestion: reparameterize and use projection algorithms.*

2.17. Consider the indirect field-oriented control (2.49) and replace the parameter α by a constant estimate $\hat{\alpha}$. Compute the error dynamics and their equilibrium points in terms of the estimation error $\tilde{\alpha}=\alpha-\hat{\alpha}$ and evaluate their stability.

http://www.springer.com/978-1-84996-283-4

Induction Motor Control Design
Marino, R.; Tomei, P.; Verrelli, C.M.
2010, XX, 351 p., Hardcover
ISBN: 978-1-84996-283-4